

# Suitability of Using Crushed Concrete Adjacent to Geotextiles in Underdrain Systems

## Second Phase: Field Trial Before Implementation

<https://vtrc.virginia.gov/media/vtrc/vtrc-pdf/vtrc-pdf/25-R5.pdf>

---

**BURAK F. TANYU, Ph.D.**  
Professor

**ALYOUB ABBASPOUR, Ph.D.**  
Research Associate

**SEZGIN SARAK**  
Graduate Research Assistant

Sid and Reva Dewberry  
Department of Civil, Environmental and Infrastructure  
Engineering  
Sustainable Geo Infrastructure (SGI) Research Group  
George Mason University

Final Report VTRC 25-R5

**Standard Title Page - Report on Federally Funded Project**

1. Report No.: FHWA/VTRC 25-R5		2. Government Accession No.:		3. Recipient's Catalog No.:	
4. Title and Subtitle: Suitability of Using Crushed Concrete Adjacent to Geotextiles in Underdrain Systems Second Phase: Field Trial Before Implementation				5. Report Date: February 2025	
				6. Performing Organization Code:	
7. Author(s): Burak F. Tanyu, Ph.D, Aiyoub Abbaspour, Ph.D., Sezgin Sarak				8. Performing Organization Report No.: VTRC 25-R5	
9. Performing Organization and Address: Department of Civil, Environmental and Infrastructure Engineering Sustainable Geo Infrastructure (SGI) Research Group George Mason University				10. Work Unit No. (TRAI5):	
				11. Contract or Grant No.: 113425	
12. Sponsoring Agencies' Name and Address: Virginia Department of Transportation 1401 E. Broad Street Richmond, VA 23219				13. Type of Report and Period Covered: Final Contract	
				14. Sponsoring Agency Code:	
15. Supplementary Notes: This is an SPR-B report.					
16. Abstract: Due to the increasing interest in the use of recycled concrete as a base course aggregate, the Virginia Department of Transportation (VDOT) identified the need for an in-depth research investigate the clogging potential of the geotextile used in highway edgedrains if crushed hydraulic cement concrete (CHCC) is placed adjacent to the drainage fabric geotextile. To answer the research needs of the VDOT and address the discrepancies in the existing literature, George Mason University conducted a laboratory-based study and published their findings (VTRC 21-R12). The study identified two major mechanisms through which CHCC reduces the flowability of the geotextile used in underdrains: physical (fine particles migrating onto the voids in between the filaments of the geotextile) and chemical (precipitation of chemicals within geotextile filaments) phenomena. The findings showed that although the drainage fabric geotextile experienced some level of reduction in its flow capacity, as was expected, the reduction was not significant enough to impact and impede the overall flow of the geotextile/CHCC system. However, the laboratory study had some limitations, e.g., while simulating the physical and chemical phenomena simultaneously, temperature, rain, and humidity variations during seasonal changes were not accounted for, the potential effects of the pavement over the top of CHCC were not included, and drainage pipes were not considered. The research reported herein is the second phase of the laboratory study and involved constructing a full-scale field test site within VDOT's Harrisonburg facility. The test site consisted of seven sections, each side of which was constructed to include a 4-inch drainage pipe covered by No. 57 stone wrapped with drainage fabric, per VDOT's UD-4 edgedrain standards. In all seven sections, an unbound base course was placed in direct contact with drainage fabric. Sections with CHCC content included an unbound base course with (i) 100% CHCC, (ii) 40% CHCC + 60% virgin aggregate (V.A.; Blend 1), and (iii) 20% CHCC + 80% V.A. (Blend 2). Replicates of these sections were constructed as paved (to simulate actual roadway conditions) and unpaved (to provide data comparable with those of the previously completed laboratory study). Additionally, the seventh section was constructed as unpaved with a 100% V.A. section, which served as the control section. The constructed site was evaluated for about 3 years, and performance evaluations were conducted approximately every 6 months by analyzing the exhumed drainage fabric geotextiles and borescope surveying the drainage pipes. The findings confirmed the observations of the previous study by capturing the physical phenomenon. However, the data from the unpaved CHCC section showed approximately 2.5 times less tufa precipitation (chemical phenomenon) on the drainage fabric geotextile than what was previously noted in the one-year laboratory study. For the paved sections, data observed over 3 years were used to predict possible tufa growth on the drainage fabric's surface in 30 years. This prediction showed that even after 30 years, the surface area of the geotextile that is covered with tufa precipitation could be less than what was observed in the one-year laboratory study. If this prediction holds true, then the drainage fabric geotextile used in this study would continue to function hydraulically in 30 years. Borecope inspections of the drainage pipes showed signs of precipitation in the sections with 100% CHCC and 40% CHCC (Blend 1) but not in those with 20% CHCC (Blend 2) and 100% V.A. Although all the drainage pipes constructed continued to function hydraulically within the duration of this study, the chemical precipitation within the 100% CHCC and 40% CHCC sections of the drainage pipes needs further monitoring. This is because the quantitative estimation of continuing chemical precipitation within the pipes requires more data than what was available within the duration of this study.					
17 Key Words: Recycled concrete, Crushed concrete, Geotextile, Drainage			18. Distribution Statement: No restrictions. This document is available to the public through NTIS, Springfield, VA 22161.		
19. Security Classif. (of this report): Unclassified		20. Security Classif. (of this page): Unclassified		21. No. of Pages: 84	22. Price:



**PROJECT REPORT**

**SUITABILITY OF USING CRUSHED CONCRETE  
ADJACENT TO GEOTEXTILES IN UNDERDRAIN SYSTEMS  
SECOND PHASE: FIELD TRIAL BEFORE IMPLEMENTATION**

**Burak F. Tanyu, Ph.D.**  
**Professor**

**Aiyoub Abbaspour, Ph.D.**  
**Research Associate**

**Sezgin Sarak**  
**Graduate Research Assistant**

**Sid and Reva Dewberry**  
**Department of Civil, Environmental and Infrastructure Engineering**  
**Sustainable Geo Infrastructure (SGI) Research Group**  
**George Mason University**

*VTRC Project Manager*  
Kevin McGhee

Virginia Transportation Research Council  
(A partnership of the Virginia Department of Transportation  
and the University of Virginia since 1948)

Charlottesville, Virginia

February 2025

VTRC 25-R5

## ABSTRACT

Due to the increasing interest in the use of recycled concrete as a base course aggregate, the Virginia Department of Transportation (VDOT) identified the need for an in-depth research investigate the clogging potential of the geotextile used in highway edgedrains if crushed hydraulic cement concrete (CHCC) is placed adjacent to the drainage fabric geotextile. To answer the research needs of the VDOT and address the discrepancies in the existing literature, George Mason University conducted a laboratory-based study and published their findings (VTRC 21-R12). The study identified two major mechanisms through which CHCC reduces the flowability of the geotextile used in underdrains: physical (fine particles migrating onto the voids in between the filaments of the geotextile) and chemical (precipitation of chemicals within geotextile filaments) phenomena. The findings showed that although the drainage fabric geotextile experienced some level of reduction in its flow capacity, as was expected, the reduction was not significant enough to impact and impede the overall flow of the geotextile/CHCC system. However, the laboratory study had some limitations, e.g., while simulating the physical and chemical phenomena simultaneously, temperature, rain, and humidity variations during seasonal changes were not accounted for, the potential effects of the pavement over the top of CHCC were not included, and drainage pipes were not considered.

The research reported herein is the second phase of the laboratory study and involved constructing a full-scale field test site within VDOT's Harrisonburg facility. The test site consisted of seven sections, each side of which was constructed to include a 4-inch drainage pipe covered by No. 57 stone wrapped with drainage fabric, per VDOT's UD-4 edgedrain standards. In all seven sections, an unbound base course was placed in direct contact with drainage fabric. Sections with CHCC content included an unbound base course with (i) 100% CHCC, (ii) 40% CHCC + 60% virgin aggregate (V.A.; Blend 1), and (iii) 20% CHCC + 80% V.A. (Blend 2). Replicates of these sections were constructed as paved (to simulate actual roadway conditions) and unpaved (to provide data comparable with those of the previously completed laboratory study). Additionally, the seventh section was constructed as unpaved with a 100% V.A. section, which served as the control section. The constructed site was evaluated for about 3 years, and performance evaluations were conducted approximately every 6 months by analyzing the exhumed drainage fabric geotextiles and borescope surveying the drainage pipes. The findings confirmed the observations of the previous study by capturing the physical phenomenon. However, the data from the unpaved CHCC section showed approximately 2.5 times less tufa precipitation (chemical phenomenon) on the drainage fabric geotextile than what was previously noted in the one-year laboratory study. For the paved sections, data observed over 3 years were used to predict possible tufa growth on the drainage fabric's surface in 30 years. This prediction showed that even after 30 years, the surface area of the geotextile that is covered with tufa precipitation could be less than what was observed in the one-year laboratory study. If this prediction holds true, then the drainage fabric geotextile used in this study would continue to function hydraulically in 30 years. Borescope inspections of the drainage pipes showed signs of precipitation in the sections with 100% CHCC and 40% CHCC (Blend 1) but not in those with 20% CHCC (Blend 2) and 100% V.A. Although all the drainage pipes constructed continued to function hydraulically within the duration of this study, the chemical precipitation within the 100% CHCC and 40% CHCC sections of the drainage pipes needs further monitoring. This is because the quantitative estimation of continuing chemical precipitation within the pipes requires more data than what was available within the duration of this study.

## **INITIAL DRAFT PROJECT REPORT**

### **SUITABILITY OF USING CRUSHED CONCRETE ADJACENT TO GEOTEXTILES IN UNDERDRAIN SYSTEMS SECOND PHASE: FIELD TRIAL BEFORE IMPLEMENTATION**

**Burak F. Tanyu, Ph.D.**  
**Professor**

**Aiyoub Abbaspour, Ph.D.**  
**Research Associate**

**Sezgin Sarak**  
**Graduate Research Assistant**

**Sid and Reva Dewberry**  
**Department of Civil, Environmental and Infrastructure Engineering**  
**Sustainable Geo Infrastructure (SGI) Research Group**  
**George Mason University**

## **INTRODUCTION**

The increasing interest in the use of crushed hydraulic cement concrete (CHCC; also known as recycled concrete aggregate or RCA) in pavement design in the years leading up to 2013 prompted a group of district material engineers at the Virginia Department of Transportation (VDOT) to develop a research needs statement (RNS) to investigate the possibility of introducing provisions related to the use of CHCC, per VDOT specifications (Tanyu and Abbaspour, 2020). Current VDOT special provisions (SP208-000100-00) limits the use of CHCC as subbase or aggregate base when a subsurface drainage system is present (VDOT, 2016a). This limitation is directly related to concerns over the loss of serviceability of underdrain systems (specifically VDOT UD-4 configuration, Figure 1) because of chemical clogging. The UD-4 underdrain configuration includes a 4-inch perforated pipe embedded in No. 57 aggregate wrapped with nonwoven geotextile (VDOT, 2008). All new pavement systems constructed under the jurisdiction of VDOT are required to include a similar drainage system. If the geotextile is clogged, the reduced serviceability of the underdrain system may potentially jeopardize the service life of the transportation infrastructure (roads and highways). Therefore, the current VDOT specification limits the use of CHCC in the presence of any drainage systems.

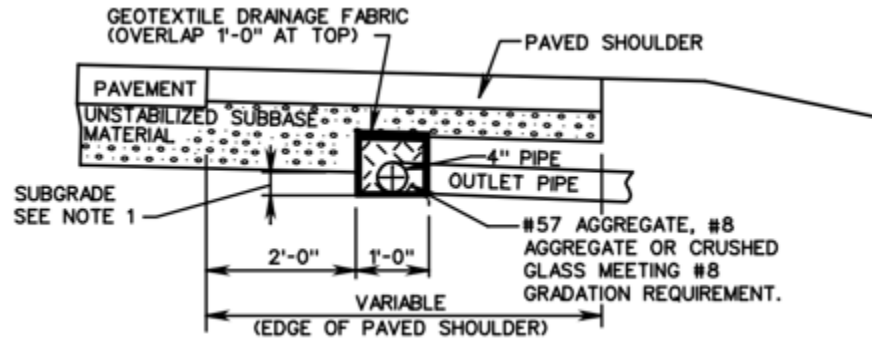


Figure 1. VDOT Standard Pavement: The UD-4 Edgedrain (Not to Scale)

In response to this RNS, Dr. Burak Tanyu and his team at the George Mason University (GMU) developed a two-phase research study. The first phase included laboratory-scale testing and simulation and was funded by the Virginia Transportation Research Council (VTRC). These simulations involved the nonwoven geotextile/CHCC interactions occurring under saturated and unsaturated flow conditions. The first phase of this research was concluded in 2016, and the final report (Report Number VTRC 21-R12) was published in November 2020 (Tanyu and Abbaspour, 2020). This completed laboratory research consisted of three major parts as follows:

- 1- The evaluation of the effect of carbonation and aging on the physical and chemical characteristics of CHCC. Freshly produced CHCC material was collected from a quarry in northern Virginia and aged for 12 months in the laboratory and 24 months in the field. The physical characteristics studied included changes in the gradation and hydraulic conductivity of the CHCC. The chemical properties studied included changes in the elemental and mineralogical content of CHCC from chemical degradation and aging.
- 2- The evaluation of the potential of chemical precipitation using theoretical geochemistry. For this, liquid samples of 100% CHCC, 100% virgin aggregate (V.A.), and two different blends mixing 40% CHCC with 60% V.A. and 10% CHCC with 90% V.A. were extracted using ASTM Batch tests. The percentages of the CHCC in the blends were determined based on the feedback received from the VTRC technical review panel (TRP). The chemical properties of the extracted liquid, including pH, electric conductivity (EC), and concentrations of leached elements, were evaluated. The findings were then used as input parameters for the geochemical modeling, using the MINTEQA2 software; the potential solid phases and theoretical conditions that could lead to the formation and deposition of solid precipitates were identified and reported.
- 3- The evaluation of the hydraulic compatibility of the nonwoven geotextile and CHCC material. This consisted of over 40 long-term filtration tests (including triplicates), using the gradient ratio (GR) test setup on various samples of CHCC and V.A.— 100% CHCC, 40% CHCC+60% V.A., 20% CHCC+80% V.A., 10% CHCC+90% V.A., and 100% V.A. Additionally, CHCC exposed to 4, 9, and 12 months of carbonation were tested to evaluate the change in their overall hydraulic

compatibility. The tests were conducted under full saturation conditions, with hydraulic gradients of 1, 2.5, and 5 applied. To identify a threshold of fines content that may cause significant physical clogging, a set of samples were also prepared, with adjusted gradation to have fines content ranging from 5% to 13%. A supplemental set of tests were then conducted using these samples to evaluate the existence of such a threshold.

The following summarizes the most important findings from the previously completed laboratory research (Phase 1):

- 1- CHCC chemistry changes with aging; specifically, its carbonate content increases with aging. These results suggest that CHCC be stockpiled for about a year or so before being used in the field. However, aging was not found to adversely affect the physical properties of CHCC.
- 2- CHCC's hydraulic conductivity does not change with aging, and the values obtained from CHCC with approximately 8% fines ranged from  $10^{-3}$  to  $10^{-4}$  cm/sec. These hydraulic conductivity values, in most cases, are comparable to those of V.A.'s with the same gradation.
- 3- Fines content (passing number 200 sieve) of approximately 9% appeared to be a threshold for notable migration of physical particles onto the nonwoven geotextile, reducing the serviceability of the geotextile when used with the CHCC, V.A., and various blends. The observations show that for samples with lower fines content, the physical clogging did not lead to a noticeable reduction in serviceability of the nonwoven geotextile/soil system.
- 4- CHCC produces calcareous tufa (calcium-based crystals that can grow on the geotextile) when the conditions are right. The potential for precipitation was also shown and characterized using geochemical analyses in this study.
- 5- Throughout the course of the laboratory study, no evidence was found that suggested that the occurrence of physical (migration of fines) or chemical (precipitate formation and deposition in the geotextile) phenomena alone leads to an extensive reduction in the filtration capacity of the geotextile or an extensive loss of serviceability of the geotextile/soil system.
- 6- Blending CHCC and V.A. appears to reduce the potential of leaching high concentrations of elements that contribute to tufa precipitation; thus, it is a recommended approach for reducing the potential for chemical clogging.

The laboratory study was conducted to simulate field conditions as closely as possible. Based on the findings, it was concluded that relating the physical phenomenon (migration of fines under seepage force and entrapment within geotextile fibers) to the reduction in filtration capacity (or serviceability) of the geotextile/soil system can be achieved by (i) conducting long term filtration tests, (ii) evaluating post-filtration geotextile permittivity, and/or (iii) measuring

the changes in the pore size distribution of geotextile from thin sections of the geotextile. However, relating tufa precipitation to the reduction in geotextile serviceability was challenging, as the laboratory hydraulic conductivity tests were performed under saturated conditions. Under saturated conditions, CHCC does not produce tufa because the liquid never reaches supersaturation and chemical precipitation to occur. Therefore, a custom-designed unsaturated test set-up was designed to determine the chemistry mechanisms governing tufa precipitation and the kinetics of tufa precipitation in an underdrain system with geotextile. In these tests, CHCC/geotextile samples were periodically wetted and dried, and geotextile samples were periodically exhumed. The percentage of the surface area of the exhumed geotextile samples covered with tufa ( $S_{\text{tufa}}$ ) was tracked for one year. Using this dataset and the chemical kinetics models of speleothem formations and natural tufa, a theoretical model was developed (for engineering design purposes) to estimate the reduction in serviceability of nonwoven geotextile/CHCC systems due to chemical precipitation (Abbaspour and Tanyu, 2021). The findings showed that in one year, the maximum  $S_{\text{tufa}}$  observed was 17%, which corresponded to an approximately 40% reduction in geotextile serviceability (Abbaspour and Tanyu, 2020a). Considering the order-of-magnitude differences between the permeability of the geotextile and that of the 100% CHCC, such reduction in geotextile performance was not considered a major concern. However, it had some limitations. First, it was not possible to assess the combined effects of the physical and chemical phenomena simultaneously. Second, the laboratory tests did not simulate the conditions of paved roadways and the drainage pipes attached to the UD-4 underdrain system. Therefore, based on the positive outcomes of the laboratory findings and due to the existing limitations, a field study was deemed necessary to confirm the validity of the laboratory findings and simulate real-life conditions.

## **PURPOSE AND SCOPE**

The research described in this report is the second phase of the study designed by Dr. Burak Tanyu and his team, and it is primarily based on data collected from the field. The main objectives of this study were to:

1. confirm whether the CHCC behavior observed in the previously completed laboratory study (i.e., fines migrate and tufa precipitates, but these phenomena do not stop the flow through the geotextile or reduce its function as a filter between the base course and the No. 57 stone) held true under field conditions;
2. determine whether the use of a 100% CHCC unbound base course was suitable for paved roadway applications and if CHCC blended with V.A. made for better performance, based on the longer-term performance evaluations; and
3. provide recommendations for VDOT to develop specifications allowing the use of CHCC (whether as 100% or as blends of CHCC and V.A.) as an unbound aggregate when geotextile is present in the drainage system.

The following specific tasks were identified in this study:

Task 1 - Designing the test site. The test site had to be specifically designed to resemble an actual roadway as closely as possible, with underdrain systems that came in direct contact with the CHCC. This task was created to design the site and the test sections that would serve as the means to achieve the main objectives of the study.

Task 2 - Characterizing the materials used at the test site. Because CHCC is a recycled material and considering the primary focus of this study, the properties of this material had to be documented and compared with those of the V.A. that was used as the control material. Additionally, this task was established to characterize and document the properties of the materials used to construct the underdrain systems.

Task 3 - Constructing the test site. Proper construction of the test site was one of the most important aspects of this study. The goal was to ensure that the construction was completed in accordance with the information developed in Task 1. This task was also necessary to document the details of the constructed features.

Task 4 - Monitoring programs at the test site. The site was monitored for 3 years in this study. Evaluating the long-term performance of the underdrain system required datasets that will explain the reasons for the performance-related observations. This task was established to design and implement a monitoring program for data collection.

Task 5 - Performance evaluations of the site. This task was aimed at ultimately documenting the hydraulic performance of the underdrain system components (nonwoven geotextile and drainage pipes) throughout the duration of this study and comparing the observations from the different test sections. The information obtained will then be used to achieve the main objectives of the study and make appropriate recommendations for implementation.

## **METHODS**

### **Overview**

The specific methods used to complete each of the tasks in this study are described in detail below.

### **Designing the Test Site**

The criteria for the test site were: (i) the site had to be constructed at a location that is owned and operated by the VDOT and (ii) the site had to have reasonable space for constructing all sections, with a suitable topography that would allow the “drainage to be based on gravity. Based on the recommendations for a typical section given by VTRC’s TRP and in order to satisfy the minimum requirements of the VDOT UD-4 Standard Pavement Edgedrain (Plate 108.05, VDOT 2016 Road and Bridge Standards), all sections included an 8-inch unbound base course and two edgedrain systems on both sides.

Each edgedrain included a 4-inch perforated corrugated pipe encapsulated within a No. 57 stone wrapped with nonwoven geotextile (served as the filter fabric). All pipes (both perforated and outlet pipes) were constructed with a minimum of 2% slope, per VDOT standards.

To develop a proper design for the site that would be used to achieve the objectives of this study, several key features were considered:

- Infiltration rainwater in the base course could not be allowed to further infiltrate the subbase layer. This was important because by not allowing the water to further infiltrate into the subbase, all water was forced to only drain out of the base course through the edgedrains. This would create the worst-case scenario in terms of evaluating the potential clogging of geotextile and the drainage pipes. To achieve this, a liner system (hydraulic barrier) had to be designed between the subbase and base courses.
- Water collected by the edgedrain system had to be allowed to drain out of the test section into storage tanks. This approach would allow for the monitoring of the drainage functionality of each section, and water samples could be collected to monitor the key indicators related to potential tufa precipitation. To achieve this, at the end of each test section, edgedrain pipes had to be connected to collection pipes, which then had to be connected to the collection tanks. The grade of all these pipes had to be designed such that all along the collection pipe system, it was never less than 2%.
- The test sections had to be designed to allow for the independent evaluation of each section without the influence of another section. This required that the base course material and any infiltration water in each section be separate from those in adjacent sections. Therefore, curb divider walls had to be designed to divide the sections as well as serve as hydraulic barriers.
- The test site had to be designed such that all the drainage pipes (including the edgedrain and collection pipes) could be monitored during throughout the study. This required that in each section, each drainage pipe system had its own “T” connector that would allow a borescope to be inserted for inspection and monitoring.
- The length of each section had to be designed to allow the research team to exhume pieces of the nonwoven geotextile approximately every 6-months throughout the study. Sampling size was targeted to be approximately 2 ft by 2 ft in dimensions to allow proper testing to evaluate performance.
- The width of each test section was to be designed to replicate a typical two-lane roadway as closely as possible within the space that would be allocated for use as the entire test site.
- Based on the previously completed laboratory study (Report Number VTRC 21-R12), it was determined that the test site would be designed to include test sections with the following unbound base course aggregates:

- 100% CHCC
- 100% V.A.
- 40% CHCC and 60% V.A. (Blend 1)
- 20% CHCC and 80% V.A. (Blend 2)

To simulate the typical roadway application and compare the field observations (Phase 2) with the findings of the previously completed laboratory study (Phase 1), sections with CHCC content had to be designed as paved and unpaved. For the sake of comparison to the previously completed laboratory study, the 100% V.A. section was also constructed as unpaved.

- The VDOT suggested the asphalt layer be 2 inches thick and the surface mix be placed directly over the base course (no prime was to be used).

### **Characterization of Materials Used at the Test Site**

To avoid bias while conducting this study, materials that would be used in real VDOT projects, such as the base course aggregates, No. 57 stone, nonwoven geotextile, and asphalt mixture, were all procured, not accepted as donated materials. The methods used to characterize each of these materials are described below.

#### **Base Course Aggregate**

CHCC, V.A., and the blends were all procured from an aggregate producer. The following processes were used to characterize each material:

- Visual observation and documentation of production and random sampling during production, following the ASTM D3665 (2012) method.
- Creation of a pile of the produced material and then reduction of the piled material into smaller portions using the quartering method, per ASTM D3665 (2012). The reduced material was then used for sampling, and the sampled materials were placed into bags and transported to GMU's sustainable geo infrastructure laboratory for testing and evaluation.
- Evaluation of the physical properties of the sampled materials, which included analysis of the grain size (in accordance with ASTM D6913/D6913M, 2017; ASTM D7928, 2017), specific gravity and water absorption of coarse and fine particles (per ASTM C127, 2012; ASTM C128, 2012), Atterberg limits (per ASTM D4318, 2010), compaction characteristics using standard effort (per ASTM D698, 2012), and permeability (per ASTM D2434, 2006). The potential geological make-up of the V.A. was also investigated via visual observations and based on the available literature.
- Evaluation of the chemical composition of the collected materials, which was achieved by creating liquid samples per the ASTM D3987 (2012) method and analyzing with inductively coupled plasma (ICP) optical emission spectroscopy (OES) to determine the

elemental concentrations. The same samples were also characterized based on measured pH and EC.

- Testing the CHCC and blend samples for their mortar content (MC) to determine the percentage of concrete matrix over aggregate. The MC was determined using the acid treatment method developed by Tanyu and Abbaspour (2020). V.A. was also treated with hydrochloric solution to test for the presence of carbonate-based compounds within the aggregate.

### **No. 57 Stone**

No. 57 stone, the crushed stone used to encapsulate the edgedrain pipes, was also procured from the same place as the base course aggregate and originated from the same rock as the base course aggregate. As such, the chemical properties of the 57 stone were considered to be similar to those of the V.A. According to VDOT specifications, the minimum and maximum particle sizes of the 57 stone and V.A. were 8 (2.36 mm) and 1.5 inches (37 mm), respectively.

### **Nonwoven Geotextile**

The geotextile used in this study was selected with the input of VDOT's TRP, in accordance with VDOT's UD-4 edgedrain requirements (VDOT, 2016). The virgin geotextile was evaluated based on the manufacturer's reported properties and for permittivity following the ASTM D4491/D4491M (2020) protocol.

### **Asphalt Overlay**

The asphalt mixture used in this study was determined by the VDOT's TRP to be a VDOT SM-9.5A mix. This is a fine to medium-surface mix with a maximum aggregate size of 3/8 inch (9.5 mm). The mixture was prepared by an asphalt company, and after placement in the field, core samples were obtained by the GMU team to evaluate the permeability of the asphalt layer.

### **Construction of the Test Site**

VDOT's leadership team at Harrisonburg Residency in Staunton District graciously allowed the test site for this study to be constructed within their property. This space met the project criterion that required the site to be located at a VDOT-owned and operated property.

The following steps were followed to develop the site:

- First, the subgrade of the areas where the test sections and collection tanks will be located was prepared.
- Then, the side slope between the footprint of the test sections and water collection tank locations was cleared, grubbed, and leveled.
- Next, subbase and curb divider walls were constructed, and the grade elevations were confirmed.

- Then, trenches for the edgedrain and collection pipes were constructed.
- Geomembrane hydraulic barriers were installed at each test section.
- UD-4 edgedrain systems were installed, and the grades of the pipes were confirmed.
- Instruments were installed at each test section, and the data collection hub was constructed.
- Base course materials were moisture-conditioned, placed, and compacted.
- A concrete pad was constructed for installing the water tanks, second data collection hub, and weather station.
- Water collection tanks were installed, collection pipes were connected to the tanks, instruments were installed into the tanks, and the second data collection hub and weather station for the site were constructed.
- Finally, asphalt was placed over the three designated sections.

The VDOT team anticipated the primary construction to required two laborers and one equipment operator, i.e., an excavator, grader, and compactor. Construction of the site was scheduled to start on May 6, 2020.

Recognizing that the start date was going to correspond to a time of the year when all VDOT crews will be very busy, the initial parts of the construction was scheduled to be completed by VDOT's Harrisonburg bridge team, while the remaining parts of the construction was to be completed by VDOT's Mt. Crawford maintenance team, based on their availability. Installation of all drainage systems and instrumentation were to be completed by the GMU team, working closely with the VDOT team. The construction of the site was to be completed right after the placement of the asphalt pavement on the designated sections.

### **Monitoring Programs at the Test Site**

The monitoring program at the test site was designed to comprise collecting data from (1) the weather station installed at the site, (2) instruments embedded within the base course sections and inside the water collection tanks, and (3) the frequent chemical analyses conducted on the water samples obtained from each collection tank. The methods used for each monitoring are explained below.

### **Meteorological Data at the Test Site**

A weather station was installed at the site to collect meteorological data (Figure 2). The weather station was located on top of the concrete pad to create a level ground, with wires inserted into the concrete pad for stability.

The weather station consisted of temperature and relative humidity sensors, a rain gauge, a barometric pressure sensor, and a water level sensor. The complete weather station was purchased from Davis Instruments and connected to a 3G remote monitoring station that enabled the researchers to monitor and download data remotely.



**Figure 2. Weather station installed at the test site**

### **Instrumentation at the Test Site**

Each test section was instrumented with a sensor located approximately at its center. The sensor was capable of recording the section's volumetric moisture contents and ground temperature (Figure 3). Each instrument from each section was connected to a data logger, which required the data to be downloaded in person to a computer periodically. The data logger system was installed within close proximity to the test sections and was powered by a solar panel (Figure 4). These instruments were installed to monitor the wetting and drying cycles of each test section.

Each water collection tank was equipped with an Onset water level logger, which is a transducer that works with the pressure water exerts on the instrument (Figure 5). This instrument is designed to track data internally until a data collection cable is connected, after which the data can be downloaded to a computer. This instrument was placed at the bottom of each tank with a yellow rope. Whenever data was to be collected, the rope was pulled up and the instrument was retracted to download the data. Monitoring the water level in each tank was important to confirm that the infiltration water from each section reached the collection tanks. This dataset was also used to compare the accumulated quantities of water from different sections.

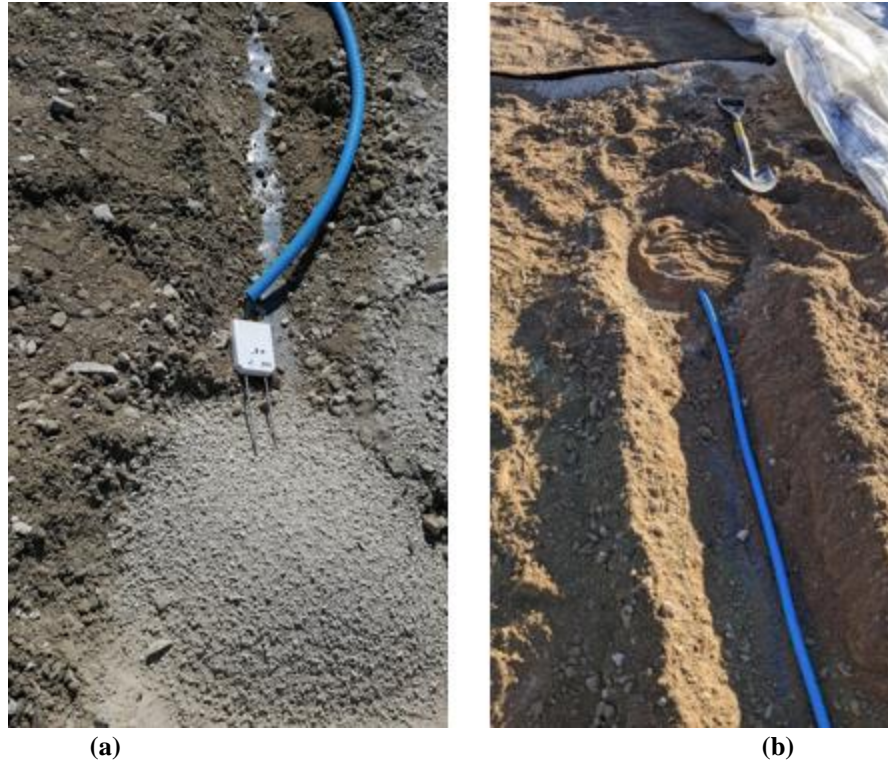


**Figure 3. Monitoring sensor (a) type and (b) installation within the base course of each test section**



**Figure 4. The data logger pole for all sensors installed within the base course at the test site**



**Figure 5. Water level logger installed at each collection tank**

The water collection tanks of the 100% unpaved CHCC test section was also equipped with Hobo pH and EC loggers (Figure 6). This dataset was used to monitor the changes in chemical variation of the outflow. Similar to the water level loggers, the pH and EC loggers also needed to be retracted periodically to download the collected data into a computer. These instruments were only installed into the collection water tanks of one section (as opposed to all sections) because of cost. The unpaved 100% CHCC section collection tanks were selected for these instruments because this section (at the beginning of the study) was believed to constitute the worst-case scenario in terms of potential tufa precipitation. One of these tanks also included a water level logger that was connected to the data hub at the weather station pole. This instrument was used to track the water level in real time to determine when to mobilize to the site for water sampling and tank emptying.



**Figure 6. The (a) pH and (b) electric conductivity (EC) logger sensors installed into the water collection tanks of the 100% unpaved CHCC test section**

### **Chemical Analyses of Water Collected from the Site**

Whenever the water level logger in the water collection tank of the 100% CHCC unpaved test section indicated that the tank was filled up to two-thirds of its capacity, the GMU team mobilized to the site to empty and collect water samples from all of the tanks. Typically, this required water sampling approximately less than every two months. The only way the water could reach the collection tanks was through the rainwater infiltrating each section. Therefore, the regularly conducted chemical analyses of the collected water provided monitoring information regarding the interaction of the infiltrated rainwater with the aggregate in each test section. To allow the collection of water samples, each collection tank had a  $\frac{3}{4}$  inch PVC sampling pipe installed (Figure 7).



**Figure 7. Water sampling pipes from the collection tanks**

The water samples collected were analyzed to track the changes in pH, EC, and calcium (Ca) and sulfate ( $\text{SO}_4$ ) concentrations (determined from the ICP-OES analyses). These datasets were used to monitor changes in leached liquid from each section over time. Previous studies on CHCC have indicated that the chemistry involved in tufa precipitation is very complex (Abbaspour and Tanyu, 2021; Abbaspour and Tanyu, 2020a; Abbaspour and Tanyu, 2019a; Abbaspour and Tanyu, 2019b; Abbaspour et al., 2018; Abbaspour et al., 2016; VDOT, 2016a; VDOT, 2016b). Therefore, the purpose of the water sample collection in this study was not to re-evaluate the complex chemistry but to use the dataset obtained to assess the likelihood of chemical precipitation and the potential chemical make-up of the precipitated material (i.e., either carbonate ( $\text{CO}_3$ ) or sulfate ( $\text{SO}_4$ )). The following very simplified approach has been developed to interpret some key indicators:

- EC indicates the ionic activity within a solution. High values indicate that certain ions are dissolving into the solution, while low values indicate that precipitation is occurring. Stabilized EC values indicate that dissolution is at a steady rate, and precipitation may or may not continue.
- The pH of the CHCC leachate is inversely correlated with the Ca concentration of the solution.
- If the pH of the collected water is high (approximately  $\geq 10$ ) and:
  - the Ca content of the solution is also high (approximately  $\geq 50$  mg/l), then calcium is most likely dissolving from the aggregate, and precipitation is likely happening (or),
  - the Ca content of the solution is low, then calcium is not dissolving (readily available Ca content is low).

- If the pH of the collected water is low and:
  - the Ca content of the solution is high, then calcium is most likely dissolving from the aggregate, but precipitation is likely not happening (or)
  - the Ca content of the solution is also low, then the dissolution of the Ca is not likely to be the predominant factor controlling the pH (some other ions in the solution are controlling the pH). Precipitation of calcium-based compounds may not be occurring.
- When Ca and SO<sub>4</sub> contents are compared:
  - If the Ca content is more than the SO<sub>4</sub> content, the precipitated material is likely to be a calcium sulfate-based compound (such as gypsum) (or)
  - If the Ca content is less than the SO<sub>4</sub> content, the precipitated material is possibly a calcium carbonate-based compound (such as calcite).

### **Performance Evaluation of the Site**

Evaluating the performance of the site involved determining the ability of the nonwoven geotextile and installed pipes (edgedrain and collection pipes) to allow the infiltration water to discharge from the system. For this evaluation, both the nonwoven geotextile and collection pipes were investigated. The performance evaluation assessments were conducted approximately once every 6 months for 3 years, after the construction of the test site was completed. The methods used for these evaluations are provided in detail below.

### **Evaluation of the Exhumed Geotextiles**

The geotextile samples were exhumed to assess the performance. This was achieved as a joint effort between VDOT and GMU, and depending on the number of crew members available, it usually required one to two days' work. Exhuming the geotextile samples included the following steps:

- 1- Marking and cutting the asphalt overlay (for paved sections only) (Figure 8).
- 2- Carefully removing the base course until the geotextile is exposed.
- 3- Carefully brushing the top of the geotextile and cutting a sample for evaluation (Figure 9).
- 4- Covering the sampling spot with new pieces of geotextile, with a minimum of 8-inch overlap on all sides (Figure 10).
- 5- Replacing the base course material and compacting it using the vibratory plate and hand tamping (Figure 11).

- 6- Placing the asphalt block inside the sampling area and sealing the joints using an asphalt joint filler (for paved sections only) (Figure 12).



**Figure 8. Marking the pavement and cutting the asphalt overlay to exhume geotextile samples from paved sections**



**Figure 9. Removing the base course material and (a) brushing the surface of the geotextile and (b) cutting a sample piece from the exposed geotextile**



**Figure 10. Placing a piece of new geotextile over the cut area before placing the base course material back onto the edg drain geotextile**



**Figure 11. Compacting the base course material back onto the edg drain geotextile**



**Figure 12. Placing the asphalt block back onto the recompacted base course aggregate**

All exhumed geotextiles were evaluated for their hydraulic ability and the surface area covered with tufa precipitation that may impede the hydraulic ability.

*Evaluating the hydraulic ability of the exhumed geotextile samples*

All exhumed geotextile samples from each test section were evaluated in the permittivity chamber for their ability to permeate water (permittivity) (Figure 13). The samples were air-dried prior to laboratory analysis, and a circular sample was cut off from the exhumed sample and soaked for at least 24 hours. The geotextile was soaked to fully saturate it before testing. The tests were started with an applied head of 10 mm until flow was stabilized. Afterwards, the applied head underwent 10-mm increments, and the permittivity ( $\psi$ ) values were recorded. For each test, triplicate virgin geotextile samples were also tested, and the ratio of the permittivity values of the exhumed and virgin geotextiles were reported in accordance with Equation 1.

$$\psi_R = \frac{\psi_{Exhumed\ geotextile}}{\psi_{Virgin\ geotextile}} \quad (1)$$

To determine the reduction in overall permittivity of the geotextile, the  $\psi_R$  determined from Equation 1 was subtracted from 1 (Equation 2). A perfect geotextile with no reduction would result in a  $\psi_R$  of 1, which would result in zero reduction in  $\psi_R$ .

$$Reduction\ in\ \psi\ (\%) = (1 - \psi_R) \times 100 \quad (2)$$



**Figure 13. Evaluating the permittivity of the geotextiles exhumed from the test site**

Although the geotextile samples tested were soaked for saturation, this process may have dissolved some of the chemically precipitated minerals. However, not all chemically precipitated compounds dissolve in water. For example, carbonate-based Ca-bearing mineral such as calcite has significantly less water solubility compared to calcium sulfate-based mineral such as gypsum. Therefore, it was important to evaluate the data obtained from the chemical analyses of the water samples gotten from the collection tanks to monitor the indicators for carbonate vs. sulfate-based ions. In cases where the calcite type of mineral precipitation was expected, permittivity test results served as the ultimate test, where the potential effects of both the physical and chemical phenomena on reduction in geotextile hydraulic ability could be evaluated. If the tufa precipitation was more likely to form gypsum, then the permittivity test served as a means to evaluate the physical phenomenon.

*Evaluating the chemical precipitation over the surface of the exhumed geotextile samples*

Parts of all exhumed geotextile samples were cleaned and evaluated under the microscope. These parts were initially air-dried and cleaned using an archeologist brush and the smooth air blow technique. Cleaning was done to remove all particles that were thought to have physically migrated onto the filaments of the geotextile. The difference between the appearance of physically migrated and chemically precipitated particles is shown in Figure 14. The cleaning process required the use of a microscope, and it typically took about a week to completely clean the geotextile samples that were exhumed from one test section.

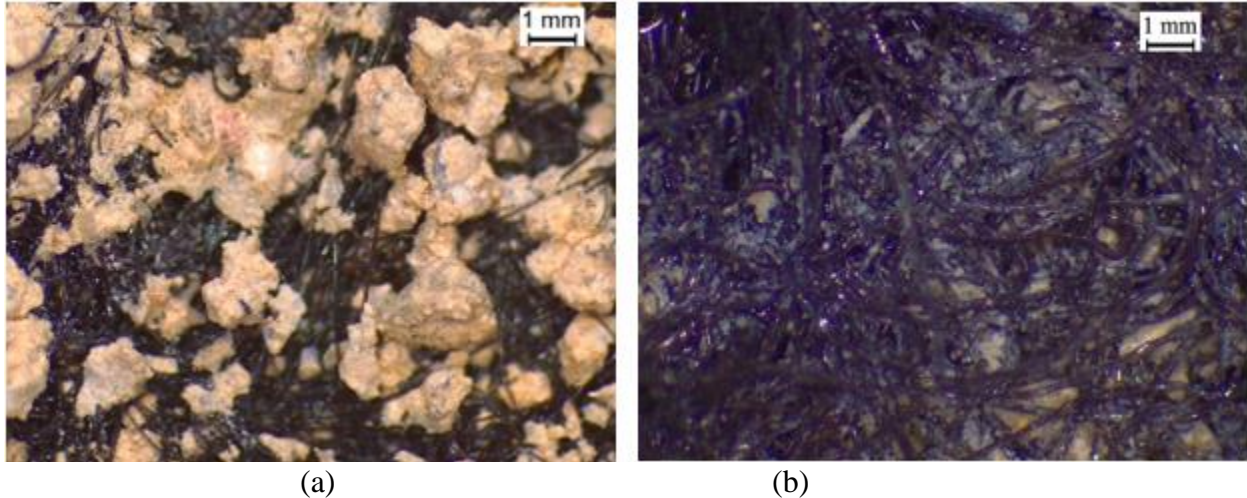


**Figure 14. A typical appearance of (a) physically migrated and (b) chemically precipitated particles on an exhumed geotextile**

After removing all the physically migrated particles from the geotextile's surface, the samples were evaluated according to the image analyses process to quantify the percentage of the surface area of the geotextile that contained CHCC tufa ( $S_{tufa}$ ). The imaging was done using a Leica M125 C microscope with an in-built 5 MP HD digital camera (Figure 15). Microscopic images, with a small overlapped area on each consecutive picture, were continuously taken from a point of interest, with a magnification of 40 on both sides of the sample. Next, the images were stitched together using the Leica LAS EZ software to create a larger image. To quantify  $S_{tufa}$ , these large images were analyzed using the Leica LAS X software. This process allowed the surface area covered with the precipitate to be identified and quantified based on the calculated unit surface of various areas.



**Figure 15. The Leica M125 C microscope with an in-built 5 MP HD digital camera with a geotextile sample under analysis**

## Evaluating the Edgedrain and Collection Pipes

Each test section was designed to have T connectors that will allow for borescope surveys of both the edgedrain and collection pipes all the way from the test section to the collection tanks. The borescope used for this purpose was manufactured by Fiberscope (and named the Viper model by the manufacturer) and has a 0.67-inch waterproof mini camera head attached to a 50-ft long cable. The instrument allowed the camera feed to be monitored directly on an LCD monitor, and the survey results were recorded on a SD card. A photo of the system used in this study is provided in Figure 16. A field implementation of the borescope survey is shown in Figure 17.

The survey data were downloaded after completion, and the video files were compared with each other to track the changes in observations over time based on each site visit. Changes in the appearance of the inner part of the drainage pipes were used to evaluate the extent of the potential physical migration of fines and chemical precipitation. These observations, coupled with the evaluation of the exhumed geotextile, were used to assess the performance of each section. Additionally, at the end of the study, an actual photograph of the collection tanks' interior was taken to document the extent of the material accumulated. Without the collection tanks, these materials would have been washed out from the collection pipes.



**Figure 16. The instrument used to survey the edgedrain and collection pipes at each section**



Figure 17. Insertion of the (a) borescope camera through the T connector and (b) monitoring and data collection on site

## RESULTS AND DISCUSSIONS

### Design of the Test Site

Figure 18 presents a layout of the test site, including the dimensions of each test section, the collection pipes connected to edgedrains in each section, and the collection tanks. The test site's design included seven different sections measuring 20 ft wide and 20 ft long each, with an overall grade difference of 2% between the beginning station point of 0+00 and ending station point of 1+45.33.

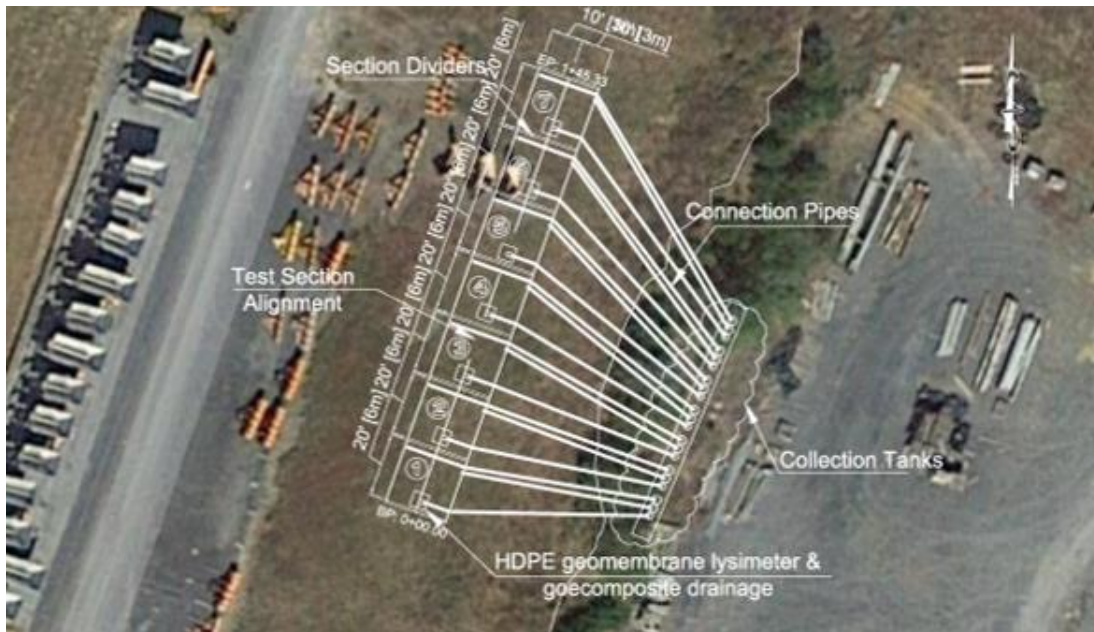


Figure 18. Schematic plan view of the designed test site (dimensions are in feet)

Each section was designed to consist of an 8-inch unbound base course. Three of the sections were designed to be paved with 2-inch asphalt, and four of the sections were designed to be unpaved. The numbers in each square in Figure 18 represent the designation used for each test section location. Below is a summary of the content of each designed test section:

- Test section 1 – Paved 100% CHCC
- Test section 2 – Paved Blend 1 (40% CHCC + 60% V.A.)
- Test section 3 – Paved Blend 2 (20% CHCC + 80% V.A.)
- Test section 4 – Unpaved 100% CHCC
- Test section 5 – Unpaved Blend 1 (40% CHCC + 60% V.A.)
- Test section 6 – Unpaved Blend 2 (20% CHCC + 80% V.A.)
- Test section 7 – Unpaved 100% V.A.

The length of the sections (20 ft) was determined to allow for the geotextile samples to be exhumed and to leave enough distance between each sample location such that they did not interfere with each other. The design length of 20 ft also allows for the geotextiles to be potentially exhumed in the future, even after completion of this study in 3 years. The width of each section ended up being slightly less than that of a typical two-lane roadway (20 ft as opposed to 24 ft) due to the geometrical constraints of the site. The V.A. section was designed to be unpaved because this created a worst-case scenario for the amount of water infiltrating the base course and allowed for a direct comparison with the previous laboratory study.

In all sections, the middle collection tank was designed to collect water from the right-side edgedrain (Figure 18). The terms “left” and “right” side are used based on the direction of these pipes when an individual faces north at the site. Figure 19 shows a close-up of the typical drainage system in each section. As can be seen in Figure 19, when facing the tanks directly, the tank designed to collect water from the left-side edgedrain was always located to the right of the right-side edgedrain’s tank. In all sections, the grade of each edgedrain was designed to be 2%. Based on preliminary estimations, it was determined that each edgedrain will be connected to a 100-gallon collection tank, allowing for a reasonable amount of water to be collected before the tanks had to be sampled and emptied. The collection tanks were designed to contain a lid system that allowed excess water to spill out in cases where the tanks filled up before they could be emptied, preventing the tank from bursting. In Figure 19, the edgedrain pipes are represented by dash lines and designed to measure 4 inches in diameter; they are also perforated and corrugated in accordance with VDOT’s UD-4 detail. The collection pipes connected to the edgedrains are designated by solid lines in Figure 19, and these pipes are also designed to be 4 inches in diameter but as smooth PVC pipes.

Figure 19 also shows the location of the divider curbs on the ends of each section. The design details of these divider walls and the geomembrane to hydraulically separate the base course from the subbase are shown in Figure 20. The divider walls were designed to be at least 12 inches deep (2 inches keyed into the subbase) and cast in place as non-reinforced concrete. The geomembrane was designed with a 40-mil high density polyethylene (HDPE) to allow ease

of handling during construction. Figure 19 also shows a feature referred to as the “lysimeter pan.” This feature was added into the design as an additional way of collecting water from each section. This is not a feature of a typical roadway, and the intention was not to promote the inclusion of such a feature in future roadway designs. The lysimeter pan was designed to allow for the collection of the infiltrated water within each base course without going through the corrugated edgedrain pipes. It was designed as an experimental feature, and a collection pipe system from the lysimeter pan was designed to connect to a 45-gallon tank.

Figure 21 shows typical cross sections of the collection pipe systems designed to convey water from both left- and right-side edgedrains and the associated T connectors allowing for borescope surveying of the drainage pipes. The design was made to strictly convey all infiltration water based on gravity, and the slope grades were no less than 2%. The elevations shown in Figure 21 only apply to the example presented. During design, ground elevations were determined separately for each section.

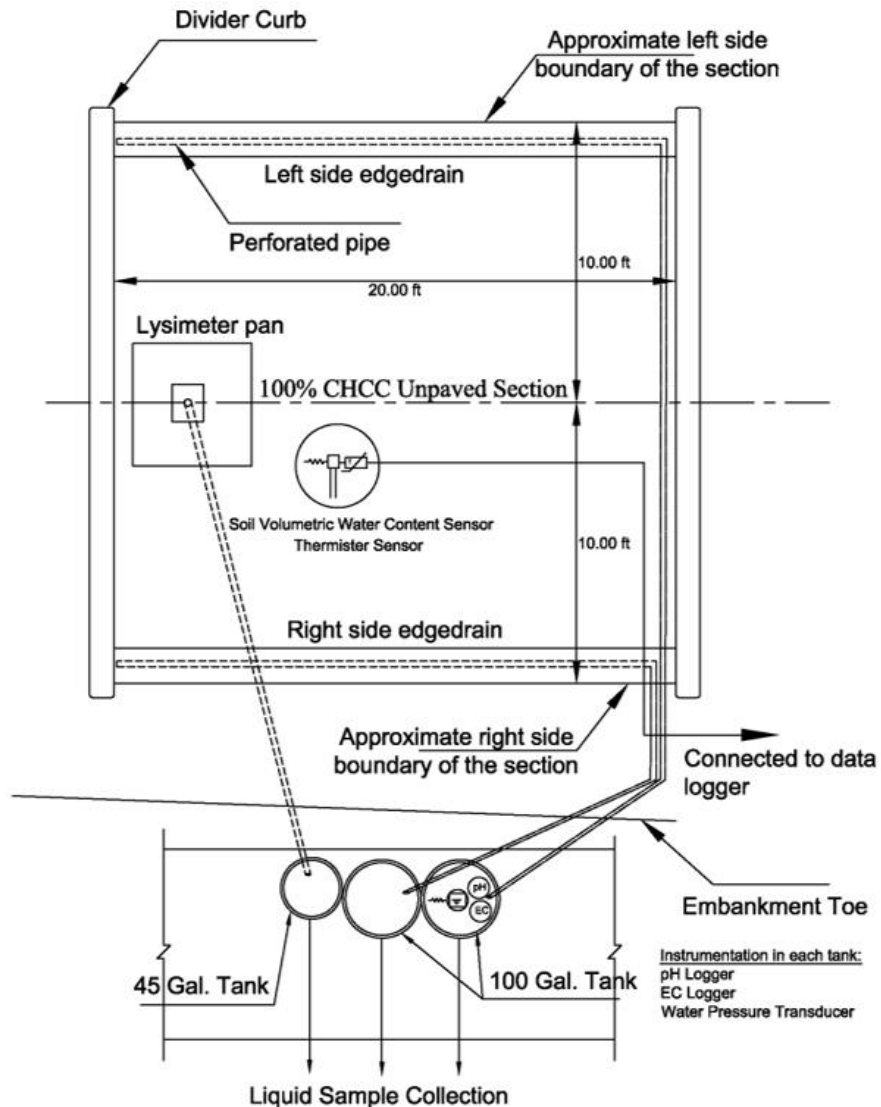


Figure 19. Plan view of a test section drainage system

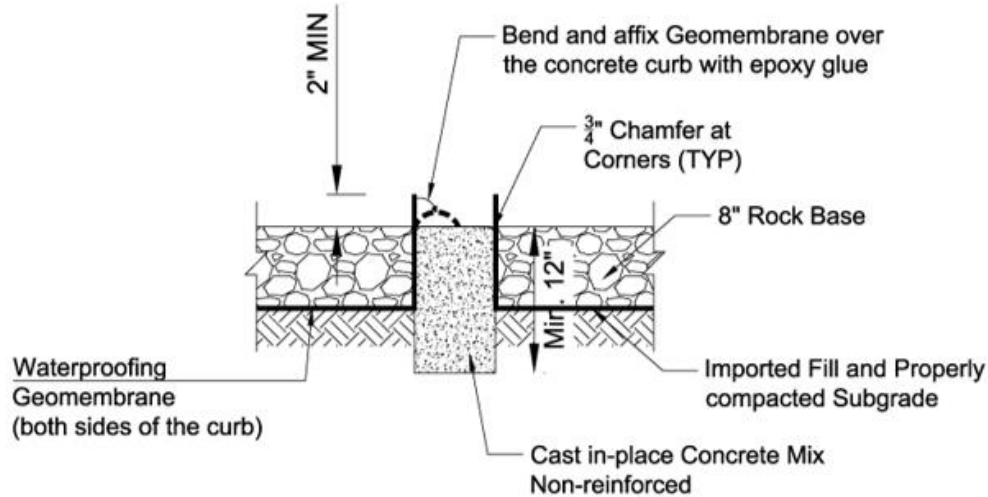


Figure 20. Details of the divider curb wall and geomembrane in each test section

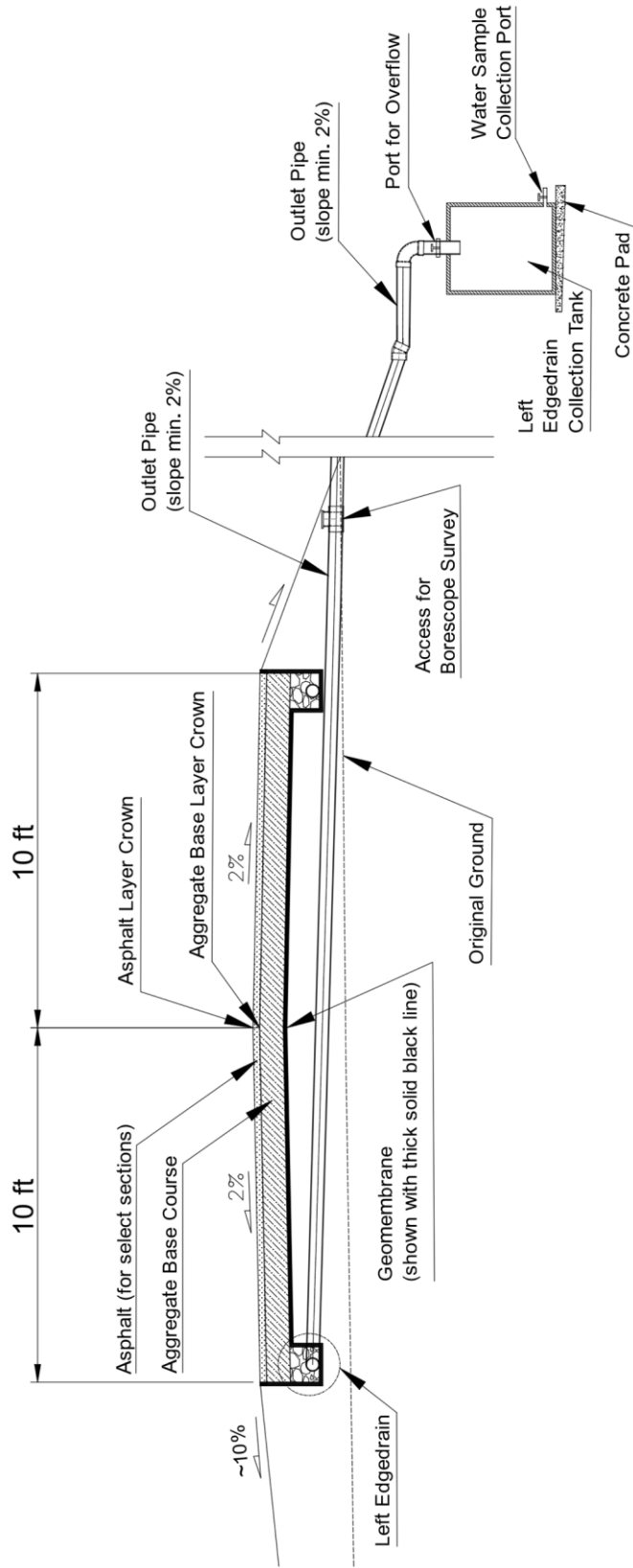
## Characterization of the Materials Used at the Test Site

### Base Course Aggregate

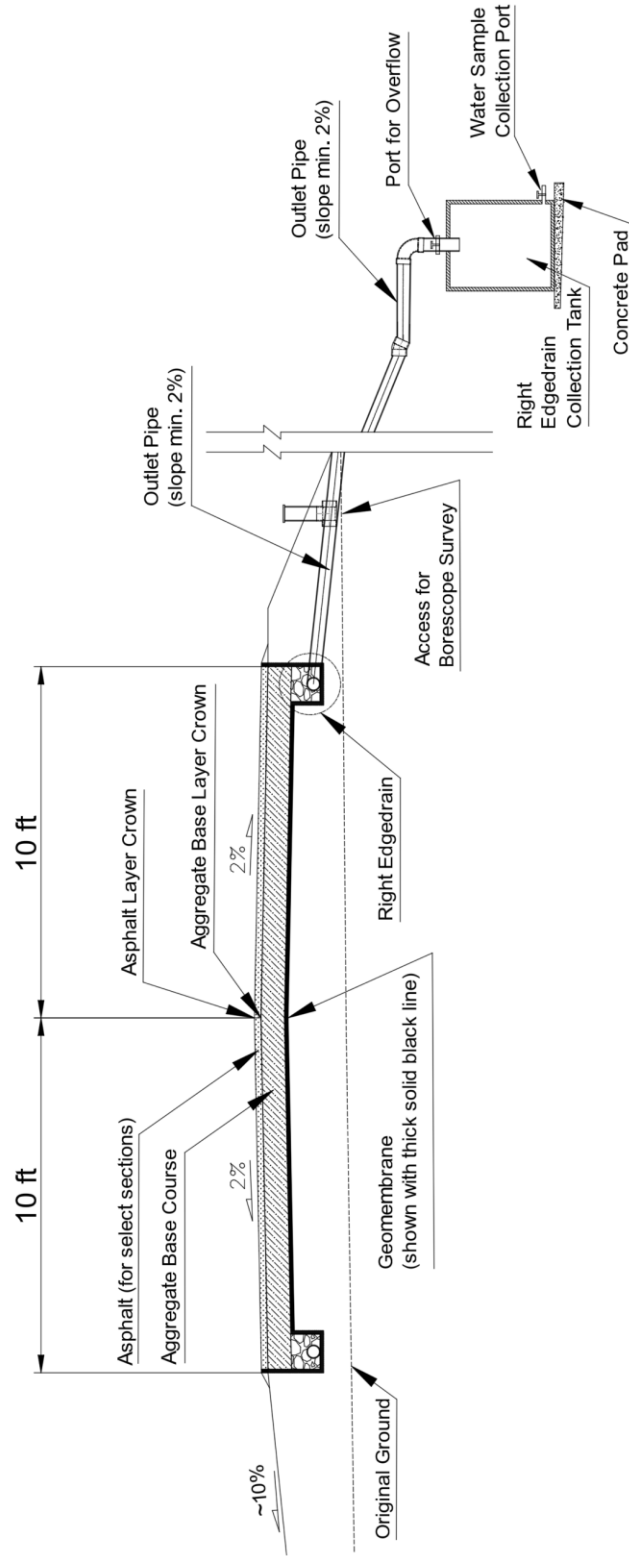
At the initiation of the project, the closest plant that was able to produce and properly mix CHCC and V.A. was located in Rockville, Virginia and operated by Luck Stone. Therefore, for this project, VDOT decided to procure all the base course aggregates from this plant.

The GMU team observed and documented the production of CHCC and the blending of CHCC and V.A. In this study, Blend 1 had a target of 40% CHCC, while Blend 2 had a target of 20% CHCC in the mixture. To produce Blend 1, Luck Stone mixed 38 tons of CHCC with 57 tons of V.A. in a pugmill to generate 95 tons of Blend 1 material. Similarly, 19 tons of CHCC material was mixed with 76 tons of V.A. to also produce 95 tons of Blend 2.

To ensure the accuracy and repeatability of the results, repeat tests (duplicates and triplicates tests) were conducted on all material characterization, and the results are presented herein. Figures 22 and 23 present the grain size distribution of 100% CHCC, 100% V.A., Blend 1 (40% CHCC + 60% V.A.), and Blend 2 (20% CHCC + 80% V.A.). As can be seen in these figures, the grain size distribution of all the materials fit into the boundaries of the VDOT 21A aggregate. However, the fines content varied noticeably among the different materials. The average percent passing the No. 200 sieve was approximately 7% for 100% V.A. and 10% for 100% CHCC. The average fines content of Blends 1 and 2 were determined to be 9% and 8%, respectively. These values were expected since the blends were created by mixing CHCC and V.A. The Atterberg's limits test results showed that all the materials were non-plastic. All materials were classified as well-graded sand and gravel with silt in accordance with the unified soil classification system (ASTM D2487, 2011). Table 1 summarizes all other physical and mechanical properties of the tested materials.



(a)



(b)

Figure 21. Typical details of the collection pipe systems from (a) left- and (b) right-side edgedrains at a test section

Table 1 shows that 100% CHCC had significantly higher water absorption, lowered permeability, and highest mortar content. This was expected as CHCC's mortar content makes it hydrophilic, which affects its water absorption and permeability (VTRC 21-R12, 2020).

All base course samples were also tested for elemental concentrations to determine the base line suite of the elements. Test results were obtained from the batch mixing of solid to de-ionized water (liquid) (S:L) ratio by mass of 1:20. Although the S:L ratio may not reflect actual field conditions; the results were used to evaluate the concentrations of elements compared to each other to evaluate the make-up of these materials. Elements that were tested included but were not limited to Aluminum (Al), Ca, Chromium (Cr), Copper (Cu), Iron (Fe), Potassium (K), Magnesium (Mg), Sodium (Na), Silicon (Si), Zinc (Zn), and sulfur (to represent sulfate ion,  $\text{SO}_4^{2-}$ ). Table 2 presents the results of these chemical analyses. The measured concentrations of elements from blended samples fall in between CHCC and V.A., which is expected behavior.

The V.A. produced in the Rockville plant is classified by the Luck Stone company as a metavolcanic rock with visible feldspar and quartz content (Luck Stone web site, <https://www.luckstone.com/locations/rockville-plant>). The CHCC data in Table 2 show high amounts of Si, indicating that the parent rock of the CHCC is also likely felsic metavolcanic in origin. The United States Geological Survey (USGS) describes majority of the rocks in Hanover County, where Rockville is located, as interlayered amphibolite and amphibole gneiss, pelitic-composition gneiss, calcsilicate gneiss, biotite hornblende-quartz-plagioclase gneiss, and garnetiferous leucogneiss (USGS, <https://mrdata.usgs.gov/geology/state/fips-unit.php?code=f51085>). This indicates that the region has a complex geology, and some of the geologic units may contain calcsilicate composition.

Previous studies have shown that among the elements found in base course aggregate leachate, calcium and sulfate ions are one of the most important (major), contributing to the formation of tufa from CHCC (Abbaspour and Tanyu, 2019a, 2020a, 2021; Tanyu and Abbaspour, 2020). The leached concentrations of Ca and  $\text{SO}_4^{2-}$  in CHCC shown in Table 2 are within the range observed in the previous laboratory study (VTRC 21-R12, 2020). However, the concentrations of leached Ca from V.A. were higher than those observed from the 100% diabase aggregate that was used in the previous laboratory study (VTRC 21-R12, 2020). This confirms that the V.A. used in this field study had some calcareous content, which has been noted in the literature for metavolcanic rocks in some parts of Virginia (as stated by USGS). A data sheet posted on Luck Stone's website also confirms that the rock quarried in the Rockville plant contains some amount of Ca (present in the form of calcium oxide). When V.A. was treated with hydrochloric acid, a limited fizzing effect was observed and weight loss in the order of 2.5% was noted. All of these observations confirm that the V.A. used in this study had slight calcareous and carbonate contents. However, the potential calcsilicate composition of the V.A. was an opportunity for this research to evaluate the precipitation potential of calcium-based compounds from a natural aggregate in Virginia.

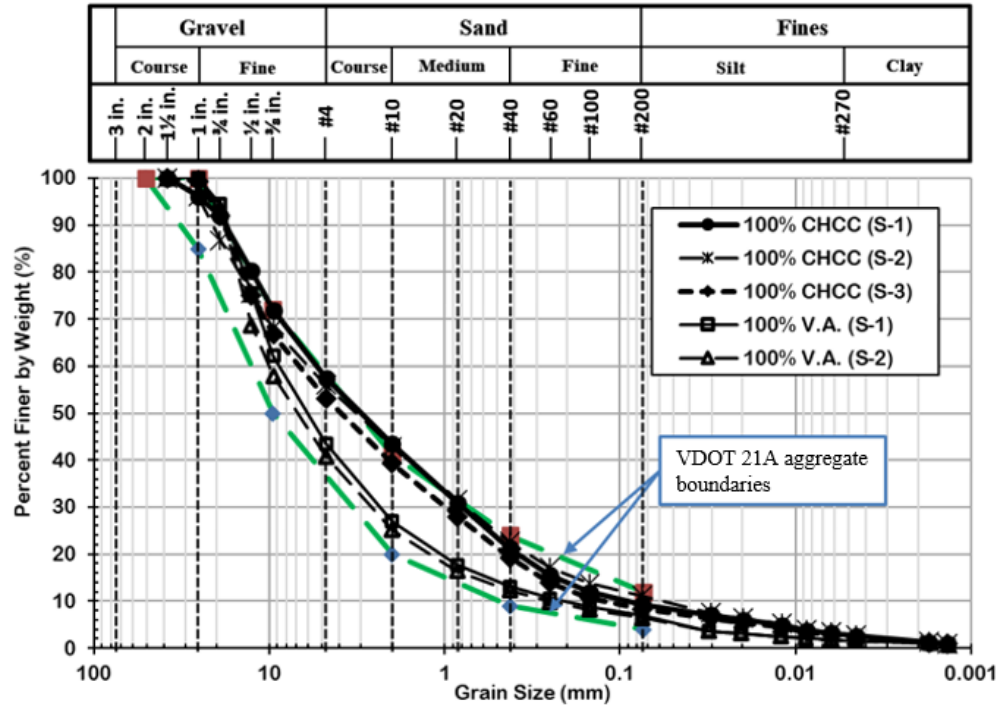


Figure 22. Grain size distribution of 100% CHCC and 100% V.A.

### Nonwoven Geotextile

The geotextile selected for constructing VDOT’s UD-4 underdrain system in this study was the Mirafi 140N (55mil), which is a nonwoven polypropylene material and meets the VDOT requirements for geotextiles to be used for drainage systems outlined in VDOT Specifications Section 245.03 (c). Properties of the selected geotextile, as reported by the manufacturer, are listed in Table 3. The geotextile was purchased from Ferguson Enterprises, Inc.

Although the manufacturer had already reported the permittivity of the geotextiles used in this study, the permittivity of each virgin geotextile was tested after each geotextile exhumation from the field to minimize the errors that may occur during evaluations. This approach resulted in 14 test values, which ranged from 1.02 to 1.30 sec<sup>-1</sup>. Knowing the thickness of the geotextile, the permeability of the geotextile was also calculated for each condition and ranged from 0.11 to 0.14 cm/sec. The range of calculated geotextile permeability values were at least an order of magnitude higher than the V.A. and three to four orders of magnitude higher than CHCC (see Table 1).

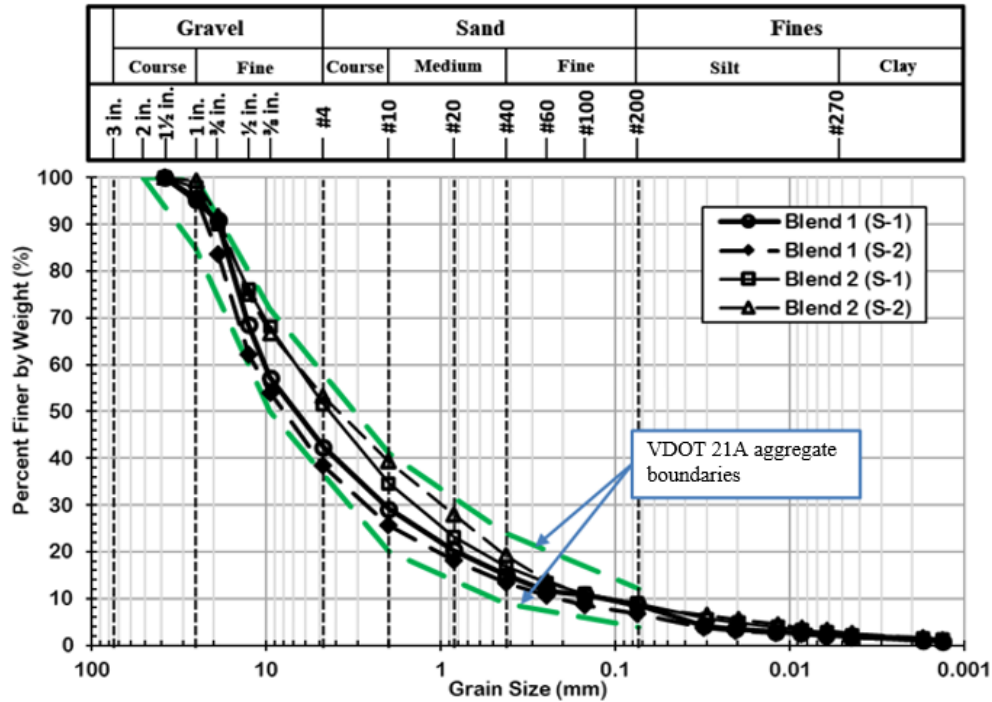


Figure 23. Grain size distribution of Blend 1 (40% CHCC + 60% V.A.) and Blend 2 (20% CHCC + 80% V.A.)

Table 1- Properties of the unbound base material used in this study

<i>Properties</i>	<i>100% CHCC</i>	<i>Blend 1</i>	<i>Blend 2</i>	<i>100% V.A.</i>
Specific Gravity of the Coarse Aggregate (per ASTM C127)				
Specific Gravity (OD)	2.23	2.50	2.57	2.65
Specific Gravity (SSD)	2.39	2.56	2.62	2.66
Apparent Specific Gravity	2.65	2.67	2.68	2.69
Water Absorption (%)	7.10	2.50	1.60	0.60
Specific Gravity of the Fine Aggregate (per ASTM C128)				
Specific Gravity (OD)	1.86	2.25	2.27	2.46
Specific Gravity (SSD)	2.16	2.41	2.43	2.56
Apparent Specific Gravity	2.64	2.69	2.70	2.72
Water Absorption (%)	15.70	7.60	7.20	4.20
Atterberg Limits (per ASTM D4318)				
Liquid Limit (%)	37	24	21	18
Plastic Limit (%)	36	24	20	17
Plasticity Index (%)	N.P. <sup>1</sup>	N.P.	N.P.	N.P.
Average Percent Passing #200 Sieve	10	9	8	7
Compaction Using Standard Effort (per ASTM D698)				
$\omega_{opt}$ (%)	16.0	9.4	8.2	8.0
$\gamma_{dmax}$ (pcf)	112.68	131.14	133.68	136.87
Permeability (per ASTM D2434) <sup>2</sup> (cm/s)	$7.3 \times 10^{-4}$	$8.6 \times 10^{-3}$	$2.9 \times 10^{-3}$	$6.3 \times 10^{-2}$
Mortar Content (%)	26.9	19.0	8.2	$2.5^3$

Notes:

1. N.P. = non-plastic
2. Permeability values are measured under an applied hydraulic gradient of 1
3. This value is not referred to as mortar content but is related to weight loss due to acid treatment

**Table 2. Results of the batch leach testing of the base course materials used in this study**

<i>Element</i>	<i>Concentration (or Unit)</i>	<i>Minimum Detection Limit</i>	<i>100% CHCC</i>	<i>Blend 1 (40% CHCC)</i>	<i>Blend 2 (20% CHCC)</i>	<i>100% V.A.</i>
Al	µg/l	0.1	85	216	633	913
B	µg/l	0.1	47	22	12	7
Ba	µg/l	0.1	64	91	170	192
Ca	mg/l	0.1	38	22	14	7
Cr	µg/l	0.5	68	34	7	3
Cu	µg/l	0.1	9	5	5	4
Fe	µg/l	10	12	31	87	136
K	mg/l	0.1	5	3	1	1
Mg	mg/l	0.1	3	2	1	1
Na	mg/l	0.1	7	6	7	6
Si	µg/l	40	6052	4312	3070	1964
SO <sub>4</sub> <sup>2-</sup>	mg/l	0.1	57	33	14	6
Zn	µg/l	0.5	4	5	7	6
pH	-	-	11.3	10.9	10.8	9.82
EC	µS/cm	-	487	347	293	289

**Table 3. Properties of the nonwoven geotextile used in the construction of the test sections (manufacturer values)**

<i>Mechanical Properties</i>	<i>Test Method</i>	<i>Unit</i>	<i>Minimum Average Value</i>
Grab Tensile Strength	ASTM D4632	kN (lbs)	0.53 (120)
Grab Tensile Elongation	ASTM D4632	%	50
Trapezoid Tear Strength	ASTM D4533	kN (lbs)	0.22 (50)
Puncture Strength	ASTM D4833	kN (lbs)	0.30 (65)
CBR Puncture Strength	ASTM D6241	kN (lbs)	1.33 (300)
Apparent Opening Size (AOS)	ASTM D4751	mm (U.S. Sieve)	0.212 (70)
Permittivity	ASTM D4491	sec <sup>-1</sup>	1.7
Permeability	ASTM D4491	cm/sec	0.21
Flow Rate	ASTM D4491	l/min/m <sup>2</sup> (gal/min/ft <sup>2</sup> )	5500 (135)

## Asphalt Overlay

Asphalt overlay was produced by Weatherman Collins Contracting, LLC located in Raphine, Virginia. Three 4-inch circular asphalt samples were collected immediately after its placement in the field for permeability testing (Figure 24a). A constant head hydraulic conductivity device was used to measure the permeability of the asphalt layers (Figure 24b). The

measured hydraulic conductivity of the asphalt samples is shown in Figure 25. The average hydraulic conductivity at a hydraulic gradient of 1 was  $3.7 \times 10^{-2}$  cm/sec.

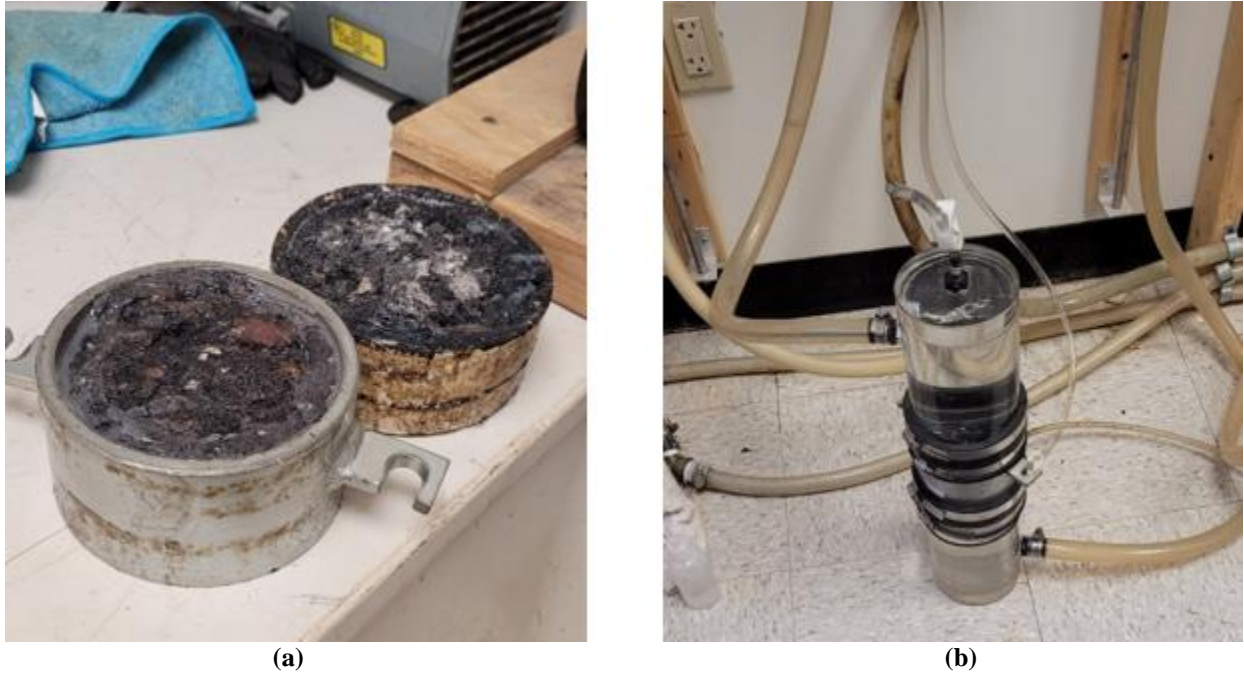


Figure 24. (a) and (b) 4-inch asphalt samples placed into a rigid wall permeameter for permeability testing under constant head conditions

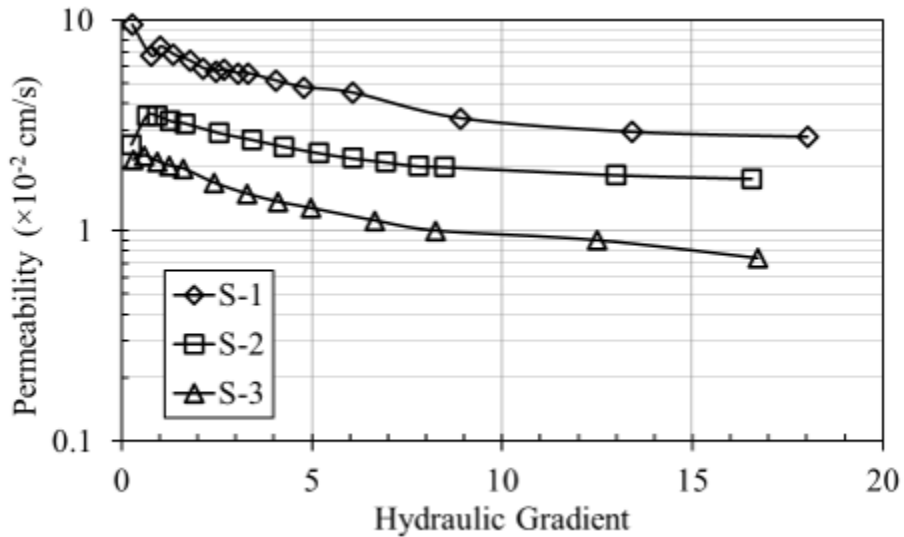


Figure 25. Measured permeabilities of the asphalt samples

The permeability of the asphalt used in this study was higher than the desired range of asphalt permeability cited in the VTRC 21-R11 report (McGhee and Smith, 2020) but comparable to the permeability of the aggregate base course used in this study (Table 1). This condition allowed more water to infiltrate the asphalt than that may typically occur in roadways

constructed by VDOT. Having a higher permeable asphalt layer allowed the research to better assess the potential of fines migration and chemical precipitation from an unbound base course aggregate that may contain CHCC.

The bitumen in asphalt overlay is known to be hydrophobic (Yadykova and Ilyin, 2022). Regarding rainwater infiltration, a combination of high permeability and hydrophobic property may result in complex conditions, especially in this study where the asphalt mixture was placed directly over the base course without any prime. Based on the determined average hydraulic conductivity of the asphalt in this study, during high-intensity rainfalls, runoff may occur, but during the low-intensity rainfalls, it is possible for notable infiltration to take place through the asphalt layer.

### **Construction of the Test Site**

A bird's eye view of the completed test site is shown in Figure 26 as obtained from Google Maps©. The construction of the site was conducted in accordance with the intended steps as described in the methods section.

The following describes the steps involved in the construction of the test site:

- First, the site was prepared for construction, organic soil was removed, and the subgrade was prepared for the placement of subbase.
- Next, the crusher run was placed to create a subbase for the test site and establish 2% grades from one end of the test site to the other (Figure 27).
- Then, the subbase was excavated according to the divider curb wall locations; the concrete form was installed, and concrete was poured to create the curb wall dividers (Figure 28).
- The sides of each section were roughly excavated to create locations for installing the edgedrain systems and connecting the left-side edgedrain pipes with smooth collection pipes (Figure 29).
- The collection pipes (4-inch smooth PVC pipes) were then installed (Figure 30). The pipe that is buried under the subbase in the left side of the photo in Figure 30 is the pipe attached to the left-side edgedrain pipe. The open end of the pipe on the right side is waiting to be attached to the perforated, corrugated right-side edgedrain pipe.
- A geomembrane hydraulic barrier was installed in each section (Figure 31).
- UD-4 edgedrain installation, including placement of nonwoven geotextile, installation of the perforated corrugated pipes (which were connected to the collection pipes), placement of No. 57 stone, and wrapping of the nonwoven geotextile over the No. 57 stone, was done (Figure 32).
- Lysimeter pans constructed with LDPE 30-mil geomembrane liners overlain by geocomposite drainage sheets were installed.

- Placement of the unbound base course with different materials in each section, moisture conditioning, compaction, and density/moisture content confirmation were done (Figure 33). All base course materials in each section were compacted to at least 95% of the maximum dry density obtained using standard effort laboratory tests (VDOT VTM 1, 2017).



**Figure 26. A Google earth© photo of the completed test site showing the locations of the three paved and four unpaved sections and the collection water tanks adjacent to the site located downslope**

- Preparation of the subgrade, installation of the formworks, and pouring of concrete for the level pad in order to allow collection tanks to be placed at the bottom of the side slope were done (Figure 34).

- The borescope access T connectors and collection pipes were installed along the slope, and the collection pipes were connected to the tanks (Figure 35).
- Finally, an asphalt overlay was placed over the three sections.



**Figure 27. Placement of crusher run as subbase**



**Figure 28. Construction of curb wall dividers**



**(a)**



**(b)**

**Figure 29. Excavations of trenches to install (a) UD-4 edgedrains on both sides of each section and (b) collection pipes that will convey water from left-side edgedrain to collection tanks**



**Figure 30. Installation of collection pipes at the end of the edg drain trenches prior to the installation of the geomembrane liner**



**Figure 31. Installation of the geomembrane hydraulic barrier (a) covering the entire section, and (b) the pieces are being welded together**

Although the site construction took place over seven months (from May through December of 2020), the following dates summarize the most important milestones achieved during the construction:

- September 1<sup>st</sup> –100% CHCC and Blend 1 were placed into test Sections 1 and 2
- September 2<sup>nd</sup> – Blend 2 was placed into test Section 3
- September 8<sup>th</sup> –100% CHCC was placed into test Section 4
- September 15<sup>th</sup> –Blend 1 and Blend 2 were placed into test Sections 5 and 6
- September 16<sup>th</sup> –100% V.A. was placed into test Section 7
- October 7<sup>th</sup> – All unbound base course sections were moisturized and compacted
- October 20<sup>th</sup> – All edg drain systems and collection pipes were connected to the tanks



(a)



(b)



(c)



(d)

**Figure 32. Installation of the UD-4 edgedrains (a), installation of the connection port for the edgedrain and collection pipe, (b) placement of the nonwoven geotextile and perforated pipe, (c) placement of No. 57 stone, and (d) wrapping of the nonwoven geotextile over the stone**



(a)



(b)



(c)



(d)

**Figure 33. (a) Placement of the loose unbound base course, (b) moisture conditioning, (c) compaction, and (d) density/moisture content confirmation**



(a)



(b)



(c)

**Figure 34. (a) Removal of organic soil and preparation of subgrade to allow for the (b) construction of the concrete pad and (c) placement of one 45-gallon and two 100-gallon collection tanks at each section**



**Figure 35. Completion of the borescope T connectors along the slope and connection of the collection pipes and tanks at each section, located downslope from the test site**

From September 1<sup>st</sup> until the asphalt layers were placed, as soon as the construction of each test section was completed, that section was covered with plastic sheets (Figure 36).



**Figure 36. Plastic sheets being placed over the entire site until the placement of the asphalt overlay**

On December 1, 2020, Test Sections 1 (100% CHCC), 2 (Blend 1), and 3 (Blend 2) were paved by the Weatherman Collins Contracting team by placing surface mix directly over the base course (no prime placed) (Figure 37). During the first site visit after 6 months, the thickness of the asphalt layer was confirmed to be 2 inches, as intended during the design (Figure 38).

Immediately after the pavement operations were completed, the plastic sheets were removed from all sections, and data collection for the study officially started. This allowed the data collection from all sections to commence at the same time. Figures 39 and 40 show the finished test sections and connected collection tanks.



(a)



(b)

**Figure 37. Placement of (a) asphalt layer over the three sections and (b) compaction of the surface**



**Figure 38. Confirmation of the thickness of the paved asphalt sections**



**Figure 39. The completed paved and unpaved test sections**



**Figure 40. Completion of the connection of the collection tanks to the collection pipes, which are connected to the edg drains at each section**

## **Monitoring Programs at the Test Site**

### **Meteorological Data at the Test Site**

In this study, meteorological data were obtained from the weather station installed at the site and included rainfall, ambient temperature, and relative humidity recordings. Results from these recordings are presented below.

Figure 41 shows the maximum recorded daily rainfall at the site, as well as the calculated cumulative rainfall between December 1, 2020, and September 8, 2023. The data show that the site cumulatively received over 2240 mm (88 inches) of rain during the operation (y-axis on the left side). The highest daily rain events were observed between August and September 2021 (i.e., 62 mm; y-axis on the right side). The trends of rain data show that the selected site was appropriate for this study as no significant periods of drought were observed. According to the USGS website, when the daily precipitation reaches above 100 mm (4 inches), the rain event is considered to be of high intensity. Figure 41 shows that all the daily rain events at the test site were below 100 mm; therefore, they were categorized as frequent but of low intensity.

Figure 42 shows the ambient temperature recordings observed at the site. The data show that in different seasons, the ambient temperatures changed as expected. On average, the temperatures were highest around August to the beginning of September and lowest around February to the beginning of March. The maximum temperature recorded was 37.6°C (99.6°F), with the minimum at -20.1°C (-4.2°F). On average, the difference between the colder and warmer seasons was approximately 30°C (86°F). Based on the minimum temperature periods seen in Figure 42, it appears that the ground was exposed to freezing temperatures between December through March. The trends of temperature data show that the selected site was appropriate for this study because it was exposed to the climatic effects of the four seasons (no time in which one climatic condition dominated).

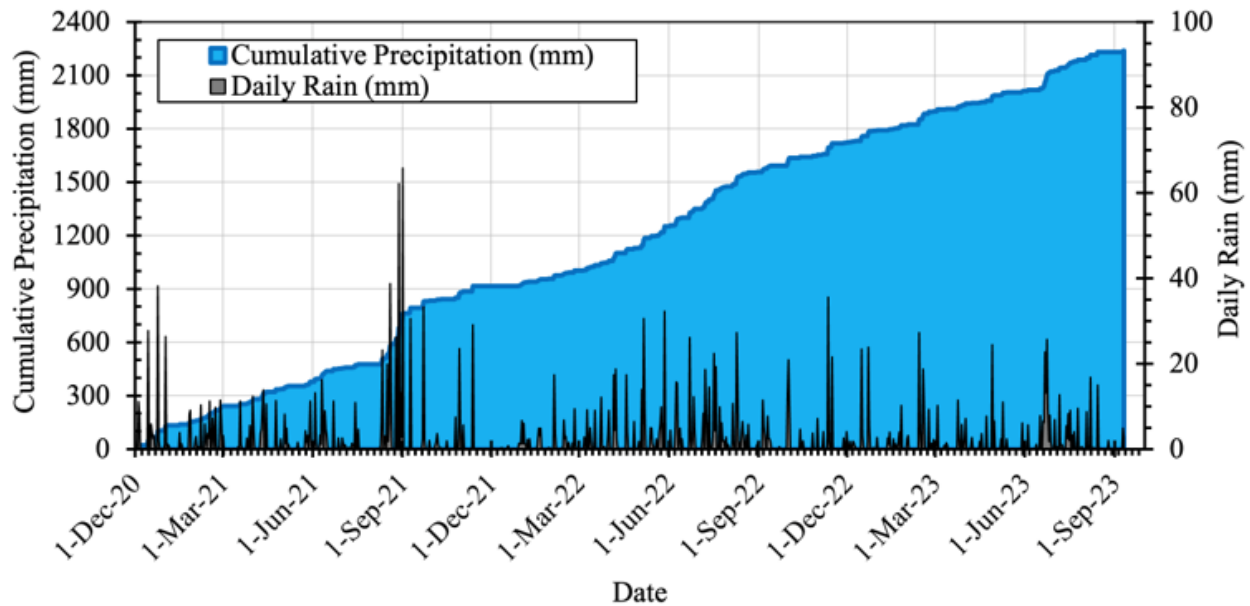


**Figure 41. Rainfall events and accumulated precipitation quantities for the site as recorded by the deployed weather station**

Figure 43 shows the recorded relative humidity (RH) data at the site. The data show that the ambient RH during the operation was mostly above 60%, with multiple peaks of above 95% throughout the wet seasons. During the driest periods, recorded RH values were between 30 and 50%. The carbonation rate of CHCC was found to be at its maximum at an RH of 40 to 80%, when the pores were moist (i.e., neither completely wet nor completely dry) (Kurdowski, 2014). The range of observed RH data shows that the selected site was appropriate for this study because most of the times, the observed RH values were favorable for the carbonation of CHCC (creating worst-case scenarios in terms of possible chemical precipitation of calcium-based compounds).

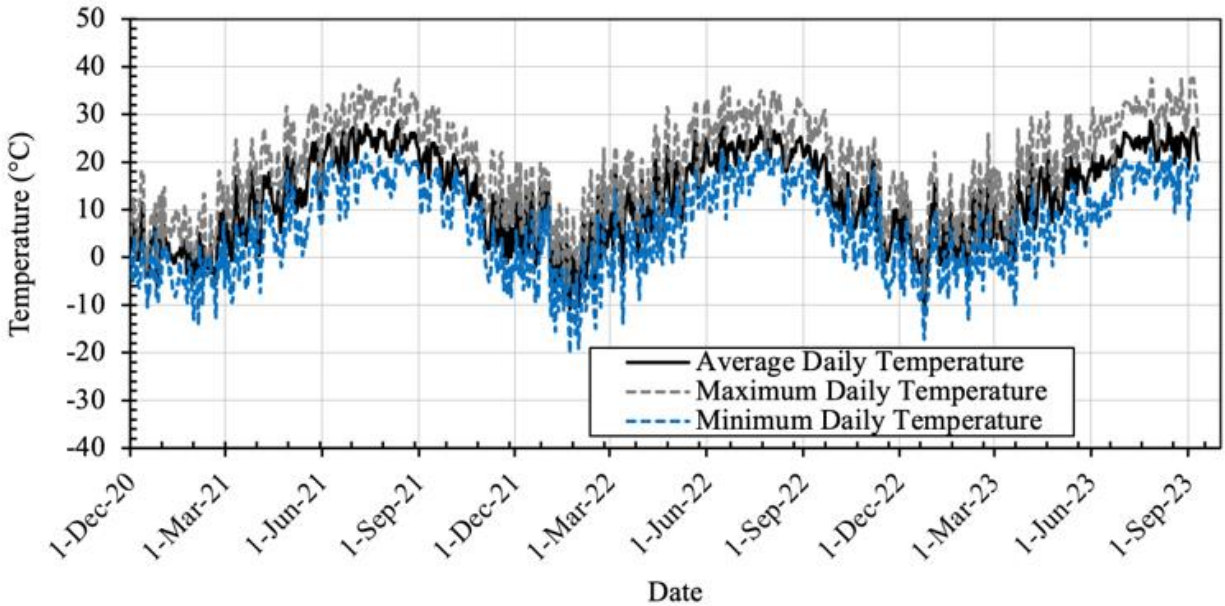


Figure 42. Average, maximum, and minimum daily temperature

### Instrumentation at the Test Site

Instrumentation and monitoring at the site were conducted by water content reflectometer/temperature sensors embedded into the base course of all sections, water level loggers placed into the water collection tanks of all sections, and pH and EC sensors placed only in the water collection tanks of the unpaved 100% CHCC section.

Figure 44 shows the data obtained from the water content reflectometer/temperature sensors embedded in each unpaved test section. The values shown represent the average conditions observed for a given day.

The temperature fluctuations of the ground seen in Figure 44 for all sections are very consistent and were expected based on seasonal changes. The data obtained from the embedded temperature sensors correlate well with the ambient temperatures observed at the site (Figure 42). Table 4 shows the maximum and minimum observed temperatures at each section during this study. Considering that the base course was only 20 cm (8 inches) thick and had no pavement layer, the similarities between the ambient and ground temperatures are expected. The data show that around February of each year, the ground temperatures were below freezing.

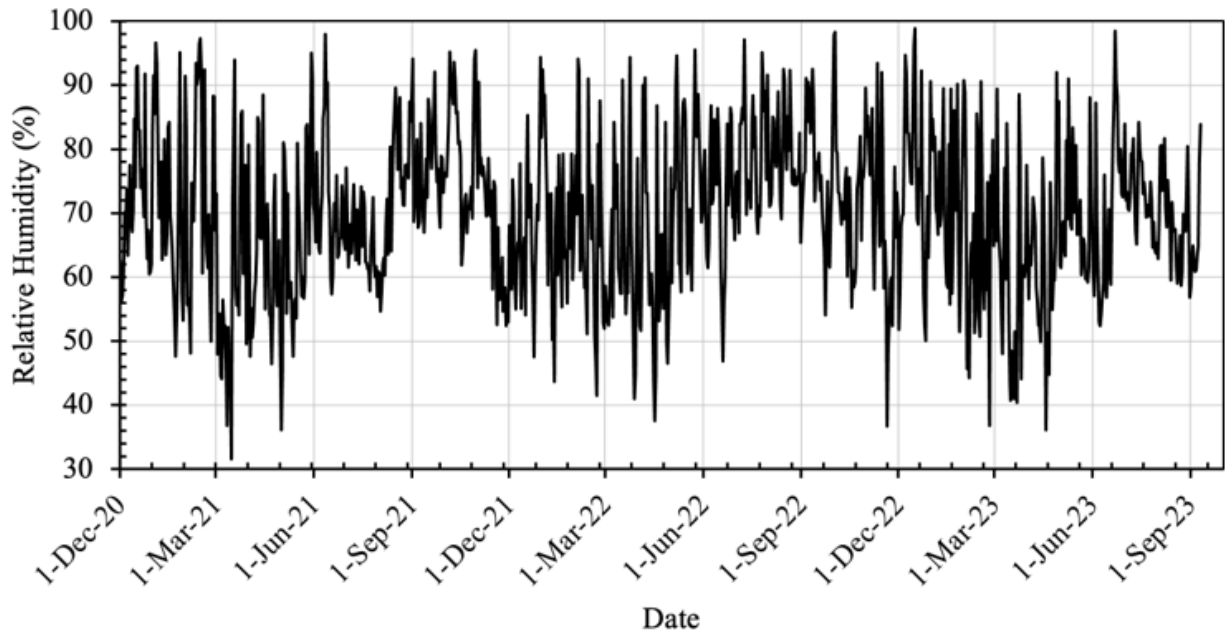
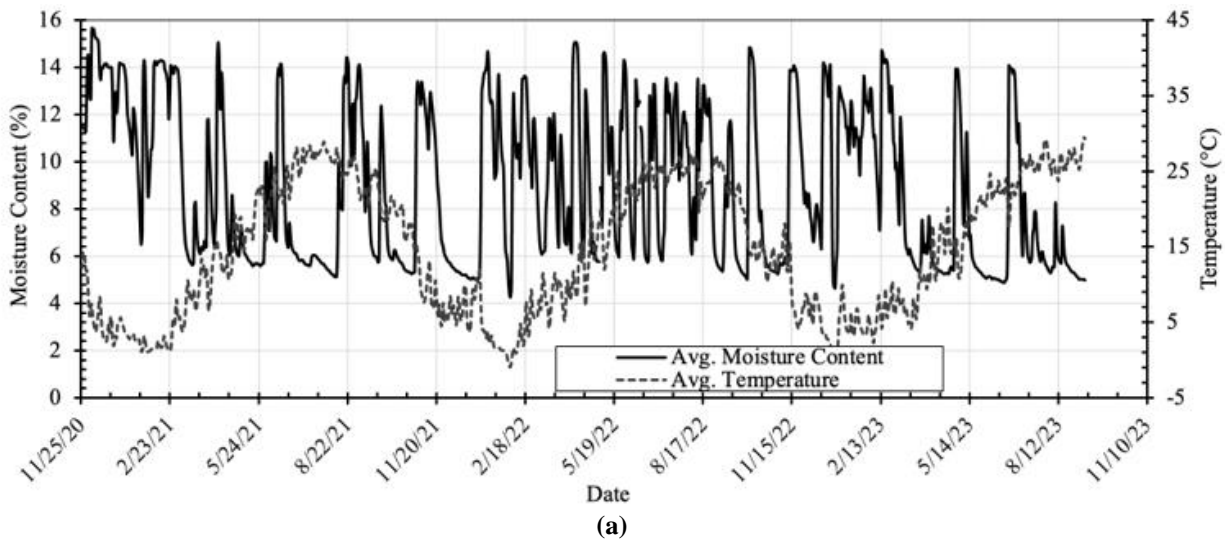


Figure 43. Recorded relative humidity at the test site



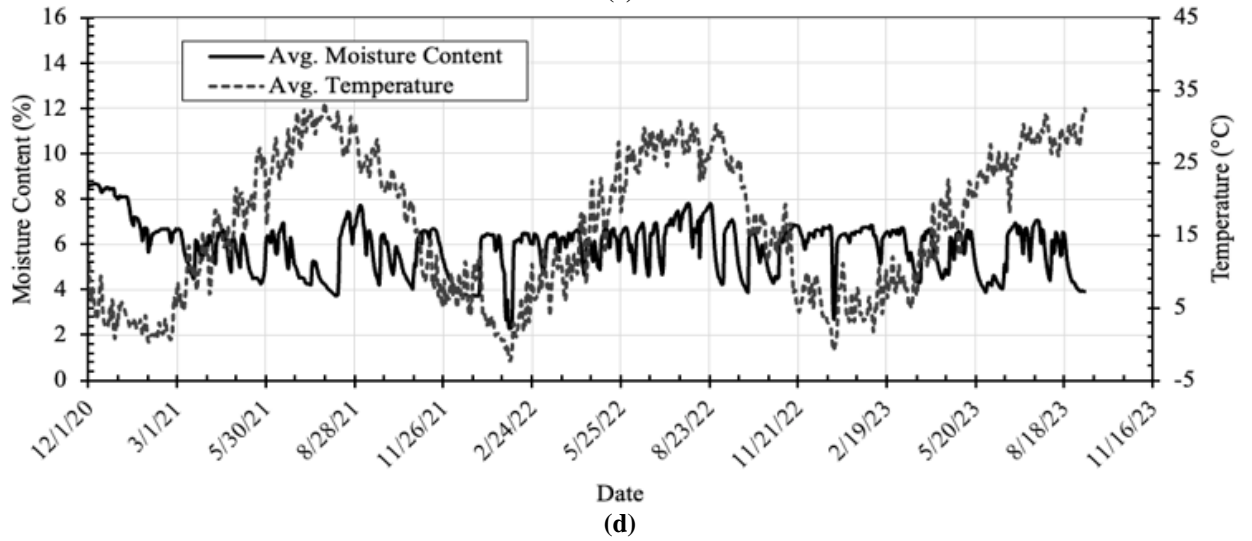
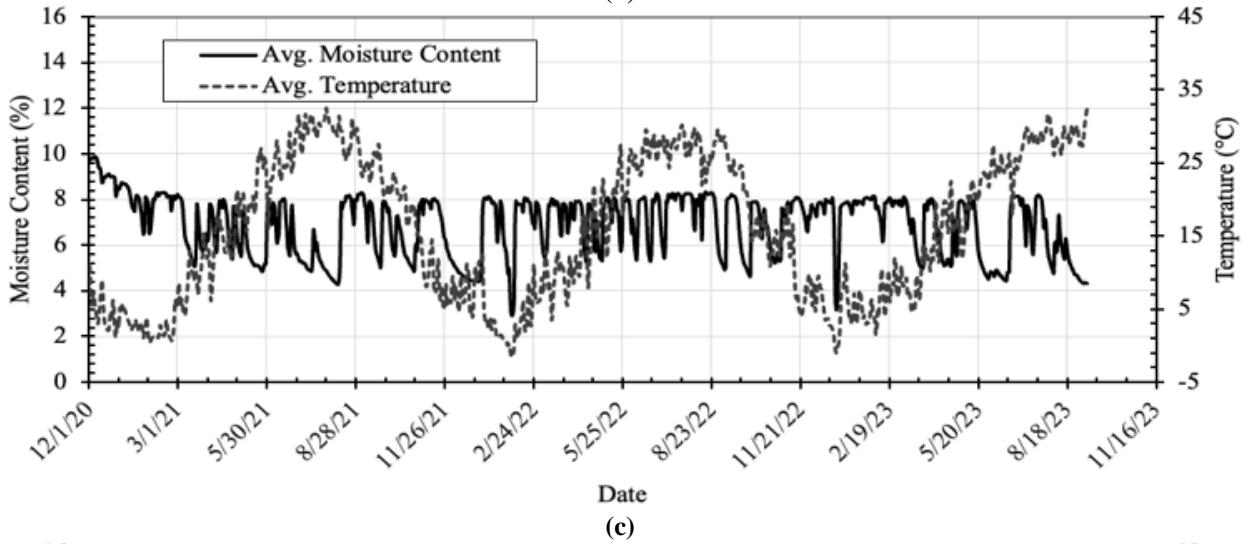
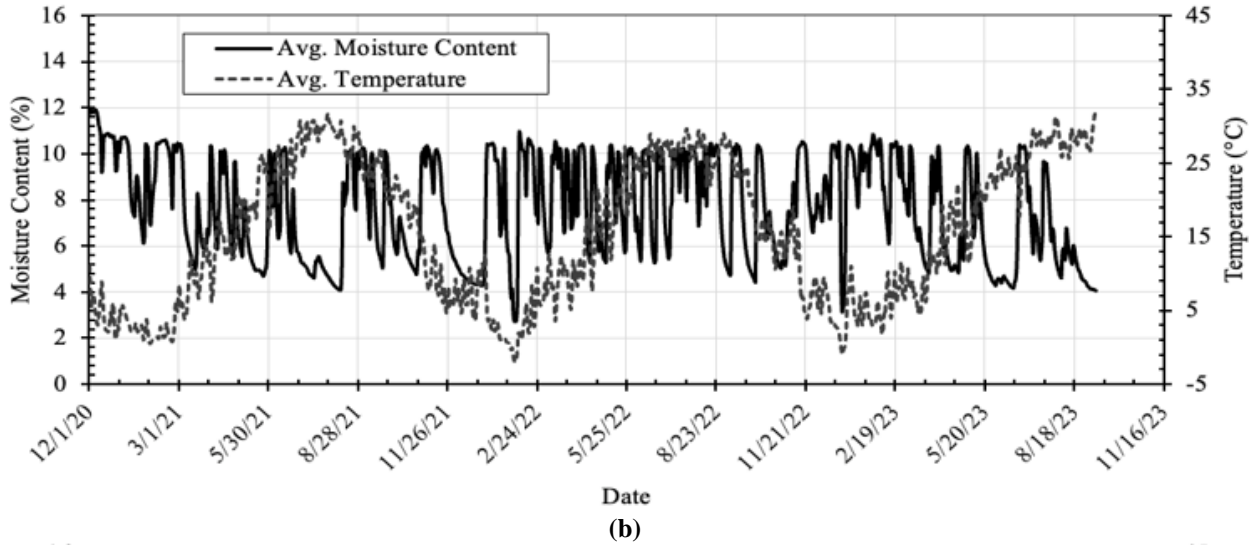


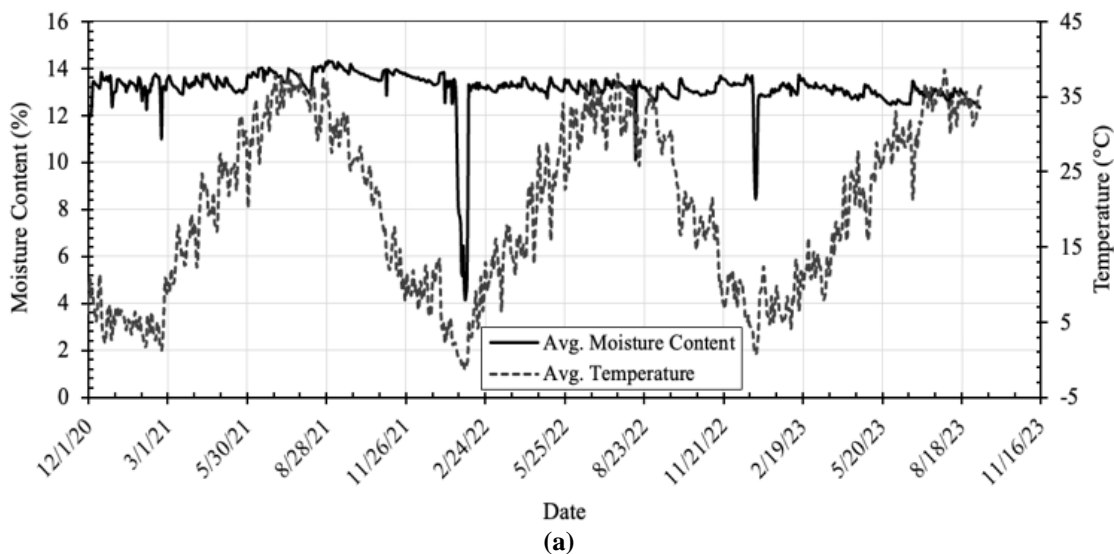
Figure 44. Daily average moisture content and temperature in the base course of the unpaved sections. (a) 100% CHCC, (b) Blend 1, (c) Blend 2, (d) 100% V.A.

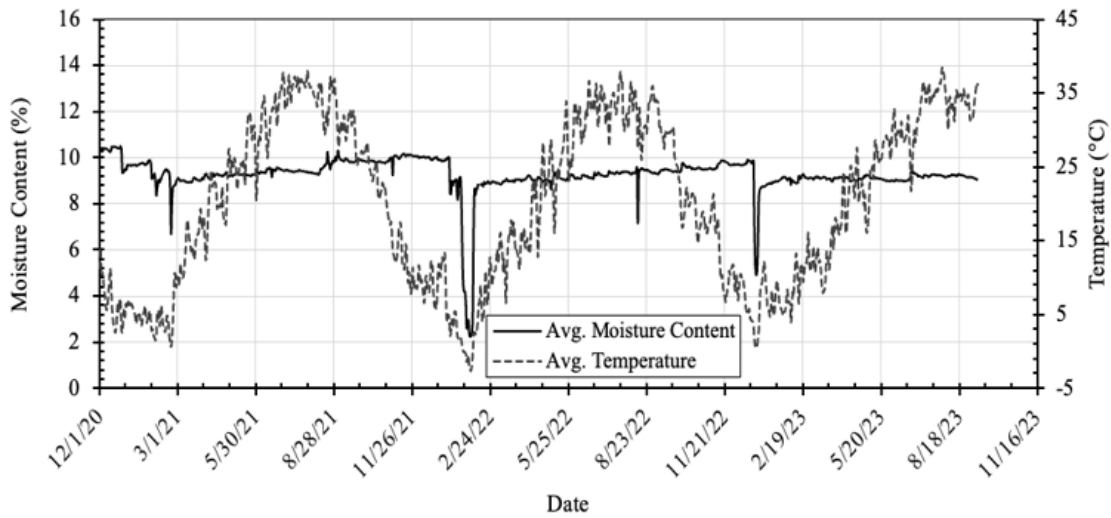
**Table 4. Comparison of typical ranges of temperature and moisture content fluctuations in unpaved sections**

<i>Section</i>	<i>Base Course Moisture Content (%)</i>	<i>Base Course Temperature (°C)</i>	<i>Ambient Temperature (°C)</i>
CHCC-U	6 to 13	-1 to 29	Avg. range of -8 to 30 (Max. 38)
Blend 1-U	6 to 10	-2 to 32	
Blend 2-U	6 to 8	-2 to 32	
V.A.-U	5 to 7	-2 to 33	

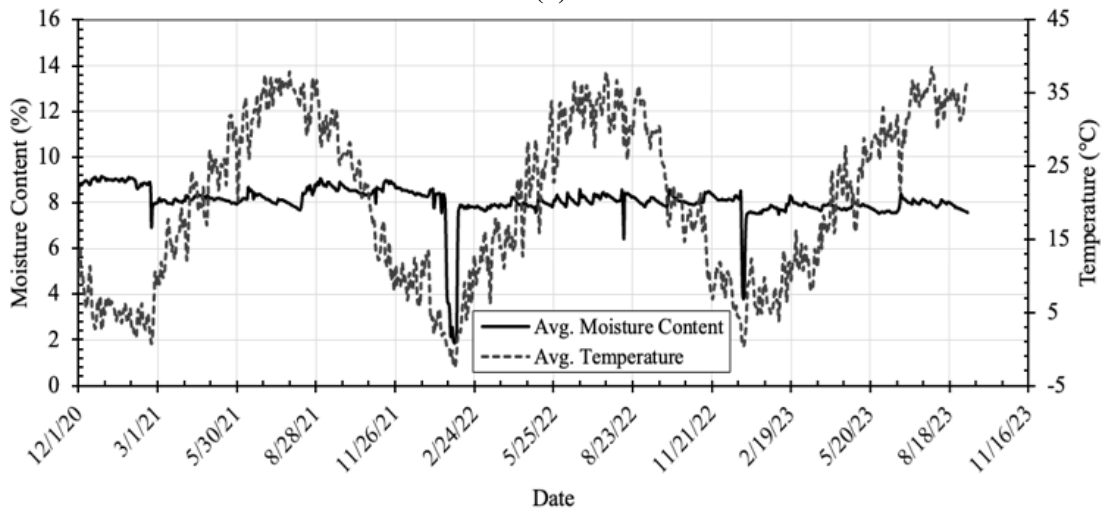
The moisture content data of each unpaved section (Figure 44) also fluctuated with time. These fluctuations correlated well with the rain precipitation (Figure 41) and ambient temperatures (Figure 42) observed at the site. This indicates that in the unpaved sections, rainwater infiltrated the base course. Table 4 summarizes the general trends observed at each section, as relates to minimum and maximum moisture content data. This comparison showed that the unpaved 100% CHCC section had the highest moisture content fluctuations while the 100% V.A. section had the lowest. These were expected behaviors since CHCC is known to be hydrophilic (Yunusa et al., 2022), meaning it tends to absorb and hold water. The moisture content ranges observed in Blends 1 (40% CHCC) and 2 (20% CHCC) correlated well with this expected behavior, where the moisture content fluctuations decreased with decreasing CHCC content. Figure 44 shows that when the ground freezes (around February) the moisture content values decrease considerably, as expected. The overall data showed the expected behaviors and confirmed the accuracy of the instrument measurements.

Figures 45 shows the data obtained from the water content reflectometers and temperature sensors embedded in each paved test section. Similar to those for the unpaved sections, the values shown for the paved sections also represent the average conditions observed for a given day.





(b)



(c)

**Figure 45. Daily average moisture content and temperature in the base course of the paved sections. (a) 100% CHCC, (b) Blend 1, (c) Blend 2**

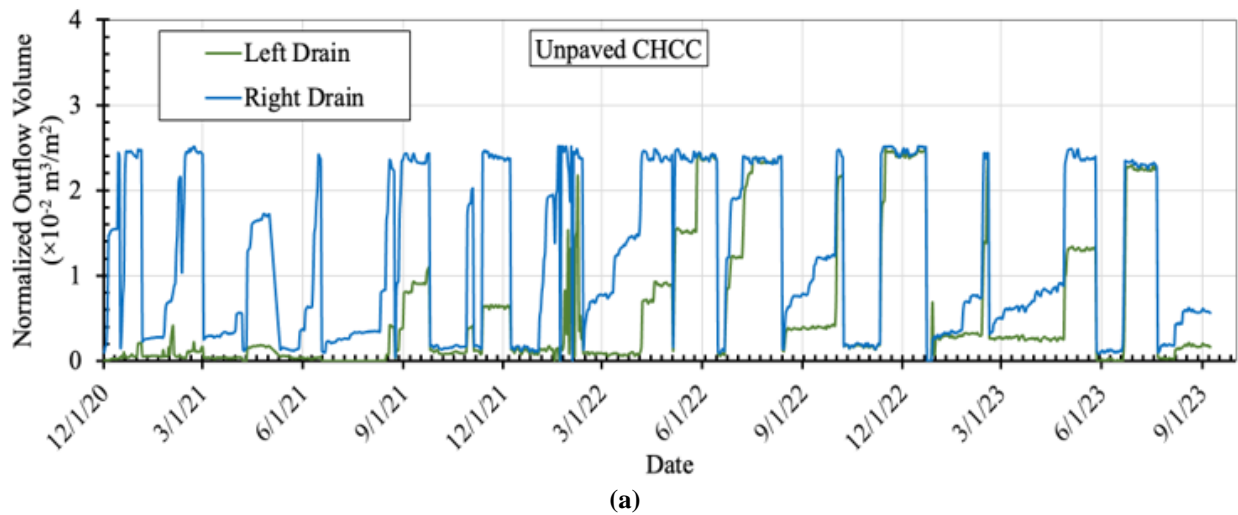
As observed in the unpaved sections (Figure 44), the temperatures shown in Figure 45 show that around February of each year, the ground freezes at the paved sections. During these times, the water contents show considerably lower values (as observed in the unpaved sections). However, in other times when the ground is not frozen, the data seen in Figure 45 is different than the data from Figure 44. In the paved sections, the moisture content fluctuations appeared to be less frequent than what was observed in the unpaved sections (Table 5). Figure 45 also shows that overall, the moisture content of the paved sections appeared to be higher for longer periods compared to that for the unpaved sections. These comparisons indicate that the base course of the unpaved sections went through more wetting and drying cycles compared to that of the paved sections.

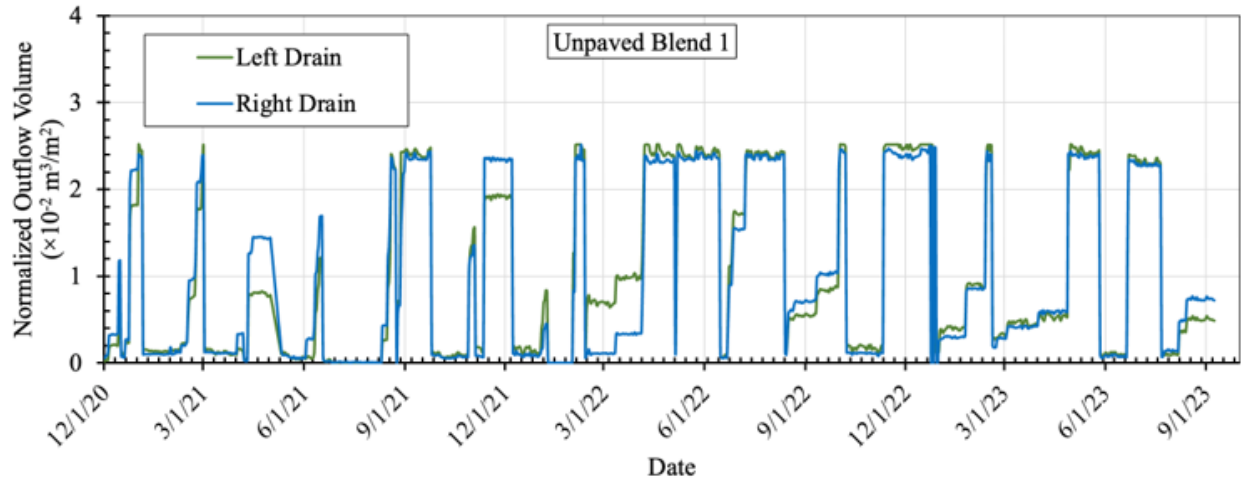
**Table 5. Comparison of typical moisture content fluctuations in the unpaved and paved sections with CHCC**

CHCC		Blend 1 (40% CHCC)		Blend 2 (20% CHCC)	
Unpaved	Paved	Unpaved	Paved	Unpaved	Paved
6 to 13	13 to 14	6 to 10	9 to 10	6 to 8	8 to 9

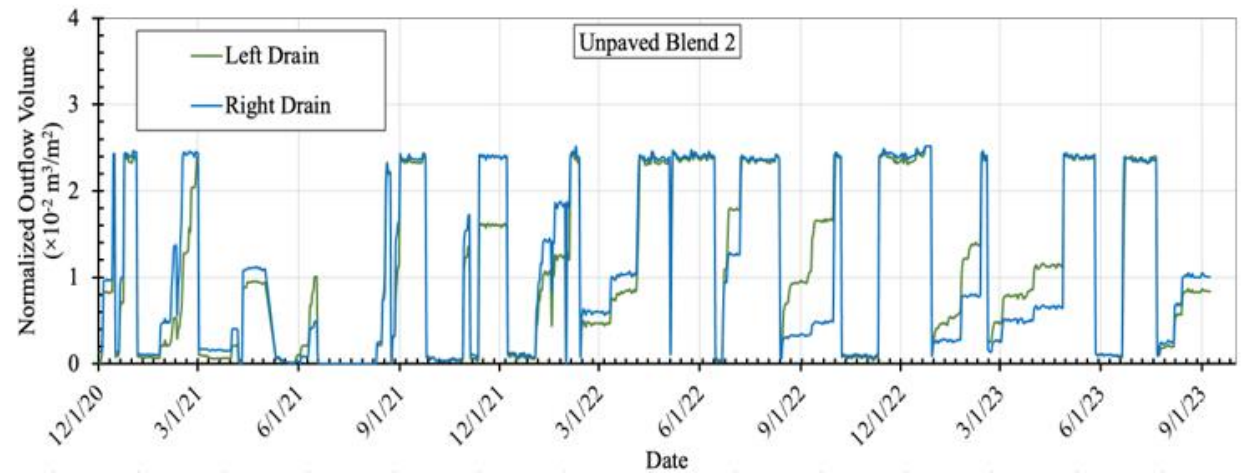
Figure 45 shows the fluctuations of the ground temperatures within the base course of each paved section. The temperature trends at the paved sections matched well with those at unpaved sections (Figure 44). However, in the paved sections, the minimum and maximum temperatures ranged between -2 and 36°C (35.6 and 96.8 °F), whereas in the unpaved sections, they ranged between -2 and 32°C (35.6 and 89.6 °F). This indicates that the base course material in the paved sections were generally warmer during moderate to warm seasons but were at the similar temperatures during winter. When the moisture content and temperature data from the paved and unpaved sections were collectively evaluated, the asphalt pavement appeared to act as a blanket, allowing the rainwater to infiltrate freely but not evaporate as freely. This resulted in higher moisture content for longer durations in the paved sections. Consequently, in the paved sections, the wetting and drying of the base course was limited compared to the unpaved sections.

Underdrain systems were constructed on both sides of each test section (Figure 32). Therefore, theoretically, each tank served to collect infiltrated rainwater from half of a given test section. Consequently, outflow volumes from each water tank were normalized based on the ratio of the volume of flow recorded within each tank (m<sup>3</sup>) to half of the square meter of each test section (m<sup>2</sup>). Figure 46 shows the normalized outflow volumes of each water tank serving as a collection point for the underdrain systems constructed on each side (left and right) of the unpaved test sections.

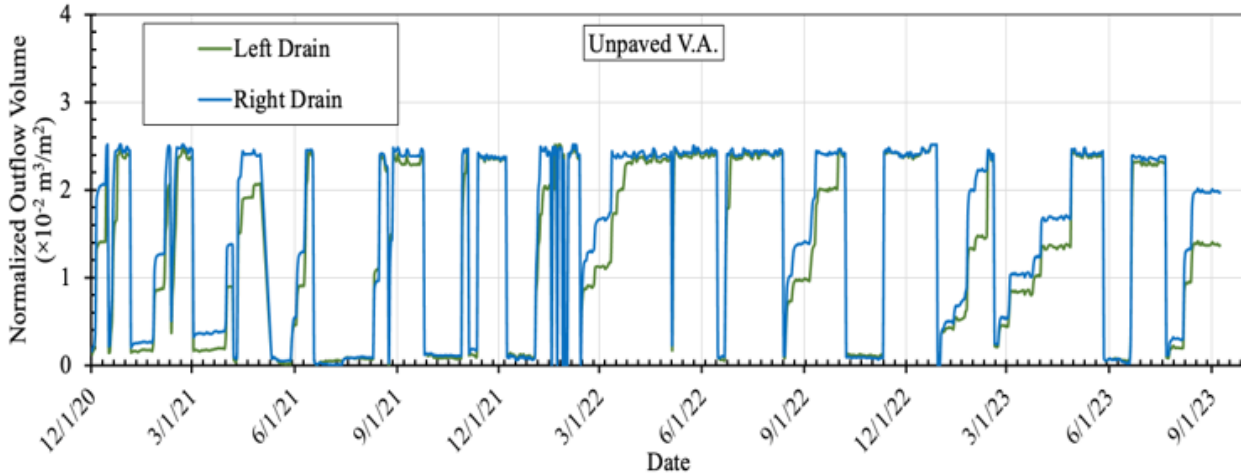




(b)



(c)



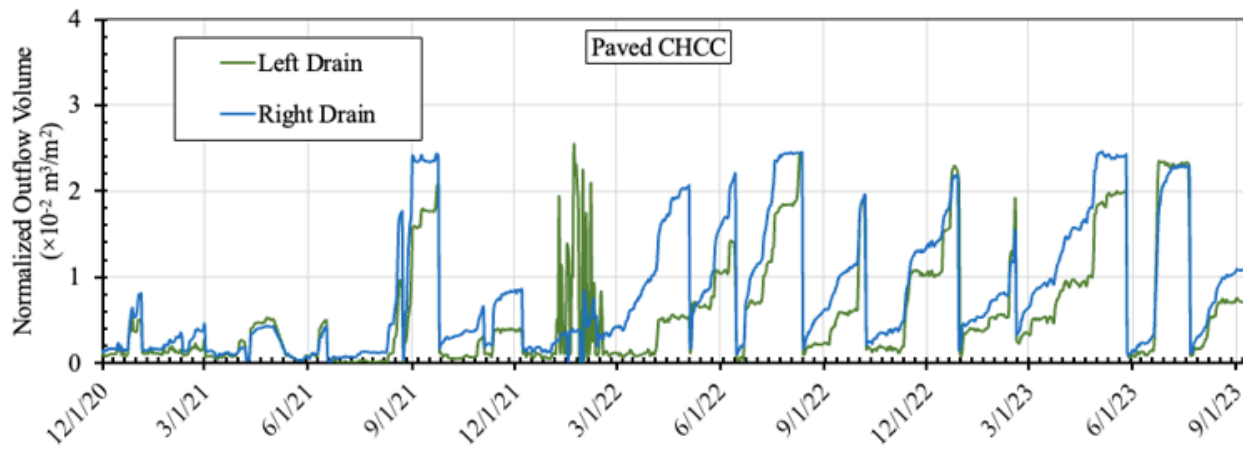
(d)

Figure 46. Normalized outflow volume recorded from the unpaved sections (a) 100% CHCC, (b) Blend 1, (c) Blend 2, (d) 100% V.A.

In general, the data shown in Figure 46 for all unpaved sections indicate that the underdrain systems were able to convey rainwater into the collection tanks. The normalized maximum capacity of each tank was determined to be approximately  $2.53 \times 10^{-2} \text{ m}^3/\text{m}^2$ . Therefore, values that level out within this range indicate that in those periods, the tanks were completely full. The excess water was allowed to drain so that the tanks would not burst. Therefore, it is not possible to determine the exact quantities of the collected water from each section. However, the data from each section clearly show that the underdrain pipes in all unpaved sections were able to convey water to the tanks. When the data in Figure 46 is compared with the rainwater data in Figure 41, the peak values match quite well, indicating that after each rain event, all unpaved sections were able to collect water through the underdrain systems.

Periodically, the research team visited the site and emptied the tanks. That is why in Figure 46, the data appear to be at maximum levels for some time followed by periods where the outflow volumes dropped down to approximately zero. Figure 46a also shows the normalized outflow volumes from the left and right edgedrain systems to be slightly different from each other at times (not always). The exact reason for this is not known, but it is likely that the difference is due to the possible slight differences in the grading of the left and right sides of the subgrade and base courses.

Figure 47 shows the normalized outflow volumes from each water tank at each paved test section. The data for the paved Blend 1 section do not represent the complete picture because there were times when the instrument in both the left and right drain tanks malfunctioned. However, the data still show that water was able to reach the collection tanks. Overall, the data of all sections indicated that rainwater was able to infiltrate the pavement, and infiltrated water was able to reach the collection tanks.



(a)

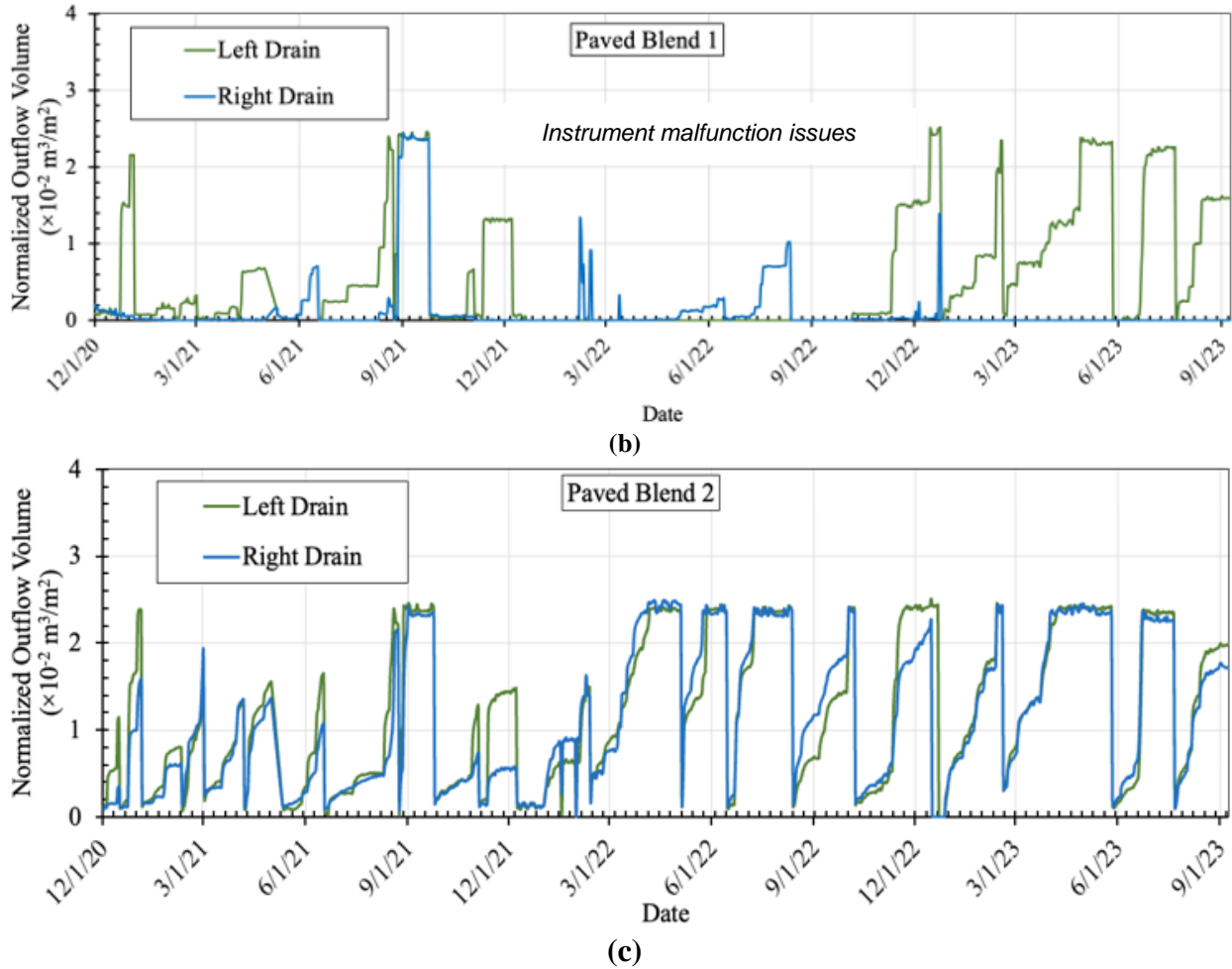


**Figure 47. Normalized outflow volume recorded for the paved sections (a) 100% CHCC, (b) Blend 1, (c) Blend 2**

When the results in Figures 46 (unpaved) and 47 (paved) are compared for the CHCC, Blend 1, and Blend 2 sections, the number of times that the water collection tanks were full was observed to be higher for the unpaved sections within the first year of the project. However, over time, the collection tanks from both the unpaved and paved sections started to become full at similar frequencies. The reason for the changes in observations in the paved sections is believed to be due to the degradation of the asphalt surface by environmental conditions (such as rain, fluctuations in temperature, and exposure to sun). Such changes are believed to create pathways for rainwater to infiltrate at a faster rate than when the asphalt layer was first constructed. In actual road applications where there is dust and other deleterious material, the asphalt becomes less permeable with time. However, if such conditions do not exist, it is not uncommon for the asphalt to start becoming more permeable over time as the material decays (Vardanega, 2014).

Although the collection tanks continued to fill up over time, it was not possible to determine the actual amount of water that infiltrated each section. This is because after the tanks filled up, the excess water poured out. However, to compare the volume of water infiltrating any two sections in the same period, the data from 07/22/23 to 09/08/23 shown in Figures 46 and 47

were evaluated. Within this period, all the tanks continued to collect water as they were not yet full. Figure 48 shows the cumulative normalized outflow volume of the tanks from all sections. The significance of Figure 48 is that the data collected represent the performance of each section after 3 years of service. The increased normalized outflow volume in both the paved and unpaved sections observed in Figure 48 are associated with notable rain events between 08/06/23 and 08/13/23, as can be seen in Figure 41. This indicates that in all sections, the distribution of infiltrated water through the underdrain system into the collection tanks is still actively occurring after 3 years.

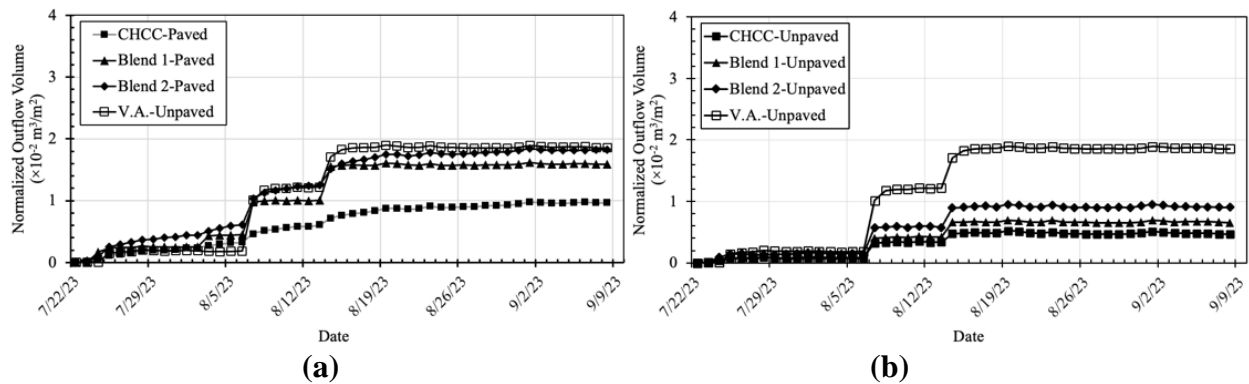


**Figure 48. Normalized outflow volumes recorded from the last cycle of water collection from the tanks**

Figure 48a compares the data obtained from all paved sections and those obtained from the 100% unpaved V.A. section. The data show that the amounts of infiltrated water conveyed to the collection tanks were very comparable in the 100% V.A. and Blend sections. If the cumulative rain accumulations from the two notable rain events on 08/06/23 and 08/13/23 are compared to the amount of water collected in the V.A. and paved Blend 2 collection tanks, the rough calculations show that in both sections, approximately 95% of the accumulated rain was collected within the collection tanks. Similar comparisons indicate that for the paved Blend 1 and paved CHCC sections, these values were 70% and 45%, respectively. The reduction in the percentage conveyance of infiltrated rainwater could be due to some potential clogging or the hydrophilic behavior of CHCC. This assessment requires further evaluation, which can be achieved by investigating the exhumed geotextiles and the borescope images of the underdrain pipe systems.

Figure 48b compares the data from all unpaved sections. For the CHCC-related sections, the unpaved sections showed a hierarchy similar to that observed in the paved sections, indicating that the most amount of water was collected by the tank at the Blend 2 section (20% CHCC), followed by those at the Blend 1 (40% CHCC) and 100% CHCC sections. However, the magnitude of the water collected in the unpaved sections was lower than what was observed in the paved sections. Considering that the data were from the warmest time of the year, the difference in performance between the paved and unpaved sections is believed to be due to the effects of evaporation. The water absorbed by the CHCC most likely evaporates, causing the amount of water being conveyed to the collection tanks to be lower. It should be remembered that Figure 48 only shows the data for the last period. If the period had been extended, the amount of water in each collection tank at the paved and unpaved sections would have likely

been at the same level. The evidence for this argument can be seen in Figures 46 and 47. Considering that the predominant application of underdrain systems was for paved conditions, the data in Figure 48 indicate valuable positive performance similarities between the V.A. and CHCC paved blend sections.

Figure 49 shows the monitoring data obtained from the instruments embedded in the water collection tanks of the unpaved 100% CHCC section. The EC probe had some issues; therefore, some of the data are missing. However, the fluctuations in pH and EC values indicate that some precipitation of Ca-based compounds might have occurred within the tanks. Higher pH conditions correlate to lower EC values and vice versa. This is an expected behavior, and the data show that the CHCC section is exhibiting the effects of carbonation due to wetting and drying cycles. Typically, a higher pH and lower EC indicates some form of precipitation of Ca-based compounds, while a lower pH and higher EC indicates a dissolution of Ca-based compounds.

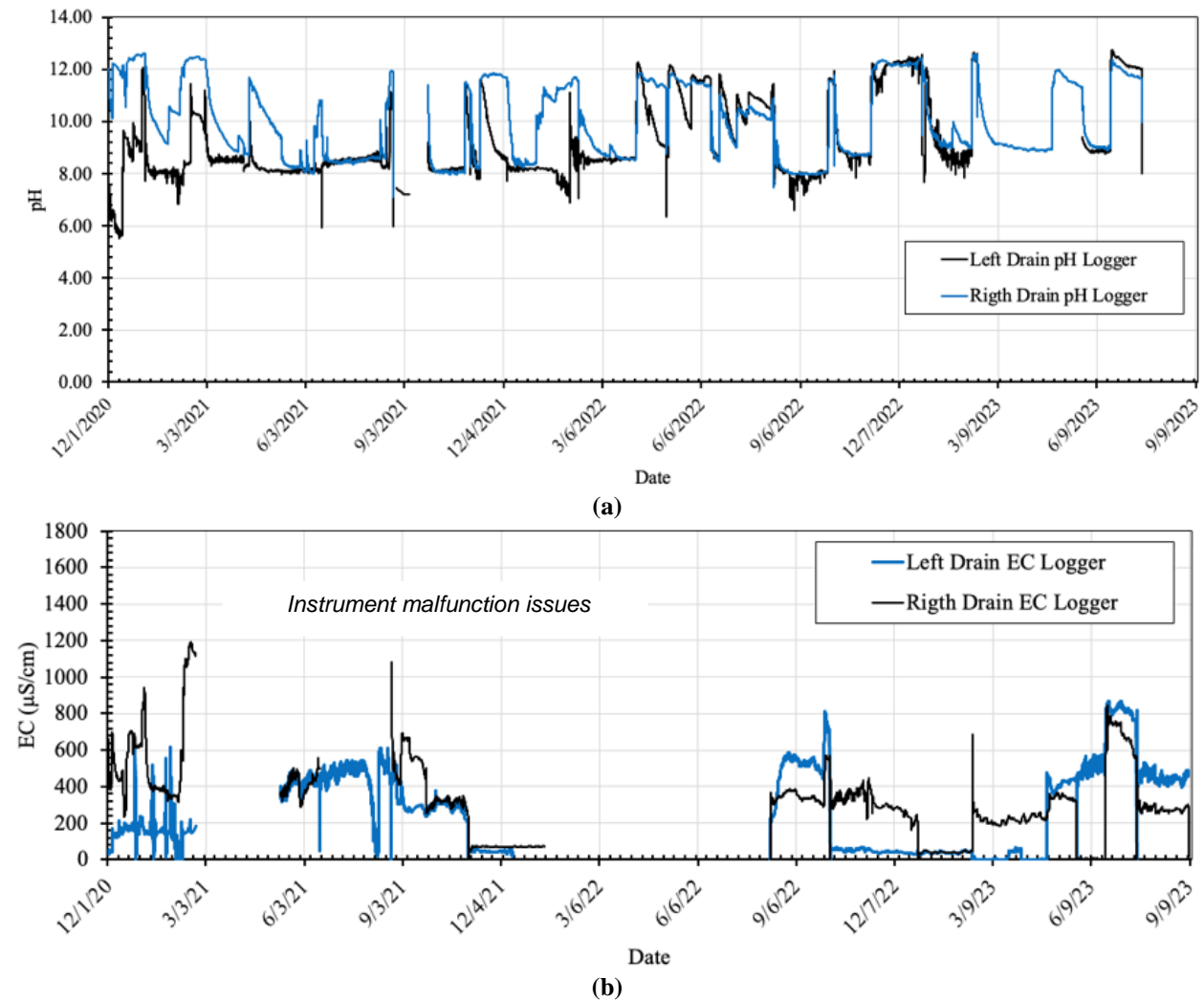


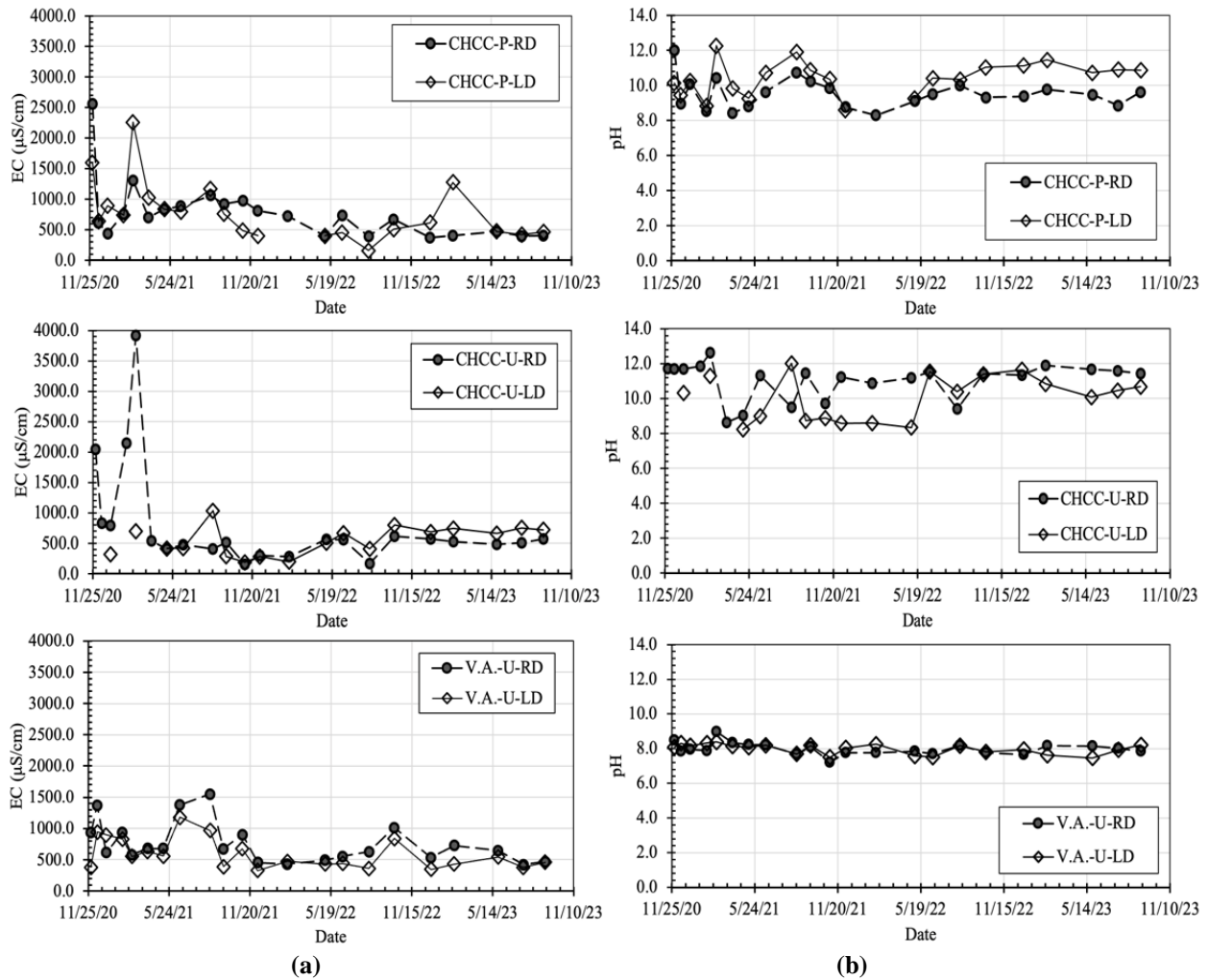
Figure 49. Monitoring data from the water collection tanks at the unpaved 100% CHCC section (a) pH, (b) electric conductivity (EC) (direct measurements from the field)

## Chemical Analyses of the Water Collected from the Test Site

Figures 50 and 51 present the results of the laboratory chemical analyses performed on the water collected from the paved and unpaved CHCC sections as well as the 100% V.A. section. For easy comparison, the vertical axis for each dataset was plotted to the same scale.

Figure 50a shows that in both the 100% CHCC (paved and unpaved) and 100% V.A. sections, dissolution of some ions occurred over time (and will most likely continue to occur). However, data from the third year of observations (i.e., November 2022 to November 2023) showed that the rate of dissolution has most likely stabilized.

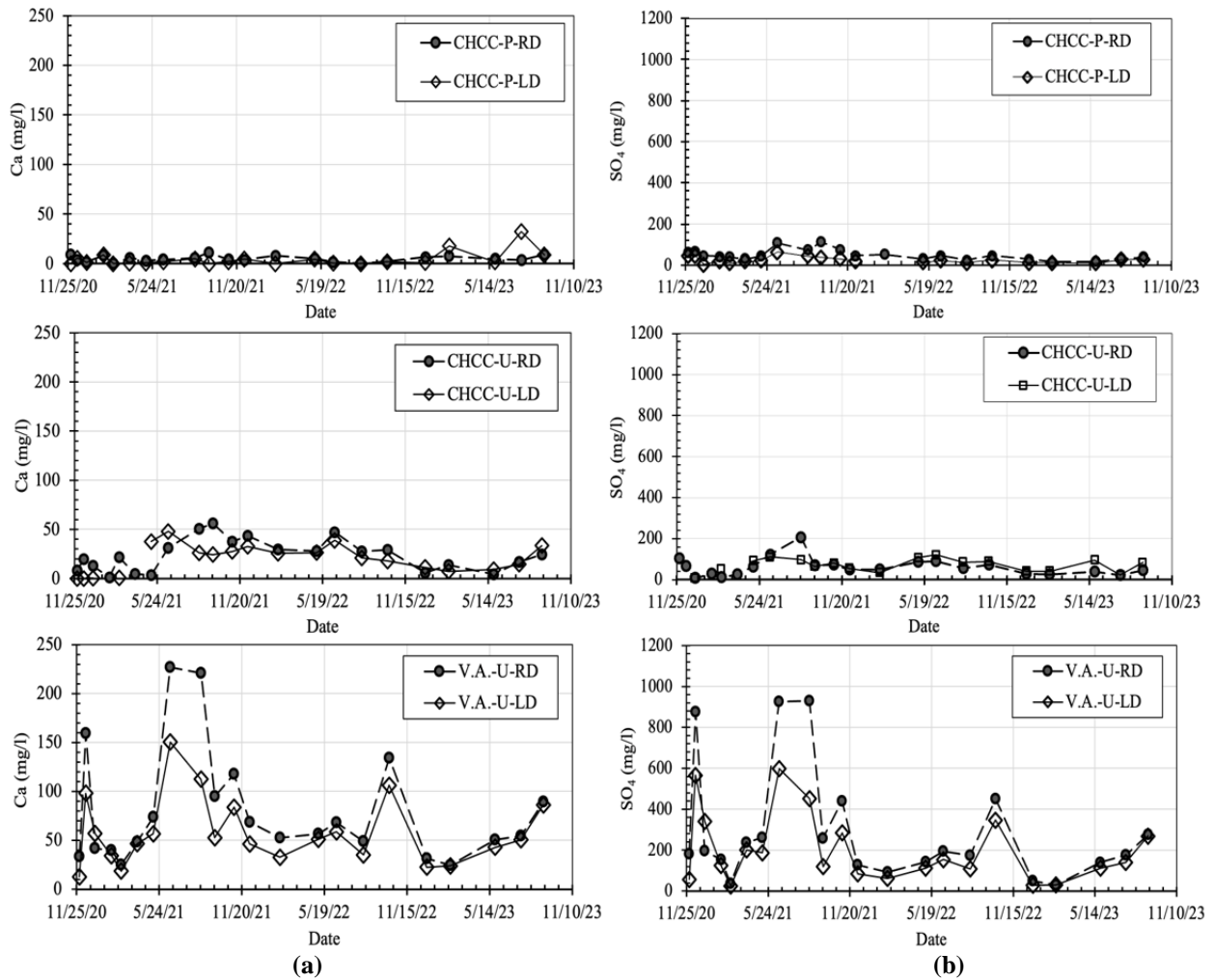
The pH data from the same time period (Figure 50b) show very similar trends for both CHCC sections. At the unpaved CHCC section, the tank associated with the right drain had a pH which fluctuated around 11.5, while in the other tank associated with the left drain, the pH fluctuated around 10.5. However, when the data from the embedded pH instrument in the same tanks were compared, as can be seen in Figure 49a, the pH values from both tanks were the same, at around 12. The data in Figure 46a show that the tank connected to the right drain of the 100% CHCC unpaved section continuously filled up faster and more frequently than that connected to the left drain. This difference is likely due to the imperfections of the construction grades in the field. However, when the information in Figures 46a and 49a are combined, it can be stated that the difference in pH measurements from the laboratory chemical analyses is most likely due to the difference of the water sitting in the tank until the data is collected by the GMU team (i.e., differences in water heights may result in differences in ion concentrations). The data in Figure 50b indicate slightly less pH values for the paved 100% CHCC compared to the unpaved 100% CHCC sections. Considering the data in Figure 48, this is an expected behavior because for a specific period, there is more water in the collection tank of the paved section (affecting the ion concentration of the solution). However, the observations were similar for the 100% CHCC paved sections, meaning that if pH was measured directly from the tank as opposed to being determined from the laboratory sample, the pH within the water collection tanks would have been around 12. Therefore, for both 100% CHCC sections, some amount of chemical precipitation is likely occurring. When the pH of the 100% V.A. section was evaluated (Figure 50b), the data did not show much fluctuation, and the pH appeared to be around 8. This indicates that the pH of the V.A. section was most likely dictated by its feldspar and quartz content, which are aluminosilicate minerals described by Luck Stone in the geological description of the rock from the Rockville plant.



*U: unpaved; P: paved; RD: right drain, and LD: left drain*

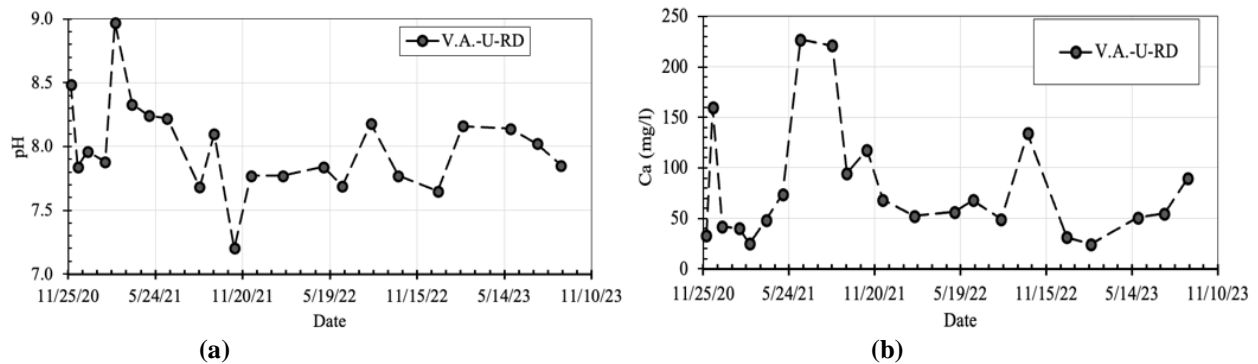
**Figure 50. Measured (a) EC and (b) pH of the water collected from the 100% CHCC (paved and unpaved) and 100% V.A. sections**

Figure 51a shows the Ca concentrations of the water from the tanks at the 100% CHCC (paved and unpaved) and 100% V.A. sections over time. When this data were coupled with the data in Figure 50, based on GMU’s interpretation approach, the chemical precipitation appeared to be occurring at a faster rate in the paved 100% CHCC section than the unpaved 100% CHCC section. This is because the overall concentration of Ca was consistently lower in the water from the paved 100% CHCC section than in that from the unpaved 100% CHCC section. In contrast, the Ca concentration of water from the 100% V.A. section fluctuated over time and was always higher than that of water from the 100% CHCC sections. The fluctuations indicate that chemical precipitation is likely also occurring at the 100% V.A. section. Figure 52 was created to better compare the fluctuations in pH and Ca concentrations occurring within the V.A. section. Data from the right drain were used as an example.



*U: unpaved; P: paved; RD: right drain, and LD: left drain*

**Figure 51. Measured leached concentrations of (a) Ca and (b)  $SO_4^{2-}$  in the water collected from the 100% CHCC (paved and unpaved) and 100% V.A. sections**



*U: unpaved and RD: right drain*

**Figure 52. Measured leached concentrations of (a) pH and (b) Ca in the water from collected from the 100% V.A. section**

As can be seen in Figure 52, there is some fluctuation in pH values and Ca concentrations within the same time periods, but these changes are in opposite directions (meaning whenever the pH is high, Ca concentrations are low and vice versa). The conditions at the time when the pH value increases and the Ca concentration decreases indicate the possibility of a chemical precipitation. The possibility of chemical precipitation from V.A. is likely as the geological make-up of the aggregate from the Rockville plant appears to contain some calc-silicate composition. When the Ca and SO<sub>4</sub> concentrations for each section are compared (Figure 51), the data show that the precipitation most likely occurred as calcite in all the sections.

Figures 53 and 54 show a comparison of the paved and unpaved Blends 1 and 2 sections, respectively. The data in these figures were compared side by side to determine the differences in pH, EC, and Ca and SO<sub>4</sub> concentrations between the paved and unpaved sections. Figure 53a shows that for the paved Blend 1 section (40% CHCC), the pH values were significantly lower than those for the unpaved Blend 1 section. When combined with the data from Figure 48, this difference could be due to the differences in concentrations within the tank due to the difference in water heights. In both sections, the EC values (Figure 53b) indicated that dissolution of ions occurred over time, and the Ca concentrations (Figure 53c) of the two sections were similar to each other. However, the concentration of SO<sub>4</sub> (Figure 53d) in the unpaved Blend 1 section was higher.

As mentioned earlier, the interpretation of the likelihood of chemical precipitation is very complex especially because at this site, the V.A. is also most likely contributing to some of the precipitation. Figure 54 (Blend 2 section) shows an even more complex dataset compared to Figure 53 (Blend 1 section). This is because in both the paved and unpaved Blend 2 (20% CHCC) sections, the pH values were around 8 (Figure 54a). This observation is similar to what was observed for the 100% V.A. section (Figure 50b). However, the rest of the indicators (EC and Ca and SO<sub>4</sub> concentrations) appear to be same for both the paved and unpaved Blend 2 sections. When compared to the 100% V.A. section, the Ca concentrations of Blend 2 are lower, indicating that precipitation may still occur.

### **Performance Evaluation of the Test Site**

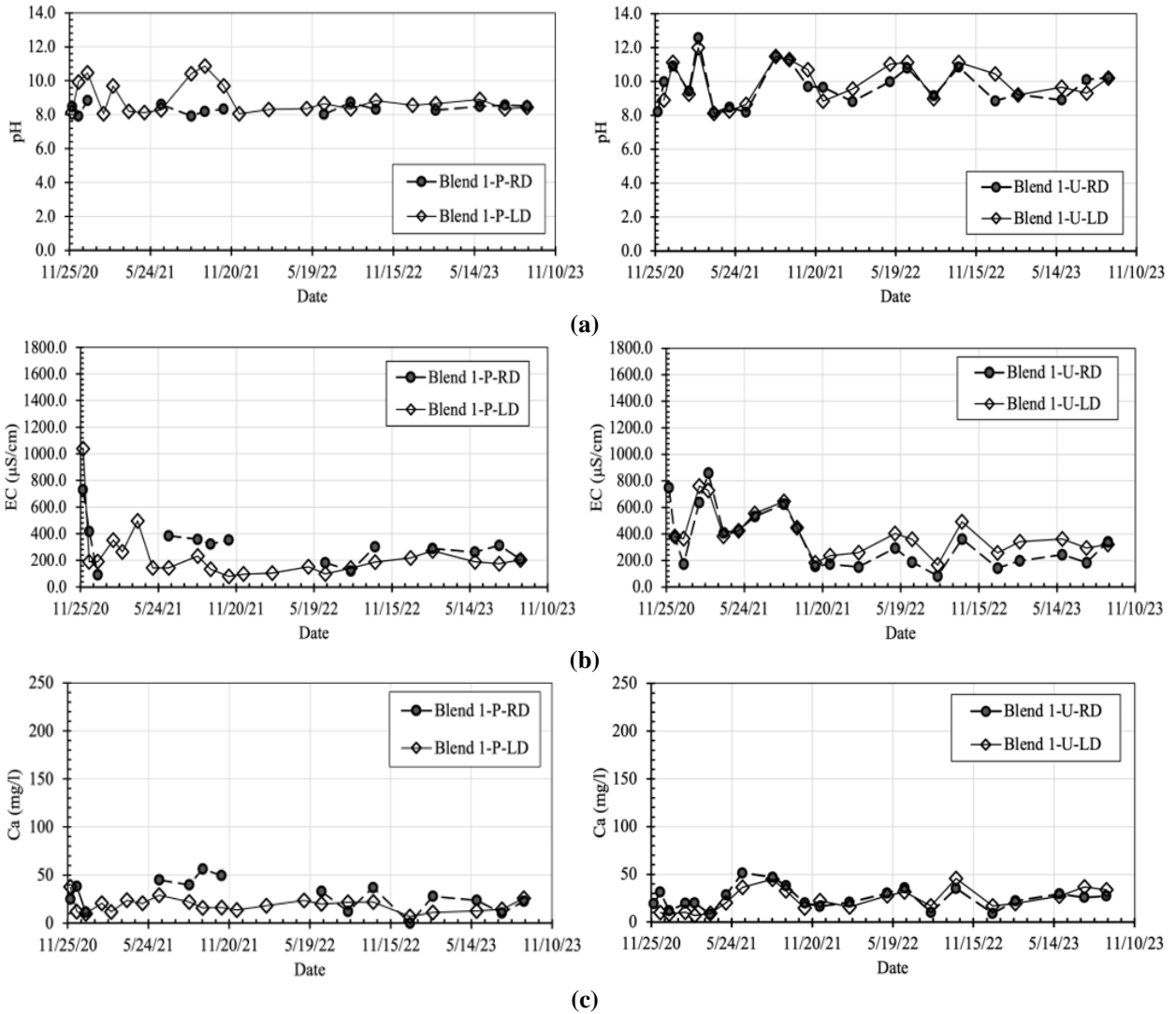
Throughout the study, five detailed performance evaluations were conducted, 6, 14, 20, 26, and 33 months after completing the construction of the site. The frequency of these site evaluation efforts was determined based on the weather conditions and availability of the VDOT crew to assist. Findings from these evaluations are presented below.

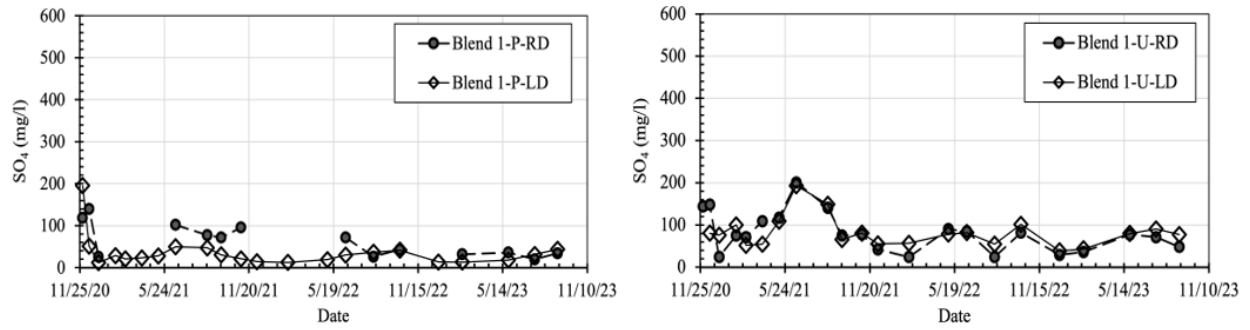
#### **Evaluation of Exhumed Geotextiles**

##### *Evaluating the hydraulic ability of the exhumed geotextile samples*

Table 6 shows a comparison of the level of reduction in permittivity of the exhumed geotextiles from the 100% CHCC (paved and unpaved) sections and the unpaved 100% V.A. section. Comparing the values gotten for each section revealed that there were no trends or significant changes related to the service time of the geotextile in the field. This was expected because the primary mechanism that governs reduction in permittivity is associated with the

migration of fines rather than tufa precipitation. This does not mean that precipitation did not take place but rather that the precipitated tufa was not as strong a contributor to the reduction in permittivity as the physical particles migrating and blocking some of the geotextile filaments. If the chemical precipitation was adversely affecting the geotextile's ability to permeate, then the end result would have been an increasing trend in permittivity reduction with time (which did not seem to be the case). Regarding fines migration, unless the particles break due to weathering (which is not an expected behavior), it is not expected that the percentage of these migrated particles would increase as a function of time (which seemed to be the case).

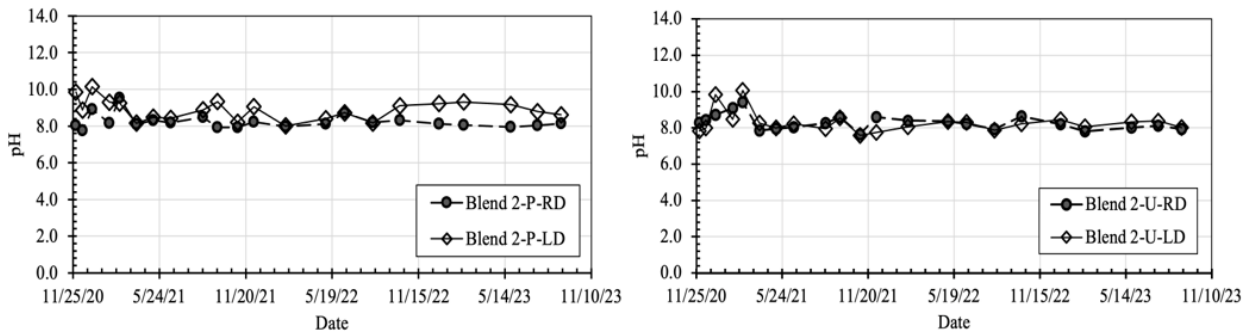




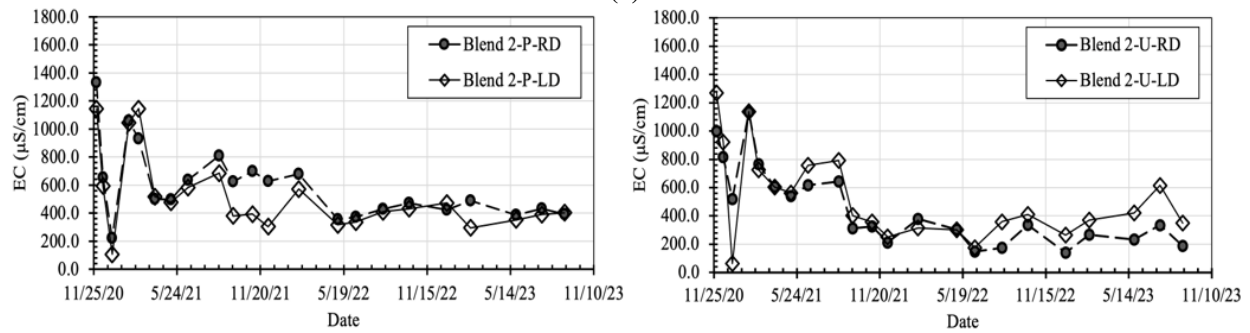
(d)

*U: unpaved; P: paved; RD: right drain, and LD: left drain*

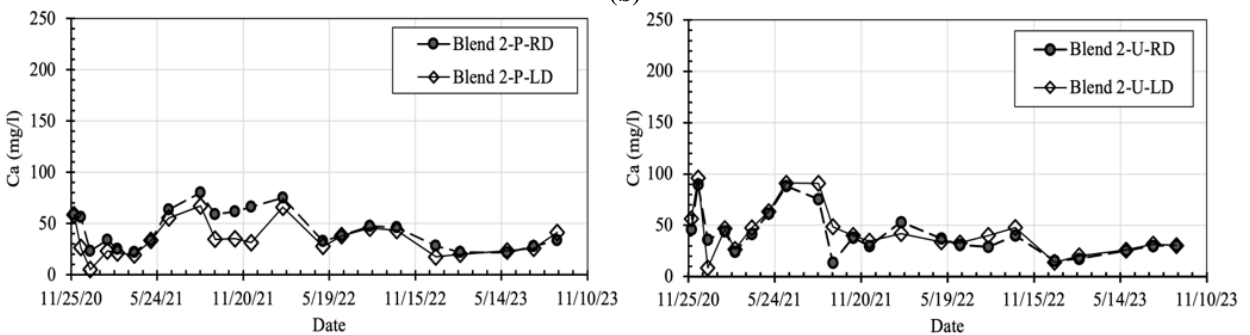
**Figure 53. Measured leached concentrations of (a) pH, (b) EC, (c) Ca, and (d)  $SO_4^{2-}$  in the water collected from the paved and unpaved Blend 1 sections**



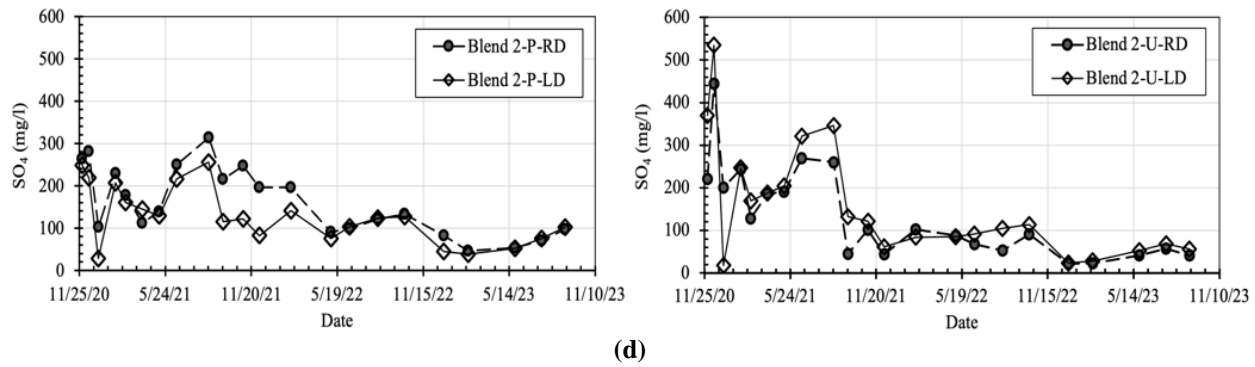
(a)



(b)



(c)



*U: unpaved; P: paved; RD: right drain, and LD: left drain*

**Figure 54. Measured leached concentrations of (a) pH, (b) EC, (c) Ca, and (d)  $\text{SO}_4^{2-}$  in the water collected from the paved and unpaved Blend 2 sections**

**Table 6. Reduced permittivity of the exhumed geotextile samples from the 100% CHCC and 100% V.A. sections**

Geotextile Sample From	Field Service Time (month)	Reduction in Geotextile Permittivity	
		Data From Tests	Maximum
CHCC-Paved	6	50%	50%
	14	21%	
	20	49%	
	26	48%	
	33	49%	
CHCC-Unpaved	6	39%	39%
	14	36%	
	20	23%	
	26	25%	
	33	39%	
V.A.-Unpaved	6	30%	36%
	14	31%	
	20	36%	
	26	22%	
	33	29%	

As can be seen in Table 6, some values in each section differ from the general range. For example, in the 100% CHCC section, majority of the percentage reduction in permittivity fall within 48% and 50%, but there is also an observation of 21%. Considering that the reduction in permittivity is not a function of time in this data set, these discrepancies are believed to be due to the location where the sample was exhumed from, as opposed to a time period. It is likely that at the point where the sample was exhumed, the base course aggregate (at the time of placement) had slightly less fines than the rest of the section. This could be because the base course materials were hauled to the site in June 2020 and kept as a small stockpile until their placement into the test sections started in September 2020. During this period, some segregation was noted (Figure 55). Even though all base course stockpiled materials were mixed as thoroughly as

possible before their placement into the test sections, the mixing was done using a front-end loader. Hence, it is possible that some small fractions did not mix as thoroughly as anticipated. This might have resulted in some locations having more fines or coarse grain content compared to the overall grain size distribution. For these reasons, comparing the performance of the geotextiles based on the worst-case scenario (maximum reduction observed) as opposed to an average value was considered more realistic. Based on this approach, the paved 100% CHCC section was found to have a higher reduction in permittivity compared to the unpaved CHCC section. This could be because the paved CHCC section was wet for longer periods than the 100% unpaved section, possibly from water migrating more of the physical particles from the CHCC on to the filaments of the geotextile. However, even the 50% reduction in permittivity did not stop the infiltration water from reaching the collection tanks (Figure 48). Table 6 shows that a notable reduction in permittivity (i.e., 36%) was also observed in the V.A. section. However, because the V.A. used in this study had lesser fines compared to the CHCC (Figure 22), the smaller reduction in permittivity observed in the V.A. sections compared to the CHCC sections was expected. Table 7 shows the data from all blend sections.



**Figure 55. A photo of the stockpiled base course materials on site during construction**

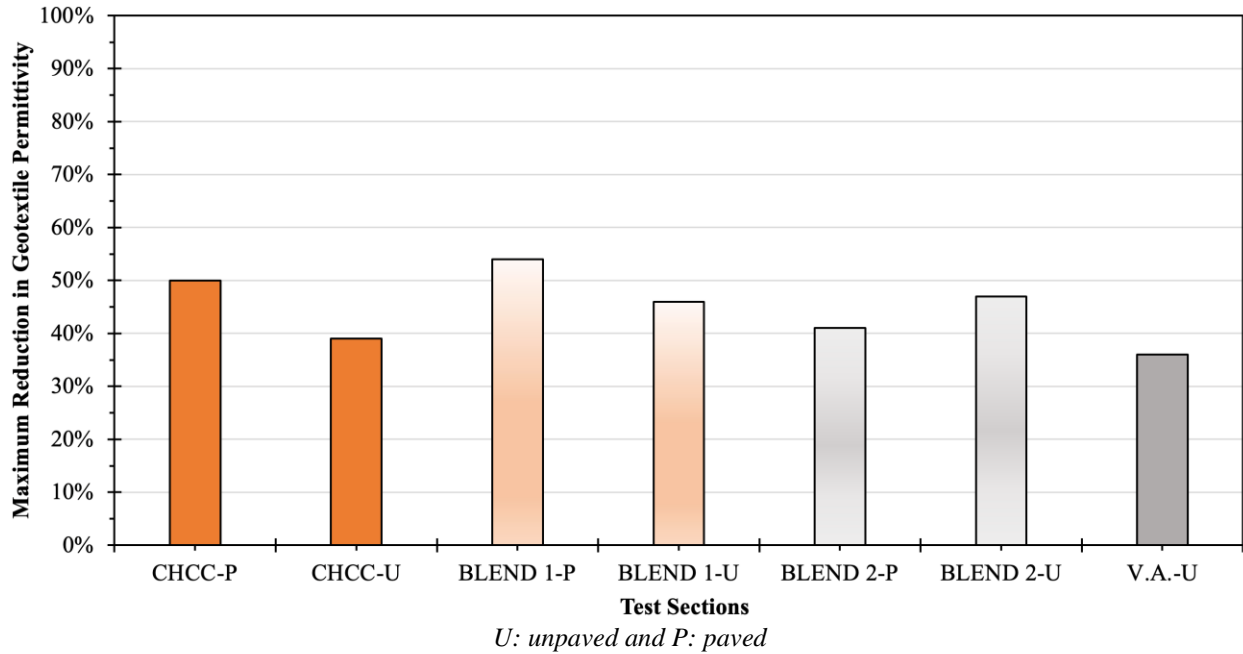
As shown in Table 7, there was no time dependent trend in the reduction of permittivity values of the geotextiles exhumed from the blend sections. For the paved sections, the Blend 1 section showed a higher reduction in permittivity compared to the Blend 2 section. Therefore, the paved blend sections showed improved performance as the percentage of CHCC in them decreased. However, this was not the case for the unpaved blend sections, as the maximum reduction values in these sections for both Blend 1 and 2 were close to each other.

Figure 56 presents a comparison of the maximum permittivity reductions observed within 33 months from all the geotextiles exhumed from each section. In both of the Blend 1 sections, the reduction in permittivity in geotextiles are slightly higher than both of the corresponding 100% CHCC sections (comparison of paved sections and unpaved sections among each other). Among the paved sections, Blend 2 performed better than Blend 1 and 100% CHCC (as expected). Among the unpaved sections, Blend 2 showed similar reduction in permittivity as Blend 1 and more reduction than the 100% CHCC section.

**Table 7. Reduction in the permittivity of geotextiles exhumed from sections with blends**

Geotextile Sample From	Field Service Time (month)	Reduction in Geotextile Permittivity	
		Data From Tests	Maximum
Blend 1-Paved	6	30%	54%
	14	48%	
	20	31%	
	26	29%	
	33	54%	
Blend 1-Unpaved	6	40%	46%
	14	38%	
	20	16%	
	26	25%	
	33	46%	
Blend 2-Paved	6	30%	41%
	14	41%	
	20	30%	
	26	34%	
	33	30%	
Blend 2-Unpaved	6	26%	47%
	14	33%	
	20	47%	
	26	35%	
	33	31%	

*Blend 1: 40% CHCC/60% V.A. and Blend 2: 20% CHCC/80% V.A.*



**Figure 56. Comparison of the maximum reduction in permittivity observed for the exhumed geotextiles from each section**

For practical purposes, the overall maximum reduction in the permittivity of geotextiles exhumed from the paved 100% CHCC, paved and unpaved Blend 1, and unpaved Blend 2 sections were closer to each other and were about 1.4 times more than what was observed for geotextile gotten from the 100% V.A. section (Figure 56). However, as shown in Figure 48, all these sections were still able to convey the infiltrated rainwater to the collection tanks. Although the reduction in permittivity in this study does not appear to be governed by the potential of chemical tufa precipitation, the photo in Figure 57, which was taken from the geotextile exhumed from the paved 100%CHCC section, shows some chemical tufa precipitation. This confirms that precipitation is occurring but has so far not taking over the hydraulic ability of the geotextile.

*Evaluating chemical precipitation over the surface of the exhumed geotextile samples*

The portions of all the exhumed geotextile samples that were tested to quantify the reduction in permittivity were also tested to determine the surface area of the geotextile that was covered by tufa precipitation ( $S_{tufa}$ ). Tables 8 and 9 present the results of the analysis of all exhumed geotextiles. One of the major observations on Table 8 is that the sections with CHCC content show  $S_{tufa}$  but so also does the 100% V.A. unpaved section. The data in Tables 1 and 2 as well as the literature indicate that the V.A. used in this study had a calc-silicate composition. The observations noted from the 100% V.A. data in Table 8 show that such composition results in chemical precipitation.

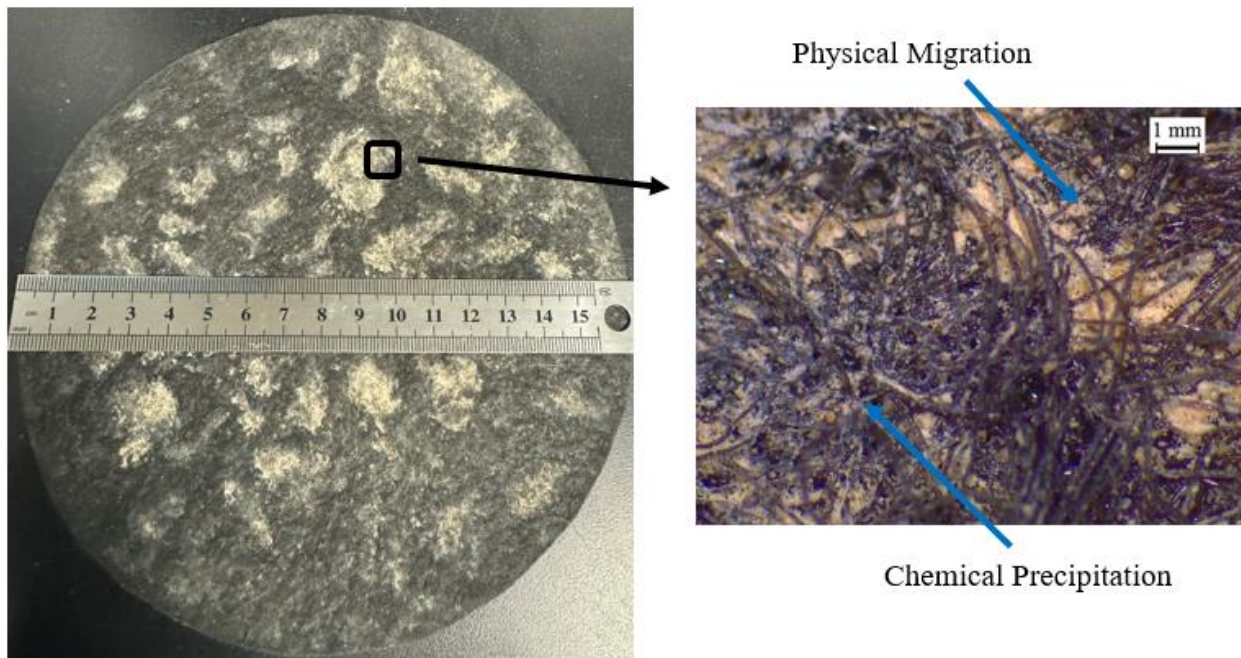


**Figure 57. A photo of the geotextile exhumed from the paved 100% CHCC section that was used for one of the permittivity tests**

Figure 58 is a graphical presentation of the results shown in Tables 8 and 9 and shows that for all sections, the  $S_{tufa}$  changed with time. For the CHCC and Blend sections, the  $S_{tufa}$  from

the first time the samples were exhumed (at Month 6) to the last time they were exhumed (at Month 33) showed notable increase. This indicates that, unlike fines migration, chemical precipitation is a phenomenon that continues with time. The  $S_{tufa}$  in the paved 100% CHCC was more than that in the unpaved 100% CHCC section (Figure 58a). This observation is consistent with the comparison of the permittivity results, where the paved 100% CHCC section showed more reduction in permittivity than the unpaved 100% CHCC section (Figure 56). The unpaved 100% V.A. also showed tufa precipitation, but, in general, the changes in  $S_{tufa}$  with time appeared to be significantly less than what was observed in the 100% CHCC sections. The  $S_{tufa}$  percentage observed on the samples exhumed from the Blend (both paved and unpaved) and paved 100% CHCC sections at 33 months appear to be similar. Overall, the  $S_{tufa}$  data appeared to support the differences in the permittivity reductions observed, meaning that the sections with higher physical fines migration also had higher chemical precipitation. However, at this stage, the chemical precipitation does not appear to be the primary factor in the reduction of geotextile permittivity, as the data on Tables 6 and 7 do not show the time dependency observed in Figure 58.

**Table 8. Percentage of the surface area of the geotextiles exhumed from the 100% CHCC and 100% V.A. sections covered by chemical precipitation ( $S_{tufa}$ )**

<i>Geotextile Sample From</i>	<i>Field Service Time (month)</i>	$S_{tufa}$
CHCC-Paved	6	5.4%
	14	5.0%
	20	8.2%
	26	8.9%
	33	9.4%
CHCC-Unpaved	6	4.3%
	14	6.2%
	20	5.0%
	26	7.2%
	33	7.4%
V.A.-Unpaved	6	4.5%
	14	4.1%
	20	2.9%
	26	3.6%
	33	5.1%

### Evaluation of the Edgedrain and Collection Pipes

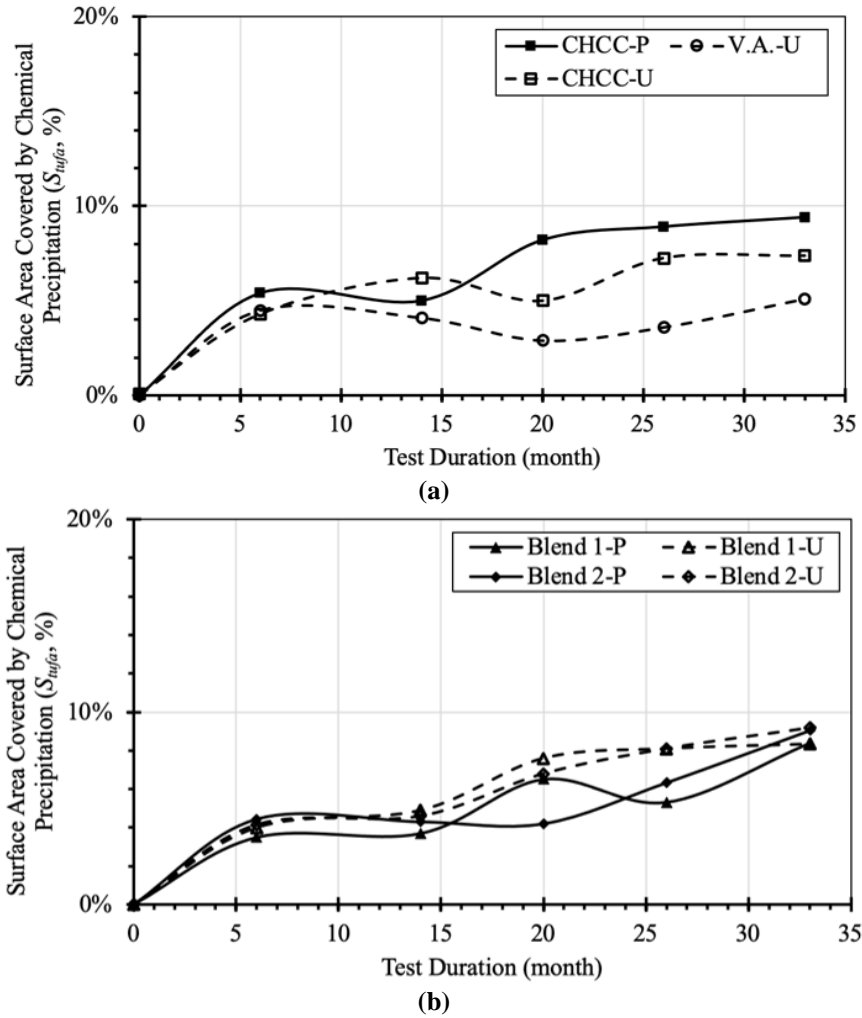
Data from the visual survey done at the 6-month mark were used as the baseline conditions and the data obtained at the 33-month mark were used to document the changes after about 3 years in service. During the evaluation at the 6th month, the borescope data from the edgedrain pipes showed no signs of debris. However, the collection pipes (smooth 4-inch PVC pipes) in all the sections showed signs of some fines content migrating through the pipes.

Similarly, some accumulated materials were noted in all collection tanks. These are positive signs that the installed pipe systems were sized appropriately and were able to properly convey water.

**Table 9. Percentage of the surface area of the geotextiles exhumed from the blend sections covered by chemical precipitation ( $S_{tufa}$ )**

<i>Geotextile Sample From</i>	<i>Field Service Time (month)</i>	$S_{tufa}$
Blend 1-Paved	6	3.5%
	14	3.7%
	20	6.5%
	26	5.3%
	33	8.4%
Blend 1-Unpaved	6	4.0%
	14	4.9%
	20	7.6%
	26	8.1%
	33	8.3%
Blend 2-Paved	6	4.4%
	14	4.3%
	20	4.2%
	26	6.3%
	33	9.0%
Blend 2-Unpaved	6	4.2%
	14	4.6%
	20	6.8%
	26	8.1%
	33	9.2%

*Blend 1: 40% CHCC/60% V.A. and Blend 2: 20% CHCC/80% V.A.*



*U: unpaved; P: paved; Blend 1: 40% CHCC/60% V.A. and Blend 2: 20% CHCC/80% V.A.*

**Figure 58. Results of the image analyses of the geotextiles exhumed from sections (a) with 100% CHCC and 100% V.A. and (b) with blends of CHCC and V.A.**

By the 33-month mark, the accumulation in all collection tanks at all the sections were noticeably more than the initial conditions. Figure 59 shows photos taken from inside the collection tanks at the end of 33 months. The conditions of the tanks for both left and right drains were not drastically different; therefore, only one of the tank photos is presented for each section.



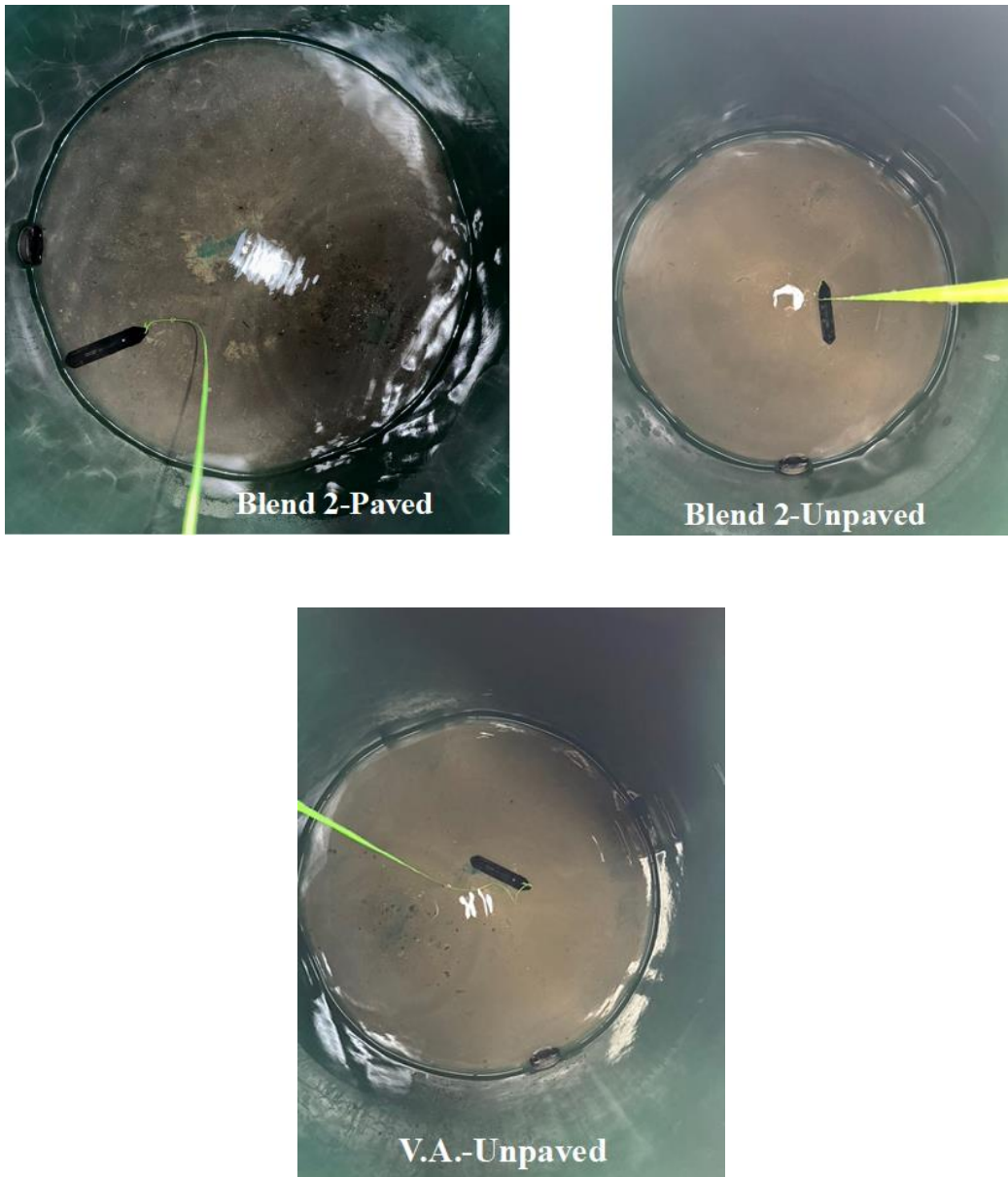


**Figure 59. Conditions of the accumulation inside the collection tanks at each section**

The accumulation in the collection tanks is an indicator that fines (whether physical particles or tufa particles) were still able to migrate all the way through the edgedrain and collection pipes. None of the borescope data from the collection pipes and edgedrains showed clogging (a condition that impedes flow). However, surveys of the 100% CHCC and Blend 1 sections (both paved and unpaved) showed that some fine amount of tufa precipitation started to form in some areas within the collection pipes. Figure 60 shows a photo of the left drain of the paved 100% CHCC section after 33 months. In the same section, the edgedrain pipes showed only very minor signs of tufa precipitation on the edges of the corrugations (Figure 61).

The corrugated edgedrains are connected to the smooth PVC pipes, which make a 90-degree turn to convey the water to the collection tanks (Figure 39a). The borescope surveys over

the years showed that this sharp turn slows down the water exiting the system. In the unpaved sections, especially the 100% CHCC and Blend 1 sections, these areas began to show tufa formation, which has gradually increased with subtle differences from one year to the next. Figure 62 shows the tufa build-up in the unpaved 100% CHCC right-side edgedrain. No such growth is observed in the collection pipes.



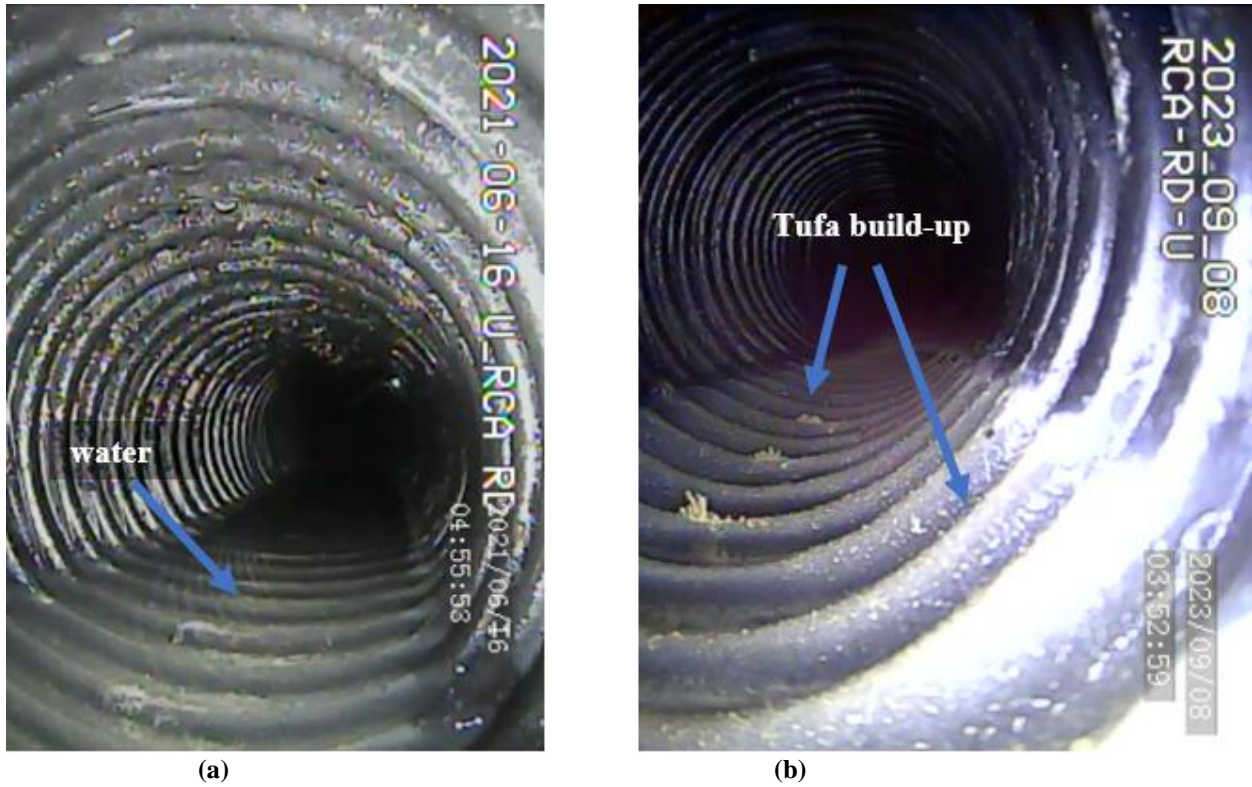
*RCA: CHCC; LD: left drain and P: paved*

**Figure 60. Tufa accumulation in the paved 100% CHCC section (a) inside the collection pipe and (b) smeared onto the borescope wire and hands**



*RCA: CHCC; LD: left drain and P: paved*

**Figure 61. Condition of the edgedrain pipe of the 100% CHCC paved section**



*RCA: CHCC; RD: right drain and U: unpaved*

**Figure 62. Tufa accumulation conditions from the unpaved 100% CHCC section (a) 6 and (b) 33 months after construction of the test site**

Figure 62 provides evidence that was not available before this field study, and that is the fact that although the nonwoven geotextile showed acceptable performance in terms of its hydraulic ability to convey water, the edgedrain is also a component of the VDOT UD-4 detail and is vulnerable to tufa build-up. Figure 62a shows conditions where there is some standing water and very slight tufa build-up along the edges of the corrugations. Figure 62b shows additional build-up 33 months after the site construction. However, the major difference between the two conditions is the appearance of the small stalagmite type of growth. In their present forms, these formations are not large enough to impede flow, but future monitoring is needed to determine whether the growth will continue at a fast rate or the constant water flow will keep the growth rate in check.

Thirty-three months after the construction, all sections were still able to convey water, and (although not shown here), majority of the areas within the pipes did not show any tufa growth. However, as presented in Figure 48, based on many factors (including the initial hydraulic conductivity), not all sections are conveying flow at the same rate.

## PERFORMANCE PREDICTIONS

### Comparison of the 100% CHCC Section in this Field Study to that in the Previously Completed Laboratory Study

Due to the limitations of laboratory conditions, the previous study was conducted with 100% CHCC, without the effects of the pavement layer. Therefore, the unpaved 100% CHCC section was used for this purpose in the current study. In the previously completed laboratory study, the surface area covered by the chemical precipitation ( $S_{tufa}$ ) was documented within 1 year (Abbaspour and Tanyu, 2020). Figure 63 presents the comparison of the  $S_{tufa}$  values from the laboratory and field studies. In both studies, the geotextile used were exactly the same.

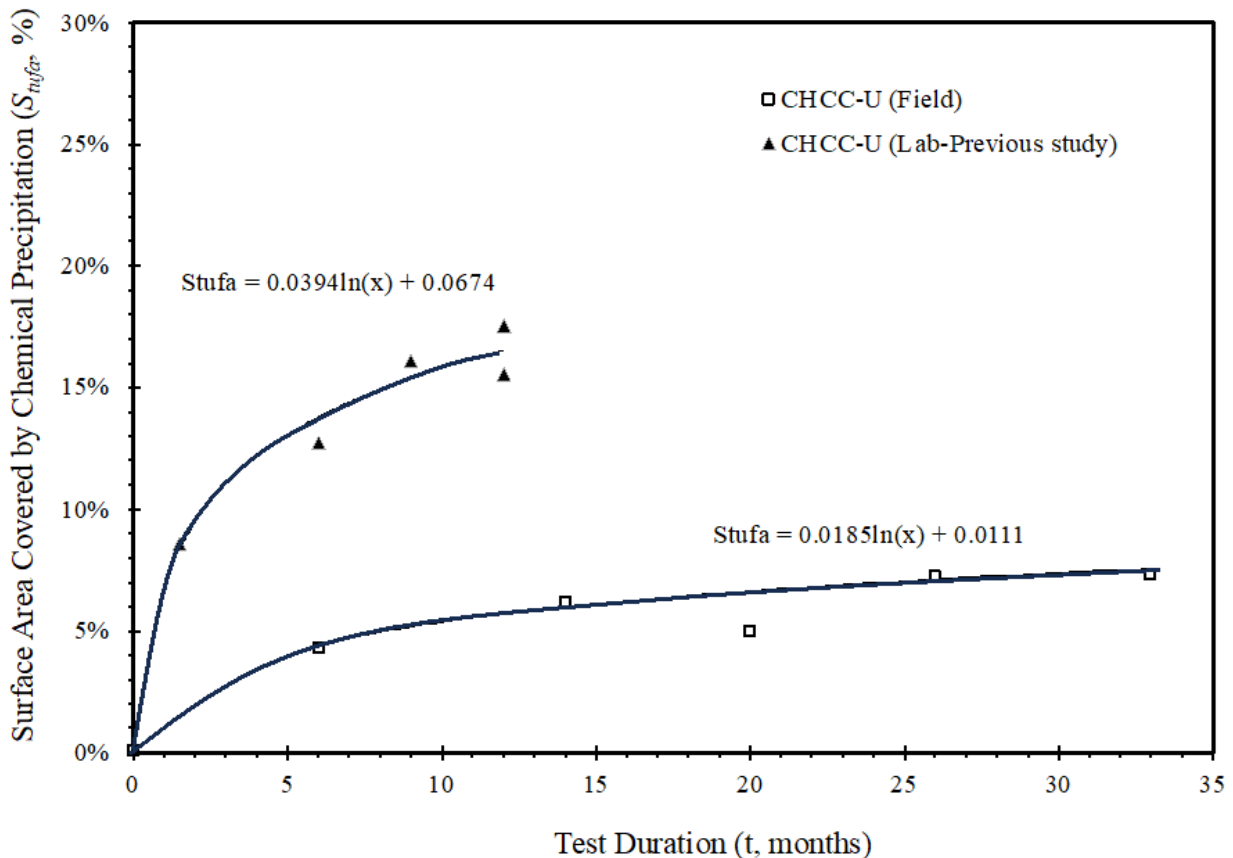


Figure 63. Comparison of the  $S_{tufa}$  in the unpaved 100% CHCC section from the previously completed laboratory study and the current field study

The laboratory study was designed and conducted to simulate the CHCC base course and geotextile interactions under constant conditions that did not account for other variables (such as changes in temperature and humidity, rainfall events (variable intensities), occurrence of wet and dry seasons, and variations in evaporation rates due to exposure to sunlight and wind). The surface area of the geotextile used in the laboratory study was about  $0.018 \text{ m}^2$  ( $0.196 \text{ ft}^2$ ), which is significantly smaller than that of the geotextile installed in the field study. In the laboratory tests, the simulated rainwater was forced to percolate through the small surface area, increasing the possibility of nucleation and deposition of CHCC tufa. Moreover, the redundancy in the field

sample was proportionally much higher than that in the laboratory simulation, and rainwater would have much more percolation paths, which, in turn, reduces the possibility of CHCC tufa nucleation and deposition on the geotextile surface. It should be noted that the two studies used two different CHCCs produced from different materials and by different manufacturers. The CHCC used in the field study has lower hydraulic conductivity and more percent fines compared to that used in the laboratory study. When the chemical properties of the leachate from both the laboratory and field studies were compared, the leachate from the field study generally showed higher pH values ( $8 < \text{pH} < 12$ ) and significantly lower Ca and  $\text{SO}_4$  concentrations. This condition is interpreted as Ca not dissolving (Ca content not being readily available) in the solid CHCC matrix. In contrast, the leachate from the laboratory study consistently showed low pH and high Ca and  $\text{SO}_4$  concentrations, especially within the first 10 months of testing (Abbaspour and Tanyu, 2020). This is a condition that favors the precipitation of CHCC tufa. In both studies, the tufa precipitation continued over time; however, by the end of the 12th month, the  $S_{\text{tufa}}$  in the laboratory study was almost 2.5 times that observed in the field (Figure 63). This comparison shows that the conditions in the field are less aggressive in terms of CHCC carbonation and having bigger geotextile surface area, resulting in less  $S_{\text{tufa}}$  on a particular location within the geotextile.

The laboratory study also included detailed hydraulic performance evaluations, and the results showed that even with 17%  $S_{\text{tufa}}$ , the geotextile was able to convey water through the filaments (Abbaspour and Tanyu, 2020). Therefore, the performance evaluations from the field study indicating that the drainage system was still working as intended in the unpaved 100% CHCC section is not a surprise. However, the laboratory study did not include an evaluation of the drainage pipes. The findings from this field study also show the importance of a potential tufa precipitation within the pipes, as can be seen in Figures 60 and 62.

### **Estimation of the Long-Term Performance of the Paved Test Sections**

The UD-4 underdrain detail is implemented by VDOT when a road is paved. Therefore, the most important performance evaluation is for the sections that are paved. The data from the field study showed that, so far, the observed reduction in permittivity of the exhumed geotextiles do not change as a function of time. This indicates that tufa precipitation is not at the stage where it affects the overall permittivity of the geotextile. At this stage, the maximum reduction in permittivity observed in geotextile samples gotten from the paved 100% CHCC and Blend 1 sections summed up to 55%, and that for the paved Blend 2 section summed up to 40%. Although a prediction of the long-term performance of the sections cannot be made based on these values, it is important to note that a 55% reduction in the permittivity of a geotextile still results in hydraulic conditions that are orders-of-magnitude better than the hydraulic conductivity of the CHCC, Blend 1, and Blend 2 sections. Therefore, to be able to make any long-term predictions, the extent of the  $S_{\text{tufa}}$  over time has to be assessed. This is because if  $S_{\text{tufa}}$  continues to fill-in the filaments of the geotextile and, at some point, start to take over the reduction in permittivity, then the performance of the geotextile will primarily start to change heavily as a function of time.

The  $S_{\text{tufa}}$  evaluations showed that, in terms of chemical precipitation, having a pavement over the top of the CHCC creates a scenario that is worse than the unpaved conditions. This is a

completely new finding, as the previously conducted laboratory study did not include the pavement. The monitoring data in this study obtained from chemical analyses of the water samples from the collection tanks indicated that the tufa precipitation in the field is most likely occurring in the form of calcite (regardless of the presence of pavement). Therefore, even though the existing drainage system appears to be in full working condition, it is important to estimate the expected  $S_{\text{tufa}}$  over time. This is because calcite is not a highly soluble mineral, and as it continues to precipitate, the extent of this precipitation may have an adverse effect on the geotextile's performance. For this evaluation, the data obtained from this field study was extended to 30 years, which is the highest flexible pavement design life criteria in VDOT (VDOT, 2022). Figure 64 shows the comparison of the estimated long-term performance of the paved CHCC and 100% V.A. sections in terms of  $S_{\text{tufa}}$ . It should be noted that the predictions shown were gotten under the assumption that the  $S_{\text{tufa}}$  rate will stay the same over time, which may or may not be true.

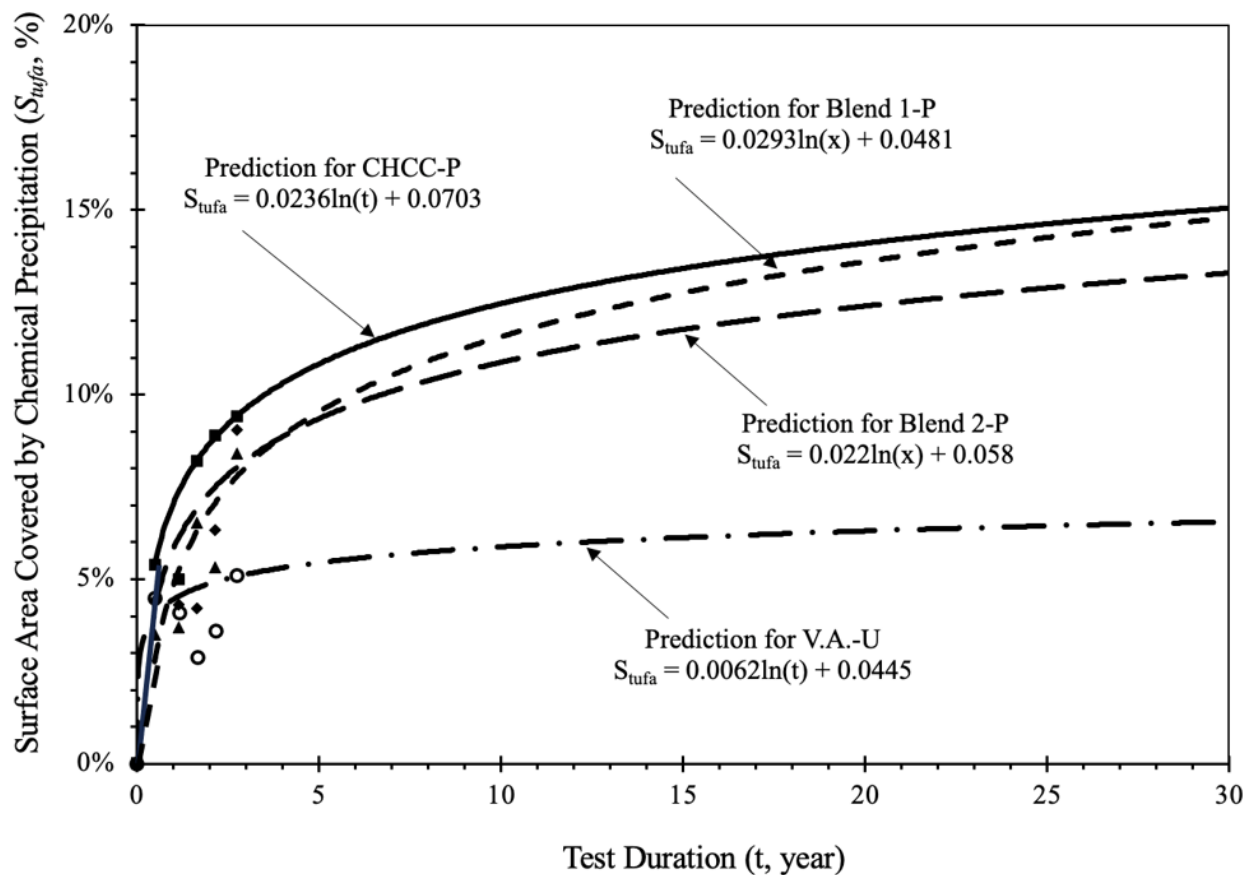


**Figure 64. Prediction of  $S_{\text{tufa}}$  over geotextile from paved sections and unpaved 100% V.A. section in this field study**

Figure 64 shows that the predicted  $S_{\text{tufa}}$  in 30 years is very similar for the paved 100% CHCC and Blend 1 sections. The predicted  $S_{\text{tufa}}$  in 30 years for the Blend 2 section was approximately 13%, which is about 10% better than that for the 100% CHCC and Blend 1 sections. In all cases, the sections with CHCC content showed higher  $S_{\text{tufa}}$  over time compared to the 100% V.A. section. This is expected because although tufa precipitation was also observed in the 100% V.A. section, the precipitation rate was significantly lesser in this section. It should be

noted that the prediction shown for V.A. is based on the highest  $S_{tufa}$  observations in this study. Therefore, the prediction line for V.A. is believed to constitute the worse-case scenario.

The previous laboratory study already showed that even at 17%  $S_{tufa}$ , the geotextile was able to perform its hydraulic functions (Abbaspour and Tanyu, 2020). However, even though the predicted  $S_{tufa}$  in the worse-case scenario on the field (100% paved CHCC section) appeared to be less than the  $S_{tufa}$  observed at the end of the one-year laboratory study (15% vs. 17% respectively), this does not mean that no concerns exist. This is because, in addition to the geotextile performance, the performance of the edgedrains and collection pipes also need to be as expected. Unfortunately, such a prediction could not be made from the data in this study. However, having access to such field test site provides an invaluable opportunity to continue monitoring the conditions within the drainage and collection pipes.

## CONCLUSIONS

- *The CHCC used in the previously completed laboratory study and that used in this field study were produced by two different manufacturers from two different locations within Virginia. CHCC is a recycled material whose content that may differ from one source to another. The experience obtained from these studies indicate that, at a minimum, the following are important properties of CHCC that should be checked when CHCC is used in an unbound base course adjacent to nonwoven drainage fabric:*
  - a. Fines content (passing No. 200 sieve)
  - b. Atterberg limits
  - c. Mortar content
  - d. pH and EC of the water that comes in contact with CHCC
- *The maximum fines contents (material passing the No. 200 sieve) of the CHCC used in this field study and that in the previously completed laboratory study were 11% and 13%, respectively. In both studies, CHCC was determined to be non-plastic, and the overall gradation was within the design range for VDOT 21A. The average mortar contents of the CHCC used in this field study and that used in the previously completed laboratory study were 27% and 34%, respectively. CHCC with these properties on both projects showed average permeability values in the range of  $10^{-3}$  to  $10^{-4}$  cm/sec.*
- *The maximum pH and EC values recorded in this field study were 12.3 and 4,000  $\mu$ S/sec, respectively. The maximum pH and EC of the CHCC solutions obtained in the previously completed laboratory study based on ASTM D3987 results were 12.3 and 1,200  $\mu$ S/sec, respectively. The difference in EC measurements between the studies relates to the finding in the previously completed laboratory study that the agitation time (the contact time between the CHCC and water) affects EC measurements. The maximum pH measured in this study exceeded the maximum allowable values in Section 245.03 (c) of the VDOT Road and Bridge Specifications for geotextile drainage fabric.*

- *The unbound base course aggregate used in this field study had a relatively high fines content but satisfied the upper limit for VDOT 21A gradation. Fines migration was noted from both the sections with natural aggregate (100% V.A.) content and those with CHCC content. The migration of these fines onto the geotextile used in this study did not adversely affect the ability of the geotextile to function as a drainage fabric. The reduction in permittivity of the drainage fabric used in this study does not appear to be changing as a function of time, as it relates to the migration of fines.*
- *The results of this field study showed that the CHCC as well as the natural aggregate (V.A.) may be susceptible to chemical precipitation if the material contains carbonate-based compounds. The findings of this study showed that for all of the unbound aggregates used in this study, the carbonate-based compound contained calcium.*
- *The previously completed laboratory study showed that chemical precipitation from CHCC may occur on the surface of geotextile used for drainage fabric. The findings of this field study confirmed that chemical precipitation on the surface of the geotextile also occurs in the field environment. Both studies also showed that the chemical precipitation from CHCC is a time-dependent phenomenon. After 3 years of field exposure, the surface area of the exhumed geotextile samples that was covered by chemical precipitation ( $S_{\text{tufa}}$ ) was less than what was observed in the previously completed one-year laboratory study. This finding shows that although the chemical precipitation is a time-dependent phenomenon, in the field, the rate of chemical precipitation appears to be slower than in the laboratory.*
- *Laboratory evaluations of the geotextiles exhumed in this field study showed that chemical precipitation occurred on the surface of the geotextile used in all sections. However, the observed chemical precipitation did not affect the ability of the geotextile to function hydraulically. The same conclusion may not be valid for geotextiles that have a smaller apparent opening size (AOS) and less permittivity than the geotextile tested in this study. The AOS and permittivity of the geotextile used in this study were reported by the manufacturer as 0.212 mm (equivalent of U.S. sieve No. 70 opening) and  $1.7 \text{ sec}^{-1}$ , respectively.*
- *The findings of this study revealed that sections with 100% CHCC and 40% CHCC (Blend 1) showed signs of chemical precipitation inside the drainage pipes, and the area covered by precipitation appeared to spatially increase over time. Precipitation was not observed in the drainage pipes of the sections with 20% CHCC (Blend 2) and 100% V.A.*
- *The findings of this field study showed that observing the water discharged from the drainage system is one way to confirm that the constructed drainage features are working as intended. However, it is important that the water is not allowed to pond near the discharge locations, as the ionically active water may result in tufa precipitation. As*

observed during the borescope evaluations, the potential of tufa precipitation was higher in the 100% CHCC and 40% CHCC (Blend 1) sections.

- *When CHCC is used in base aggregate materials, chemical precipitation (tufa build-up) may not only occur in the drainage fabric but also in the drainage structures (pipes and outlets). Borescope evaluations of the drainage pipes showed signs of precipitation in sections with 100% CHCC and 40% CHCC (Blend 1) but not in sections with 20% CHCC (Blend 2) and 100% V.A. Even though all the constructed sections were able to continue to hydraulically function within the duration of this study, the chemical precipitation within the drainage pipes at the 100% CHCC and 40% CHCC sections need further monitoring. This is because quantitative estimation of continuing chemical precipitation within the pipes requires more data than what was available within the duration of this study.*

## **RECOMMENDATIONS**

1. *VDOT's Materials Division should collaborate with VTRC to develop RNS considering the following:*
  - *Further characterization of CHCC produced by different sources in Virginia, as well as characterizing other allowed materials in VDOT's Special Provision (SP208-000100-00) that may potentially impact the drainage fabric due to chemical precipitation.*
  - *Evaluation of the compatibility of the CHCC gradation and pH with the range of drainage fabric geotextile currently allowed in Section 245.03(c) of VDOT's Road and Bridge Specification.*
  - *Soliciting a pilot project with a 20% CHCC and 80% V.A. blend as an unbound base course aggregate adjacent to UD-4 edgedrains with a nonwoven geotextile drainage fabric that has manufacturer-reported AOS and permittivity of 0.212 mm (equivalent of a U.S. sieve No. 70 opening) and  $1.7 \text{ sec}^{-1}$ , respectively. Long-term monitoring of this pilot project should include periodic exhumation of geotextile fabric to check for chemical precipitation and borescope monitoring of the underdrain pipes.*
2. *As agreed with the Harrisonburg Residency facility, all remaining field test sections that were constructed for this study will be paved by VDOT. VTRC should consider continual monitoring of this site.*

## **IMPLEMENTATION AND BENEFITS**

### **Implementation**

Regarding Recommendation 1, VDOT's Materials Division will need to work with VTRC to develop RNS and present it to the Pavement Research Advisory Committee by Fall 2025.

Regarding Recommendation 2, VTRC and VDOT's Materials Division will need to discuss the need for any further actions by December 2025.

### **Benefits**

This research provides information that can be used by VDOT to make decisions on using CHCC as an unbound base course aggregate adjacent to nonwoven geotextiles that are used as part of the UD-4 drainage detail. Allowing the use of CHCC as an unbound base course aggregate may have economic benefits and will promote sustainable practices in terms of recycling a material that may otherwise be disposed. This research also provides benefits associated with material characterization and the percentage of CHCC to be used.

Identifying a range of pH, EC, mortar content, and gradation values for CHCC produced in Virginia and other allowed material in the Special Provision will allow for better assessment of the suitability of these materials to be used adjacent to drainage fabric. Determining the compatibility of the geotextiles used in edgedrain construction with the gradation and pH of CHCC produced in Virginia will help determine the suitability of using a wide range of the geotextiles currently allowed by VDOT as drainage fabric. Long-term monitoring of the field site constructed as part of this study and completing a pilot project will confirm the findings of this study and provide essential information to develop a special provision for using CHCC.

## **ACKNOWLEDGMENTS**

Financial support for this study was received from the Virginia Transportation Research Council (VTRC). The members of the technical review panel for this project, who reviewed this final report, consisted of Dr. Harikrishnan Nair, P.E. (associate director at VTRC); Mr. David Shiells, P.E. (district materials engineer at VDOT); Dr. Edward J. Hoppe, P.E. (associate principal research scientist at VTRC); Dr. Wansoo Kim, P.E. (soils, aggregates, and buried structures program manager at VDOT); Mr. Chaz Weaver, P.E. (district materials engineer at VDOT); Dr. M. Shabbir Hossain, P.E. (associate principal research scientist at VTRC); and Ms. Vanna Patterson Lewis, P.E. (engineering coordinator of FHWA's Virginia division).

The initial need for this research was identified by Mr. John Schuler - Assistant State Materials Engineer and Mr. David Shiells. Mr. Shiells and Mr. Kevin Wright - Implementation Team Lead of VTRC, have been great help in identifying the project site and making the connection between the GMU and the VDOT teams. We are very grateful to all of the VDOT's Harrisonburg facility leadership especially Mr. Edward (Dale) Perry - Maintenance Manager for allowing and supporting this site to be constructed within their facility. The construction of this site would not have been possible without the help of the VDOT's Harrisonburg bridge (crew supervisor Mr. Joseph Calhoun) and Mt. Crawford maintenance teams (crew supervisor Mr. Stacey Michael) and continuous support by Mr. Wright. Additional special appreciation is extended to Mr. Gary W. Via, Jr and the rest of the Mt. Crawford maintenance team for providing assistance every time the GMU team exhumed geotextiles.

The logistics involved in identifying a site was complex. There were two possible sites, and time constraints required that materials be ready for both sites. In the northern Virginia area, the authors would like to thank Mr. Joe Fitterer of the Chantilly Crushed Stone for graciously helping to produce fresh CHCC on-site and creating the blends using pugmill based on the requirements of the GMU team. However, due to location of the selected site, this material was never used in the construction of this test site. Mr. Dan Babish of Luck Stone and members of the Luck Stone Rockville, VA plant helped produce another set of CHCC materials and created the blends also using pugmill. Virgin aggregate material was also produced at Luck Stone's Rockville plant. Mr. William Walker, the central laboratory manager at Luck Stone, worked with the GMU team to conduct quality control tests for the produced materials.

Mr. Todd Harman of Hallaton donated the geocomposite and HDPE geomembrane liners used in the construction of the test sections. Hallaton also provided in-kind technical support for the installation and welding of the geomembrane liner, with the help of Mr. Russ Villegas, who came to the job site. Mr. Villegas's help was essential in correctly installing the liner system so that all the infiltration water had no way out of the test section unless through the edgedrains.

This test site is the first of its kind in the United States, and it would not have been possible to create this site without all this support.



## REFERENCES

- Abbaspour, A., Tanyu, B. F., 2021. Chemical clogging and geotextile serviceability in subdrains adjacent to recycled concrete. *Geosynthetics International* 28, 402–420. <https://doi.org/10.1680/jgein.20.00051>
- Abbaspour, A., Tanyu, B.F., 2020a. Parameters Affecting Tufa Precipitation from Recycled Concrete Aggregate, in: Reddy, K.R., Agnihotri, A.K., Yukselen-Aksoy, Y., Dubey, B.K., Bansal, A. (Eds.), *Sustainable Environment and Infrastructure, Lecture Notes in Civil Engineering*. Springer International Publishing, Cham, pp. 71–81. [https://doi.org/10.1007/978-3-030-51354-2\\_7](https://doi.org/10.1007/978-3-030-51354-2_7)
- Abbaspour, A., Tanyu, B.F., 2020b. CO<sub>2</sub> Sequestration by Carbonation Processes of Rubblized Concrete at Standard Conditions and the Related Mineral Stability Diagrams. *ACS Sustainable Chem. Eng.* 8, 6647–6656. <https://doi.org/10.1021/acssuschemeng.9b07690>
- Abbaspour, A., Tanyu, B.F., 2019a. Tufa precipitation from Recycled Concrete Aggregate (RCA) over geotextile: Mechanism, composition, and affecting parameters. *Construction and Building Materials* 196, 317–329. <https://doi.org/10.1016/j.conbuildmat.2018.10.146>
- Abbaspour, A., Tanyu, B.F., 2019b. Evaluate Hydraulic Compatibility of Geotextile and RCA in Underdrain Systems Under Turbulent Flow Regime, in: *Geosynthetics Conference 2019*. IFAI, Houston, Texas, U.S.A.
- Abbaspour, A., Tanyu, B.F., Aydilek, A.H., Dayioglu, A.Y., 2018. Methodology to evaluate hydraulic compatibility of geotextile and RCA in underdrain systems. *Geosynthetics International* 25, 67–84. <https://doi.org/10.1680/jgein.17.00034>
- Abbaspour, A., Tanyu, B.F., Cetin, B., 2016. Impact of aging on leaching characteristics of recycled concrete aggregate. *Environ. Sci. Pollut. Res.* 23, 20835–20852. <https://doi.org/10.1007/s11356-016-7217-9>
- ASTM C127, 2012. Standard Test Method for Density, Relative Density (Specific Gravity), and Absorption of Coarse Aggregate. ASTM International, West Conshohocken, PA.
- ASTM C128, 2012. Standard Test Method for Density, Relative Density (Specific Gravity), and Absorption of Fine Aggregate. ASTM International, West Conshohocken, PA.
- ASTM D698, 2012. Standard Test Methods for Laboratory Compaction Characteristics of Soil Using Standard Effort (12 400 ft-lbf/ft<sup>3</sup>(600 kN-m/m<sup>3</sup>)). ASTM International, West Conshohocken, PA.
- ASTM D2434, 2006. Standard Test Methods for Measurement of Hydraulic Conductivity of Coarse-Grained Soils. ASTM International, West Conshohocken, PA.
- ASTM D2487, 2011. Standard Practice for Classification of Soils for Engineering Purposes (Unified Soil Classification System). ASTM International, West Conshohocken, PA.
- ASTM D3665, 2012. Standard Practice for Random Sampling of Construction Materials. ASTM International, West Conshohocken, PA.
- ASTM D3987, 2012. Standard Practice for Shake Extraction of Solid Waste with Water. ASTM International, West Conshohocken, PA.

- ASTM D4318, 2010. Standard Test Method for Liquid Limit, Plastic Limit, and Plasticity Index of Soils. ASTM International, West Conshohocken, PA.
- ASTM D4491/4491M, 2020. Standard Test Method for Water Permeability of Geotextiles by Permittivity. ASTM International, West Conshohocken, PA.
- ASTM D6913/D6913M, 2017. Standard Test Methods for Particle-Size Distribution (Gradation) of Soils Using Sieve Analysis. ASTM International, West Conshohocken, PA.
- ASTM D7928, 2017. Standard Test Methods for Particle-Size Distribution (Gradation) of Fine-Grained Soils Using the Sedimentation (Hydrometer) Analysis. ASTM International, West Conshohocken, PA.
- Edil, T.B., Tinjum, J.M., Benson, C.H., 2012. Recycled Unbound Materials (Final Report, MN/RC 2012-35). Minnesota Department of Transportation, Saint Paul, Minnesota.
- Gupta, N., Kluge, M., Chadik, P.A., Townsend, T.G., 2018. Recycled concrete aggregate as road base: Leaching constituents and neutralization by soil interactions and dilution. *Waste Management* 72, 354–361. <https://doi.org/10.1016/j.wasman.2017.11.018>
- Kurdowski, W., 2014. *Cement and concrete chemistry*. Springer Science & Business.
- Luck Stone, Rockville Plant Geology. Retrieved 10/03/2023 from <https://www.luckstone.com/locations/rockville-plant>.
- McGhee, K. K., Smith, B. L., 2020. Impact on Compaction of Virginia’s Dense-Graded Asphalt Surface Mixtures from Recent Changes To Design and Construction Acceptance Criteria (No. FHWA/VTRC 21-R11). Virginia Transportation Research Council (VTRC).
- Tanyu, B., Abbaspour, A., 2022a. Evaluating the Longevity and Condition of the Geotextiles Used in The Past in Geo-Infrastructures Constructed with Recycled Concrete Aggregatens (RMRC Final Report). Recycled Materials Resource Center University of Wisconsin-Madison, George Mason University, Madison, WI.
- Tanyu, B., Abbaspour, A., 2022b. Suitability of Using Crushed Concrete Adjacent to Geotextiles in Underdrain Systems Second Phase: Field Trial Before Implementation Part I: Construction and End-of-One-Year Evaluations (Unpublished Report). Virginia Transportation Research Council, George Mason University, Charlottesville, VA.
- Tanyu, B., Abbaspour, A., 2020. Evaluation of Use of Crushed Hydraulic Cement Concrete (CHCC) as an Additive to Base Course/Subbase Material (Final Report No. Final Report No. FHWA/VTRC 21-R12). Virginia Transportation Research Council, George Mason University, Charlottesville, VA. <https://doi.org/10.13140/RG.2.2.32533.96483/2>
- The United States Geological Survey (USGS), Hanover County Geology. Retrieved 10/03/2023 from <https://mrdata.usgs.gov/geology/state/fips-unit.php?code=f51085>.
- The United States Geological Survey (USGS), Rates of Rainfall. Retrieved 10/03/2023 from <https://water.usgs.gov/edu/activity-howmuchrain-metric.html#:~:text=Very%20heavy%20rain%3A%20Greater%20than,than%2050%20m%20per%20hour>.
- Vardanega, P. J., 2014. State of the art: Permeability of asphalt concrete. *Journal of Materials in Civil Engineering*, 26(1), 54–64.

- VDOT, 2017. Virginia Test Method (VTM) 1: Laboratory Determination of Theoretical Maximum Density Optimum Moisture Content of Soils, Granular Subbase, and Base Materials – (Soils Lab), May 8, 2017
- VDOT, 2016a. Road and Bridge Specifications - Special Provision for Section 208 - Subbase and Aggregate Base Material (SP208-000100-00). Virginia Department of Transportation, Richmond, VA.
- VDOT, 2016b. Road and Bridge Specifications. Virginia Department of Transportation, Richmond, VA.
- VDOT, 2008. Road and Bridge Standards, 2015th ed. Virginia Department of Transportation, Richmond, VA.
- VDOT, 2007. Road and Bridge Specifications. Virginia Department of Transportation, Richmond, VA.
- VDOT, 2022. Manual of Instructions, Chapter VI: Pavement Design and Evaluation. Virginia Department of Transportation, Richmond, VA.
- Yadykova, A. Y., Ilyin, S. O. 2022. Rheological and adhesive properties of nanocomposite bitumen binders based on hydrophilic or hydrophobic silica and modified with bio-oil. *Construction and Building Materials*, 342, 127946.
- Yunusa M, Zhang X, Cui P, Tian X. Durability of Recycled Concrete Aggregates Prepared with Mechanochemical and Thermal Treatment. *Materials (Basel)*. 2022 Aug 22;15(16):5792. doi: 10.3390/ma15165792. PMID: 36013924; PMCID: PMC9416652.